

# Intuitive Teleoperation of a Robotic Arm and Gripper with Soft Pneumatic Haptic Feedback

by

Raagini Rameshwar

A Dissertation

Submitted to the Faculty

of the

WORCESTER POLYTECHNIC INSTITUTE

In partial fulfillment of the requirements for the

Degree of Doctor of Philosophy

in

Robotics Engineering

August 2023

APPROVED:

---

Professor Cagdas Onal  
Primary Advisor  
Worcester Polytechnic Institute

---

Professor Berk Calli  
Committee Member  
Worcester Polytechnic Institute

---

Professor Yunus Telliel  
Committee Member  
Worcester Polytechnic Institute

---

Professor Jing Xiao  
Committee Member  
Worcester Polytechnic Institute

# Acknowledgements

- My advisor: Professor Cagdas D. Onal PhD, for his unending technical and mental support, and for helping making this process and my research truly enjoyable;
- Committee Members: Professors Berk Calli PhD, Yunus Telli PhD, and Jing Xiao PhD, for their support and invaluable feedback;
- Colleagues: Shilpa Thakur, Mason Mitchell, Eric Rogers, Ann Marie Votta, Dr. Erik Skorina, Sihui Li;
- My parents, Rameshwar Sundaresan and Satya Rameshwar;
- All my users who participated in user testing
- The Amazon Robotics Fellowship through the Robotics Engineering Department at Worcester Polytechnic Institute
- This dissertation is based upon work supported by the National Science Foundation (NSF) under Grant Nos. DGE-1922761 and IIS-2024802. Any opinions, findings, and conclusions or recommendations expressed in this material are those of the authors and do not necessarily reflect the views of the NSF.

# Abstract

Robot teleoperation is a transformative field of study that can enable workers to safely perform tasks in dangerous environments. Robot arm teleoperation is particularly suited to help remotely perform delicate or intricate manipulation tasks in fields like medicine, space and ocean exploration, and hazardous waste management. The quality and usability of a teleoperation system, particularly a robot arm teleoperation system, depends on how much the user is immersed in the system and feels that the robot manipulator is an extension of their own body. We explore this sense of immersion, or “telepresence”, through the mapping scheme between the human user and robot manipulator, and through the use of realistic haptic feedback. In this thesis, I discuss our work towards a teleoperation system with safe, realistic haptic feedback for intuitive control of a robotic arm and gripper. The system involves a motion capture system that the user wears to control a robotic arm and sensorized gripper, and soft pneumatic haptic devices. We present several iterations of our system, and discuss the development of a novel user-to-robot mapping scheme as well as the development of soft “haptic muscles”, a term we coin for our pneumatic haptic feedback devices. We also present several stages of user testing, and discuss how we used each set of results to design the next iteration of our system. Our most recent system iteration is a teleoperation system that allows novice users to pick and place objects comfortably, with a task completion time of 18 seconds across all users. It also allows users to pick and place delicate objects without damaging or deforming them, and we find that the soft haptics decrease the user’s applied force by 53%.

# Dissertation Structure

The structure of this dissertation is as follows:

Chapter 1 discusses an introduction to robot arm teleoperation, its applications, and current research in the field.

Chapter 2 discusses an overview of the system we have built and how the different subsystems work together.

Chapter 3 discusses the design, development, and testing of the motion capture subsystem and our human-robot mapping algorithms.

Chapter 4 discusses the design, development, and testing of our soft pneumatic haptic devices.

Chapter 5 discusses the development of the robotic end effectors we use in testing our system.

Chapter 6 discusses several phases of user testing, the results of the testing, and how we used each set of results to improve the system.

Chapter 7 discusses the wider implications of this work as it applies to various industrial and research sectors.

Chapter 8 concludes with a summary of our findings and our planned future work.

# Table of Contents

Acknowledgements . . . . .	i
Abstract . . . . .	ii
Dissertation Structure . . . . .	iii
List of Figures . . . . .	xiv
List of Tables . . . . .	xv
<b>1 Introduction</b>	<b>1</b>
1.1 Robot Arm Teleoperation . . . . .	1
1.2 Related Work . . . . .	3
1.2.1 Motion Capture . . . . .	4
1.2.2 Haptic Feedback . . . . .	6
1.2.3 Sensorized Robotic End Effectors . . . . .	8
1.2.4 Teleoperation Systems . . . . .	8
1.2.5 Human-Robot Interaction Studies . . . . .	9
1.2.6 Methodology . . . . .	10
1.3 Contributions . . . . .	11
1.3.1 Haptic Feedback Mechanism . . . . .	11
1.3.2 Motion Capture System . . . . .	12
1.3.3 Robotic End Effector . . . . .	13
<b>2 System Overview</b>	<b>14</b>
2.1 Integrated System . . . . .	14

2.2	Research Phases Overview . . . . .	16
<b>3</b>	<b>Motion Capture System and User Mapping</b>	<b>19</b>
3.1	Motion Capture Hardware . . . . .	19
3.1.1	Data Glove . . . . .	19
3.1.2	IMU Bands . . . . .	23
3.2	User to Robot Mapping Schemes . . . . .	24
3.2.1	Joint to Joint Mapping Scheme . . . . .	24
3.2.2	Cartesian Mapping Scheme . . . . .	27
<b>4</b>	<b>Haptic Muscles</b>	<b>36</b>
4.1	Haptic Muscle Design and Control . . . . .	36
4.2	Plastic Haptic Muscle Prototype . . . . .	37
4.3	Fabric-Silicone Haptic Muscle Prototypes . . . . .	39
4.3.1	Design Requirements . . . . .	39
4.3.2	Fabrication Process . . . . .	40
4.3.3	Material Selection Experiments . . . . .	42
4.3.4	Force Output Validation . . . . .	47
<b>5</b>	<b>Robotic End Effector</b>	<b>50</b>
5.1	Simulated 3-Fingered Robotiq Gripper . . . . .	51
5.2	5-Fingered Anthropomorphic Gripper . . . . .	52
5.2.1	Ada Hand - Open Source Design . . . . .	52
5.2.2	Soft Force Sensors . . . . .	54
5.2.3	5-Fingered Gripper Validation . . . . .	54
5.2.4	5-Fingered Gripper Conclusions . . . . .	55
5.3	2-Fingered Robotiq Gripper . . . . .	55
<b>6</b>	<b>User Testing</b>	<b>58</b>
6.1	Phased User Testing . . . . .	58

6.2	Phase 1 . . . . .	58
6.2.1	Phase Setup . . . . .	58
6.2.2	System Description . . . . .	59
6.2.3	User Test Description . . . . .	59
6.2.4	User Test Results . . . . .	60
6.2.5	User Test Conclusions and Future Work . . . . .	61
6.3	Phase 2 . . . . .	61
6.3.1	Phase Setup and Hypotheses . . . . .	61
6.3.2	System Description . . . . .	62
6.3.3	User Test Description . . . . .	62
6.3.4	User Test Results . . . . .	63
6.3.5	User Test Conclusions and Future Work . . . . .	65
6.4	Phase 3 . . . . .	66
6.4.1	Phase Setup and Hypotheses . . . . .	66
6.4.2	System Description . . . . .	66
6.4.3	User Test Description: Grasp Quality . . . . .	66
6.4.4	User Test Results: Grasp Quality . . . . .	67
6.4.5	User Test Description: System Teleoperation . . . . .	68
6.4.6	User Test Results: System Teleoperation . . . . .	69
6.4.7	User Test Conclusions and Future Work . . . . .	71
6.5	Phase 4 . . . . .	72
6.5.1	Phase Setup and Hypotheses . . . . .	72
6.5.2	System Description . . . . .	72
6.5.3	User Test Description: Novice Haptic Study . . . . .	73
6.5.4	User Test Results: Novice Haptic Study . . . . .	74
6.5.5	User Test Description: Novice Teleoperation Study . . . . .	75
6.5.6	User Test Results: Novice Teleoperation Study . . . . .	76
6.5.7	User Test Description: Expert Teleoperation Study . . . . .	77

6.5.8	User Test Results: Expert Teleoperation Study . . . . .	78
6.5.9	User Test Conclusions and Future Work . . . . .	79
<b>7</b>	<b>Broader Impacts</b>	<b>81</b>
7.1	Broader Impact . . . . .	81
7.2	Responsible Innovation In Different Sectors . . . . .	82
7.2.1	Space Exploration . . . . .	82
7.2.2	Warehouse Logistics . . . . .	83
7.2.3	Medical Care . . . . .	84
7.3	Teleoperation-Driven AI . . . . .	85
7.4	STEM Education and Outreach . . . . .	86
<b>8</b>	<b>Conclusions and Future Work</b>	<b>88</b>



# List of Figures

1.1	Our teleoperation system allows a user to wear a motion capture system and control a robotic arm and gripper. Force sensors on the robotic gripper read forces during teleoperation, and these forces are transferred to the user via the haptic muscles. . . . .	3
2.1	A system diagram showing how the main subsystems interact. The system uses ROS as its software communication hub, and data is passed as topics from subsystem to subsystem. Our areas of novel contribution are bordered in red. . . . .	15
2.2	This software flow shows how data flows from the user to the robotic arm and gripper, and how data from the robotic gripper flows back to the user. . . . .	18
3.1	An optical curvature sensor sitting on the user’s thumb. The infrared emitter and receiver are outlined in green and the flexible black tube in yellow. The curvature sensor sits atop the haptic device (clear plastic). . . . .	20
3.2	This plot shows an example of the optical sensor outputting curvature signals when worn by a user. When the user’s finger is straight, light from the LED reaches the receiver, resulting in a high signal. As the user gradually curves their fingers, the light is blocked, resulting in a low signal. This provides an accurate reading of the user’s finger curvature. We find that the signal is consistent when the finger is fully open or closed, and gradually decreases as the user’s finger bends. . . . .	21
3.3	The StretchSense SuperSplay is an off-the-shelf data glove with capacitive curvature sensing. The curvature sensors are flexible layers that change capacitance when stretched. . . . .	22

3.4	We use a linear mapping to convert the user’s current position to a desired position for the robotic gripper. We get the user’s minimum and maximum values through a calibration routine at the beginning of each teleoperation test. . . . .	23
3.5	The user wears 3 IMUs, on the upper arm, forearm, and wrist, to capture their arm motions. The IMUs are connected to each other and the microcontroller using I2C.	24
3.6	The human arm and robot are mapped joint-to-joint. The user’s shoulder controls the first two joints, the elbow controls the third, and the wrist controls one of the robot’s wrist joints. . . . .	25
3.7	We asked a user to wear the motion capture system and rotate their elbow parallel to the ground, which teleoperates the elbow joint of the robotic arm. We capture the user data as well as the current joint position output by the robot arm, and plot both here. We find that joint-to-joint mapping is a low-latency form of control because there are no complex kinematics to calculate. . . . .	26
3.8	This is a plot showing the results of workspace mapping with scaling. We capture user data and use a scaling constant to map the user position into the robot workspace. The plot shows an example of the user moving in the x-axis and the resulting motion of the robot arm. We show the user’s raw position, the scaled position, and the robot end-effector’s final position. . . . .	30
3.9	This plot shows the results of workspace mapping using the proposed alignment technique. We capture user data and use the user’s calibration values to align the user and robot workspaces. The plot shows an example of the user moving in the x-axis and the resulting motion of the robot arm. We show the user’s raw position, the scaled position, and the robot end-effector’s final position. . . . .	33

3.10	We asked one user to wear the motion capture system and draw a circle in the air with their hand. We then use both the scaling and alignment mapping methods to calculate the robot’s desired position from the same movement. This plot shows the user movement, the desired robot position using the workspace scaling method, and the desired robot position using the workspace alignment method. The alignment method produced a semi-circle that is wider than the scaling method, showing how the user is able to reach a larger workspace using the alignment method. . . .	34
3.11	We asked a user to wear the motion capture system and teleoperate the robot arm in the x-axis, moving left and right several times. We captured their movement and the robot’s end-effector position over time to show the latency between the two. We show the robot and user movement in the x-axis and calculate an average latency of 250ms. . . . .	34
4.1	We control the haptic muscles using solenoid valves that have a constant input air source. By driving the solenoid valve with PWM signals, we can output a certain percentage of the air source to inflate the haptic muscle. . . . .	37
4.2	Initial prototypes of haptic muscles fabricated using heat-sealable plastic deflated (left) and inflated (right). . . . .	38
4.3	Cotton-spandex fabric a) in a neutral state b) stretched parallel to the ribs and c) stretched perpendicular to the ribs. . . . .	40
4.4	The manufacturing process to construct one haptic muscle. We coat a trapezoid-shaped piece of fabric with silicone (A-C), spray mold release in the center (D), and add another fabric-silicone piece to create a pouch (E). After inserting an air tube (F), we sew the pouch into a toroid (G). . . . .	41
4.5	A complete fabric-silicone haptic muscle deflated (left) and inflated (right). . . . .	42

4.6	To perform the Minimum Detectable Change test, we ask a user to wear the haptic muscle, then inflate it partway. We then increase and decrease the PWM duty cycle input in a square wave pattern, gradually increasing the input pressure at each step. The test begins at 40% inflation then slowly increases, with a jump back to 40% inflation between each increase. . . . .	43
4.7	User results for the “MDC Test”, indicated the change in pressure detected for all three haptic muscles. The haptic muscle made with Ecoflex has the highest sensitivity with the lowest variance. We performed this test on 16 users who had no experience with wearable haptics. . . . .	44
4.8	The transient pressure response of three haptic muscles to immediate (step) full inflation input. This plot shows results from one haptic muscle of each type, and there may be variations across haptic muscles of the same material due to manufacturing differences. . . . .	46
4.9	The duty cycle vs pressure plot for all three haptic muscles, as well as one standard deviation and linear fits. This confirms that the relationship between our input and resulting pressure are approximately linear after an initial duty cycle offset. This plot shows the results after 3 cycles of inflating the haptic muscles, and we show the average, standard deviations, and trendlines across all cycles of each haptic muscle. . . . .	47
4.10	(a) The setup to track compression forces and restoration forces while inflating the plastic (bottom left) and Ecoflex0030 (bottom right) haptic muscle. It consists of a tendon-driven 3D-printed finger, a force-sensitive resistor (FSR) to track compression, and a load cell to track restoration force. (b) The results of the compression tests for both haptic muscles. (c) The results of the restoration tests for both haptic muscles. . . . .	48

5.1	We use a linear mapping to convert a user’s current finger position to a gripper position. We begin teleoperation by having the user open and close their hand while wearing the data glove. We capture the data glove’s signals in the open and closed position and set this as the user’s working range. We can then linearly map the user’s working range to the robot. . . . .	51
5.2	We 3D print the Ada hand in three distinct pieces. The palm and fingers are one piece, printed from NinjaFlex, a flexible filament. The wrist and back plates are two pieces, printed from rigid ABS. . . . .	52
5.3	The fingers of the robotic hand are tendon driven and underactuated. The Ninjaflex fingers allow the fingers to conform to different shapes and perform a variety of grasps such as cylindrical, spherical, tripod, and pinch grasps. . . . .	53
5.4	We sensorize the Ada Hand by adding a chamber in the fingertip to house a hall-effect sensor and a small magnet. This is a novel version of a sensor previously proposed in [1]. The sensor reads finger deflection during grasping which we can interpret as grasp force. . . . .	55
5.5	We sensorize the Ada Hand by adding a chamber in the fingertip to house a hall-effect sensor and a small magnet. This sensor reads finger deflection during grasping which we can interpret as grasp force. In this plot we show a user wearing the data glove presented in Chapter 3 and using it to teleoperate the Ada Hand to grasp a soft toy and a rigid box. The curve shows the sum of the force sensor outputs across all five fingers of the soft gripper. We observe that the force output for a soft object is less than that of a rigid object. . . . .	56
5.6	We add resistive force sensors and silicone pads to the gripper fingers to add sensing and compliance to a rigid off-the-shelf Robotiq gripper. . . . .	57

5.7	We asked a user to use a game controller to open and close the gripper around a loaf of bread, and collected the force sensor output. We observe that the user initially squishes the loaf and then opens the gripper somewhat to grasp it more lightly. We see, therefore, that we can use the force sensor data to communicate grasp strength. . . . .	57
6.1	The simulated setup we presented at the Waste Management Conference in 2018. Users wore the motion capture system and controlled the simulated robotic arm. The plot on the right shows the force output from the gripper as the user grasps a cube. The user felt haptic feedback proportional to the force output through the haptic muscles. . . . .	60
6.2	To test the usability of the system, users were asked to grasp a small box and a water bottle and place them into the larger black box. . . . .	63
6.3	During the timed portion of the user test, 5 out of 9 users were able to complete the entire task in under 5 minutes, and 2 out of 3 experienced users completed the task in under 2 minutes. On average users took less time to pick and place the box than the bottle, but experienced users dealt with both objects fairly quickly. . . . .	64
6.4	To test our system, users picked up 5 randomly ordered objects, each with and without feedback, and placed them in a box. Objects are placed on the table one at a time. . . . .	69
6.5	Pick and place user study results with/without feedback for experienced users and inexperienced users. We tested 12 users, 8 inexperienced and 4 experienced. The center point is the average time to complete the pick-and-place task for each object, and the error bars represent the standard deviation among users. . . . .	70
6.6	User test setup simulating remote teleoperation with a robotic arm and gripper. (a) The setup includes a camera pointing at the robot with the video fed to the monitor, and a barrier to prevent the user from seeing the physical robot. The user wears a data glove with haptic muscles and controls the arm with the glove and a keyboard. (b) The user watches a monitor which streams live video of the robot arm. . . . .	74

6.7	We performed a pick-and-place test with 10 users and 4 objects of varying size and stiffness to gauge how well they can use the system. The results that users perform an average pick and place in 18.63 seconds. We find that the new human-robot mapping scheme improves both average performance and standard deviation of task completion time. This shows that more users are more comfortable with the system with very few outliers who struggled more. . . . .	77
6.8	We performed a pick-and-place test with 10 users and 4 objects of varying size and stiffness to gauge how well they can use the system. We find that, in general, users complete the pick and place more quickly as they gain experience with the system. In this plot we show a sample of 5 users and their average pick and place times over the course of testing. The trendline shown shows a slight downward trend when comparing completion times over all 6 runs of the experiment. . . . .	78
6.9	We performed a pick-and-place test with 10 users and 4 objects of varying size and stiffness to gauge how well they can use the system. After each run of picking and placing 4 objects, we asked them to fill out a NASA Task Load Index survey. We calculate "average negativity" as the average of the user's responses to the task load questions. We find that the presence of haptic feedback decreases users' average negativity and therefore mental load during the task. . . . .	79
6.10	Teleoperation experiment to pick and place a soft fruit bar by an experienced user: (a) without haptic feedback and (b) with haptic feedback. The plots show normal force applied during the task, as well as the state of the fruit bar at the end of the attempt. . . . .	80

# List of Tables

4.1	Haptic Muscle Sensitivity Test Results . . . . .	45
6.1	This table shows our 4 main phases of development and what version of each subsystem was involved in each phase. . . . .	59
6.2	User performance in picking and placing a cylindrical bottle (9 users, 6 inexperienced and 3 experienced) . . . . .	64
6.3	User performance in picking and placing a rectangular box (9 users, 6 inexperienced and 3 experienced) . . . . .	65
6.4	Grasp Quality Test with Visual Feedback . . . . .	68
6.5	Grasp Quality Test with no Visual Feedback . . . . .	68
6.6	Novice Haptic Test Results (12 users) . . . . .	74



# Chapter 1

## Introduction

### 1.1 Robot Arm Teleoperation

Robot arms are becoming indispensable in many industrial and research sectors, such as space and underwater exploration [2], surgery units in hospitals [3], warehouse logistics, and manufacturing plants [4]. They are strong, precise, and durable, allowing them to perform repetitive tasks that are dangerous or cumbersome for a human to do. Many robot arms today are either autonomous, and programmed to perform one task repetitively, or they are remotely controlled, because the environment in which they work is unpredictable or constantly changing. Remote control of robot arms, or robot arm teleoperation, is a way for people to perform non-repetitive tasks in changing environments that may be remote or dangerous. It is a way of combining human perception and skill with robot strength and precision. Robot teleoperation is already enhancing space research [5] and helping perform minimally invasive surgery [6] as well as helping do work in hazardous environments [7][8].

Current modes of robot teleoperation in industry and research are mostly dependent on control pads, joysticks, or game controllers. This tends to limit the kinds of tasks a robot arm can do, so there are still many remote or dangerous tasks that require human intervention. The key to pushing the field of robot teleoperation is “telepresence”, a concept that allows human perception and robot capabilities to work more closely in harmony. Telepresence during teleoperation is defined as

feeling that the teleoperated agent is an extension of the user's body, or that the user and avatar are the same being.

One example of telepresence can be seen in virtual reality games, where users are sometimes so immersed in the virtual world that they forget that their body exists in a different place, and they collide with furniture or walls. VR-accidents aside, telepresence is very useful during robot teleoperation. Studies have shown that a heightened sense of telepresence during teleoperation of virtual agents can increase task speed and decrease mental load. It is clear, therefore, that telepresence is one of the major goals of robot teleoperation research. To achieve telepresence in robot teleoperation requires two major things: intuitive human-robot mapping and haptic feedback [9][10].

Human-robot mapping refers to how the user moves in order to move the robotic arm, and this can range from only using their fingers to using their whole body. The closer a user's motions during teleoperation are to their motions in real life, the more immersive the telepresence experience. It is also important to take advantage of the human sense of proprioception, or where one's body is at all times. If the experience is truly immersive and the motion control truly intuitive, a user will easily understand how to move their own body to control the robotic arm.

Haptic feedback refers to the sense of touch, which is something people use to accomplish even simple tasks with ease. During teleoperation, haptic feedback can provide information to a user that vision alone cannot. For example, it can tell a user how well they have grasped an object, the weight of an object, and sometimes even its texture. Haptics can also help users navigate cluttered environments and even use the environment to their advantage, like pushing an object against a table or wall to orient it and pick it up more securely. Haptics during teleoperation help form a closed-loop system, where the user controls their own actions based on feedback from the teleoperated robot. This enhance the telepresence experience and allow users to accomplish more complex, touch-based tasks. The nature of the haptic feedback is crucial to its usefulness, and it is important that a user is able to quickly interpret the haptics and respond with the correct motion controls.

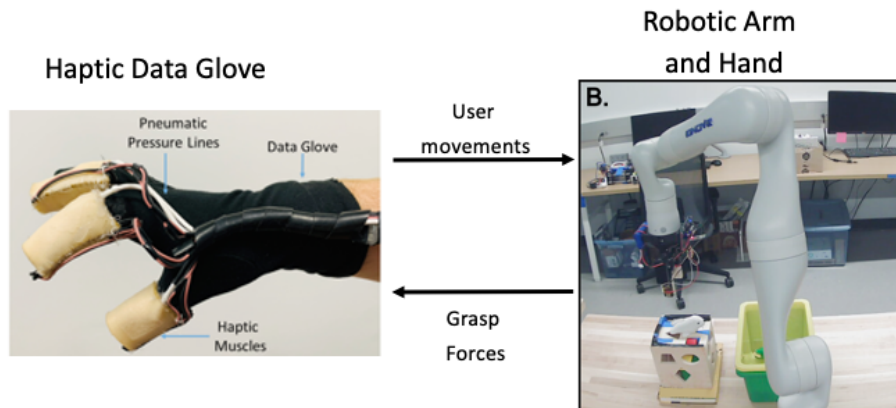


**Figure 1.1:** Our teleoperation system allows a user to wear a motion capture system and control a robotic arm and gripper. Force sensors on the robotic gripper read forces during teleoperation, and these forces are transferred to the user via the haptic muscles.

In this work, we present a full closed-loop teleoperation system that explores the idea of telepresence through novel human-robot mapping and haptic feedback mechanisms. The system allows a user to wear a lightweight and portable motion capture system and use natural body motions to control a robotic arm and gripper. The robot gripper has soft force sensors at the fingers that read grasp forces during teleoperation. These grasp forces are transmitted to the user through pneumatic haptic feedback devices that give the user a sense of grasp quality and strength. This system allows users to intuitively teleoperate a robot arm and remotely handle delicate or fragile objects. We present our work on all the technical subsystems involved in this research, as well as the execution of several phases of user testing to prove the system’s usability and the efficacy of the haptic feedback.

## 1.2 Related Work

Our main areas of novelty lie in the motion capture, haptic feedback, and gripper subsystems. We thus focus on these areas in the literature.

## 1.2.1 Motion Capture

There are several methods of capturing user movements or intention to remotely teleoperate robotic arm systems. The most popular in commercial settings is using a control pad that allows the user to jog the arm in space or control its joints using joysticks, and easily program and run trajectories. A similar and less featured method is to use a simple gamepad like an XBox controller, a single joystick, or a keyboard and mouse [11][12][13][14][15]. While these methods are very reliable for tasks that are repetitive and require set trajectories, they become cumbersome and difficult when the environment is unpredictable and changing. For example, controlling an arm with a game controller requires a user to switch between “position” and “orientation” mode, which is time-consuming and unintuitive [16]. Some touch-based controllers are more full-featured, such as the touchscreen presented in [17], but is still unintuitive enough to limit the task range of a novice user.

The other category of teleoperation methods is through body motions, where the user controls a robotic arm by moving their own body. Because this teleoperation method mirrors how people complete tasks everyday, it allows users to perform more complex tasks quickly and solidifies the telepresence experience [18]. We find in our literature review that papers using body-based teleoperation test their systems with more complex tasks, such as folding laundry, working with connectors, and opening doors. It therefore seemed most reasonable to delve into how various researchers capture their users’ body movement data.

There are many ways to develop a motion capture system for remote teleoperation, and they differ widely in setup time, user comfort and mobility, portability, and cost. One very popular method is vision-based motion capture, which requires the user to remain in view of the cameras detecting their motion [19][20] and can sometimes suffer from vision occlusion. Additionally, depending on the algorithm used for pose estimation, a vision-based system may introduce latency to the teleoperation system that is undesirable. Alternatively, it may require a very powerful computer to run the system. Another popular method for teleoperation is using virtual reality headsets with handheld trackers. These headsets, for example the HTC Vive, ship with very fast pose estimation algorithms that allow users to control characters in video games, and these algorithms are easily integrated into teleoperation systems.

Finally, there are teleoperation systems that use wearable sensors to estimate the pose of the user and their arm. These tend to use rather expensive sensor suites with complex algorithms to estimate poses based on inertial measurement unit readings, such as the sensor suite sold by Perception Neuron and used in [21]. This method is growing more popular because the setup time is very low, it has high portability, and the user also has high mobility and is very comfortable, especially if the sensors are small and the attachment method allows for movement and adjustability [22]. We chose the path of wearable sensors because of its simplicity and lightweight nature, but we chose to create our own sensor suite, which resulted in a low-cost and full-featured motion capture system. The Perception Neuron, one of the few inertial sensor based motion capture systems on the market, sells for 4500USD, while our motion capture system costs under 120USD. While our motion capture system uses only 3 IMUs and the Perception Neuron ships with 17 sensors, scaling our system to use 17 sensors would still cost under 500USD.

Because we chose to pursue a wearable motion capture system, we also had to consider how to sense the user's finger movements to control a gripper. There are many data gloves on the market and in the literature that do this very effectively [23][24][25]. One solution is to use inertial measurement units on the fingers to detect their motion and bending angles, similar to our method for detecting arm motions. Another solution that is gaining popularity is various forms of flexible sensors that are stitched or glued to the fingers of a glove, which results in a more lightweight and maneuverable wearable. Flexible sensors can be resistive, capacitive, based on fiber optics, and even use single-walled carbon nanotubes [26]. In this work we have two data gloves, one novel design based on optical curvature sensors and an off-the-shelf option with capacitive sensors. The glove with optical curvature sensors is lightweight and flexible, but also durable. It is also a very low cost option, costing under 2USD for one sensor and 20USD to manufacture a glove. In contrast, the off-the-shelf capacitive option costs USD5000 for a pair of gloves.

One of the major considerations when developing a teleoperation system with body-based motion capture is how to map the user's body movements to the robot arm. This is particularly challenging when the robotic arm is not anthropomorphic. The simplest way to do this is "end-to-end" mapping, where the user's position and orientation directly control the robot's position and orien-

tation. This method is functional, but can be difficult when controlling a 7dof arm with redundant joints because we must depend on the IK algorithm to choose between multiple solutions. Though the user does not have to worry about the robot arm's individual joints in general, there are some edge cases where the user may become confused about how to move the arm from one position into another. Several papers present algorithms addressing this confusion.

One method to control redundant manipulators is to use the end-to-end method but use a single joint angle from the user to obtain a unique solution, thus allowing the user to more directly control the robot's joints [27]. Another method is to use the end-to-end method but scale the workspace of the user to match the robot workspace, thus ensuring that both are working in comfortable workspaces to avoid singularities [28]. Yet another method uses deep reinforcement learning to not only map the user's position to the robot, but also perform obstacle avoidance and singularity avoidance [29].

It is difficult to gauge how intuitive and easy-to-use these systems are, because every researcher performs different tasks and uses a different method of motion capture to gauge pose estimation. We therefore decided to try several methods ourselves as will be discussed in Chapter 2. One is a joint-to-joint method normally used with robotic hands [30], another is an end-to-end method with scaling, and the third is an end-to-end method with workspace alignment.

## **1.2.2 Haptic Feedback**

Haptic feedback is an important aspect of an effective teleoperation system [10]. There are several modes of haptic feedback, which vary in effectiveness depending on the application. Tactile feedback, or cutaneous feedback, is transmitted using vibration, temperature, or pressure close to the skin and usually indicates contact with an object [31][32][33]. Kinesthetic feedback is transmitted by applying a force to a user's body and can indicate a resistive force, such as grasping an object [34]. The literature shows that kinesthetic feedback is an effective way to transmit quality-of-grasp to a user, and enhances grasp stability which allows for more delicate manipulation [35]. There are two types of kinesthetic haptic feedback, admittance and impedance. Admittance feedback systems calculate a desired user position based on force, and communicate that force to the user

by locking them into the desired position [36]. Impedance feedback calculates the desired force based on position and applies some force or torque to the user [37].

The goal of kinesthetic feedback is to apply real forces on a user's body to simulate how real-world objects apply similar forces. There are several ways to do this, and we focus here on haptic systems that act on a user's fingers to transmit manipulation forces. One popular way to apply kinesthetic feedback is through tendon-driven mechanisms attached to the fingers. When actuated, the tendons pull on a user's fingers and open the user's hand, thus preventing their hand from closing. This is a very realistic simulation of how objects in one's hand prevent the hand from closing further than the size of the object. In the literature, there are several authors who use tendon-driven systems to provide kinesthetic haptic feedback [38][39]. In [40], for example, the authors present a data glove where the user's fingers are attached to mechanical linkages, driven by motors on the glove. The users use the glove to drive a remote-controlled car around a maze, curling their fingers to control the car's speed. If the car is about to crash, the linkages pull the user's fingers straight, applying both kinesthetic feedback and preventing the user from crashing the car. In a similar vein, the authors in [36] use shape-memory alloy brakes to stop a user's fingers from closing past a certain threshold.

One issue with tendon-driven kinesthetic haptic systems is that they tend to be bulky and require motors attached to the user's hand. This bulk increases if the system also includes cutaneous feedback, as having both types for feedback can be very useful for manipulation tasks. An overly bulky system might limit user mobility and comfort, and thus limit the kinds of tasks that can be completed with the system [32]. Additionally, the presence of tendons attached to user's fingers can be a safety hazard if safety limits are not included, and this may limit the amount of force that can be applied to the user.

More recently, researchers are looking towards more lightweight and comfortable haptic systems, such as those made of fabric [41] or with very efficient motor designs [42]. We pursue the route of fabrics and pneumatics for our haptic device, as it enables us to safely and controllably apply forces to users' fingers. Rather than using motors and linkages, we use soft robotic principles and are inspired by pneumatic artificial muscles (PAMs). PAMs are able to inflate and

apply high forces relative to their size, but are also inexpensive to manufacture, and inherently adjustable and compliant. Their soft structure makes them particularly suitable for human-robot interaction because they can apply high forces safely and comfortably. They are a compliant and lightweight replacement for motor-tendon systems that apply kinesthetic feedback to users' fingers [43][44][45].

### **1.2.3 Sensorized Robotic End Effectors**

There are many robotic grippers in literature that can read grasp forces. Many are rigid grippers that use position or velocity control to grasp known objects, combined with a custom or off-the-shelf sensor like the BioTac from SynTouch [46][47]. Other rigid grippers use force control to ensure that the grasped object is not damaged or deformed. There are also many soft grippers in the literature, which are compliant and thus require less complicated control schemes to grasp a variety of objects without damaging them. Adding force sensing to compliant grippers is quite challenging because the sensors must also be compliant, and there are several examples of using resistive, capacitive, barometric, and strain sensors that are mounted in unique ways to soft grippers [48]. Resistive and capacitive sensors are, however, prone to drift and sensitive to changes in temperature and humidity. To address this issue, our group in the Soft Robotics Lab developed a soft force sensor consisting of a 3-axis hall-effect sensor and magnet separated by a soft substrate such as silicone. As force is applied to the magnet, it moves with respect to the hall effect sensor, and the sensor outputs the magnetic field in the x, y, and z axes. We can then interpret the hall effect sensor output as force in 3 axes [1]. The sensor is novel in the space of soft force sensing, and we build on this work by integrating it into a 3D-printable anthropomorphic hand.

### **1.2.4 Teleoperation Systems**

Thus far, most of our references have dealt with motion capture and haptic systems that exist in isolation, either to teleoperate a system without haptic feedback, teleoperate a system that is not a



robotic arm, or provide haptic feedback in a virtual environment. We therefore provide a survey on current teleoperation systems that do include haptic feedback.

Several teleoperation systems that require haptic feedback rely on systems that can perform tracking and feedback at the same time, such as joysticks and desktop haptic devices. In these cases, a user controls a robotic arm in space with a joystick, and the haptic feedback is the joystick or haptic device pushing back on the user. This is particularly useful for obstacle avoidance or tasks where the user applies pressure to another object such as dentistry simulations [49][50]. They are less useful for tasks that require manipulation or picking and placing objects. Other systems use bilateral teleoperation, where the user controls a “leader” robot using their body, and the teleoperated robot follows the leader. In this case, haptic feedback can be felt through the leader robot resisting the user’s movement and thus applying torques to the user [51].

In teleoperation systems with wearable motion capture and haptic feedback, the haptics are generally cutaneous, using either pneumatics, electrotactile feedback, or vibration motors [52][53][54]. This is because these systems are more easily condensed into wearable forms.

### **1.2.5 Human-Robot Interaction Studies**

Much of our work is based on user studies and user-oriented design, so we consider the research surrounding how to perform human-robot interaction (HRI) studies and how to integrate these studies into design processes. We find that the literature is very varied and there is very little standardization in HRI, and this is mainly because HRI research is very specific to the robotic platform and the task space being studied [55]. Several frameworks have recently been proposed for conducting HRI studies, but they are specific to particular aspects of HRI, such as emotional connection [56], or spatial cognition during collaborative tasks [57]. Additionally, many of these models concern situations where users are interacting with autonomous systems [58]. We find that the field of robot teleoperation is extremely technical, so the literature we have referenced does not do an adequate job of applying HRI models or techniques to teleoperation systems or subsystems. We therefore consider the adjacent field of human-computer interaction (HCI), where the systems being studied are rather more predictable and the user studies more rigorous and consistent.

In our work, we are inspired by HCI literature and consider both quantitative and qualitative feedback [59][60][61][62][63]. We track performance metrics such as time to task completion and force application during the task, but also ask users questions related to cognitive workload (CWL), and our questions are inspired by the NASA Task Load Index which is commonly used in human-computer interaction studies [64][65]. Our results, therefore, are a combination of quantitative and qualitative, and relate to specific subsystems and the system as a whole. We are therefore able to draw deeper conclusions about what aspects of the teleoperation system are working and what needs improvement.

### **1.2.6 Methodology**

When developing a teleoperation system, which contains many parts, it is important to consider how best to test and validate the system. When considering the literature, we find that, in general, testing a full teleoperation system with several complex subsystems is fairly challenging. Many of the works we have referenced specifically explore one subsystem, such as developing a motion capture system or haptic device for a virtual reality environment, or developing a soft gripper for autonomous pick-and-place. The works we have referenced with full teleoperation systems generally test the whole system at once with a few users, and thus cannot make strong claims about which individual subsystem contributes to the success of their system, nor what needs improvement. Therefore, our goal to develop a more "usable" teleoperation system must also address what "usable" means.

Through the course of this study, our methodology is based on the idea that a teleoperation system is both a set of technologies combined into a technical system, and that a teleoperation system is an entire technology that interacts with a human user. We therefore perform several types of experiments through the study. One type is subsystem validation, where we test a particular subsystem to prove that it works in isolation. Another is subsystem exploration, where we answer questions and explore different options within a subsystem. These two types of experiments will be presented in their corresponding subsystem chapters and are generally isolated experiments, or

experiments that combine two subsystems to validate their integration. When the subsystem is particularly novel, the validation experiment is also generally novel.

The last set of tests are experiments where we add a level of unpredictability by adding a human user in the loop, and these tests are presented in Chapter 6. These tests are also divided into subsystem tests, where we gauge how well users interact with a particular subsystem where we have added novelty, and full system tests where we gauge the efficacy of the teleoperation system in general.

The experiments described above fit into the iterative process we have used to develop a better teleoperation system. We develop a system using subsystem validation and exploration experiments, then perform user tests to understand how people interact with the system. The results of the user studies, both quantitative and qualitative, drove the design and implementation of the next iteration of the system. In this way, we move closer towards a system that is truly usable based on user-oriented design processes.

## **1.3 Contributions**

Our overarching contribution is a usability study on what makes an effective teleoperation system that includes haptic feedback, and how best to test a complete teleoperation system. Over the course of this work, we have completed several iterations of this system and tested them in isolated environments without human users, and as part of full teleoperation systems. We therefore have developed a strong idea of what makes a teleoperation system successful, and how to test individual components of the system with and without human users in the loop.

While some of our subsystem components are off-the-shelf, others are novel components that we have developed during this work. We list our subsystem-level contributions below:

### **1.3.1 Haptic Feedback Mechanism**

We present a impedance-type kinesthetic haptic device that is wearable, lightweight, and full-featured. We have coined the term "haptic muscle" to describe this novel device and it was patented

in 2017 [66]. The haptic muscle applies both contact and kinesthetic forces to the user’s finger, by both squeezing the finger and applying a moment force to the knuckle, gently keeping the finger open. The haptic muscle is pneumatically-driven and sits around the finger, making it both comfortable and safe to use because there is no risk of overextending the user’s fingers.

We present two versions of the haptic muscle. The first is an extremely lightweight and easy-to-manufacture version made from heat-sealable plastic. The second is made from a fabric-silicone composite that offers more comfort, smaller resolution of detectable feedback, and a more controllable application of force. We prove these improvements using multiple tests: a unique “minimum detectable change” user study, and a force application test using a novel test bench that measures the forces applied on a finger by the haptic muscles. We also prove in teleoperation tests that the haptic feedback allows users, both novice and expert, to handle fragile or brittle objects without deforming or damaging them.

### **1.3.2 Motion Capture System**

We present an arm motion capture system based on inexpensive wearable sensors that provides real-time measurements of user motions. Similar wearable systems are based on very expensive sensors and require complex algorithms to output real-time positions. Our system is lightweight, easy to set up, and suitable for a variety of body types due to the adjustable nature of the wearable components. Additionally, because it is based on inertial measurement units that track global orientations, the system is entirely portable and allows the user to move freely during teleoperation. It requires only a few minutes of calibration to attune itself to an individual user.

We also present several schemes that use the angles from the inertial measurement units to control the robotic arm. Most mapping systems are based on end-effector positioning alone, and use tracking systems such as large motion capture studios or virtual reality trackers on the user’s head and arm. Because our system is based on wearable IMUs, our mapping does not deal with occlusion issues, where the sensors cannot track the user. With our various mapping schemes we try to work towards maximum intuition and workspace usability. We define intuition as the ability of the user to move the robotic arm into a desired position quickly and efficiently. Our first scheme

is a direct joint-to-joint mapping which is a one-to-one mapping between the user and robot joints. This is very intuitive to use because the robot arm behaves exactly like a human arm. The other scheme is an end-effector workspace mapping, where we perform a mapping between the user's and robot's workspaces in cylindrical coordinates. This method maximizes both intuition and workspace range because there is a simpler translation from the human to robot motions, but the scheme is designed to use the entirety of the robot's workspace.

Along with motion capture for the arm, we present a novel method of capturing user's finger motions during teleoperation. The proposed method uses optical curvature sensors attached to a soft glove. The sensors consist of an infrared LED and infrared receiver connected by a black tube that blocks other light. When the user's finger is straight, the receiver outputs a high signal. As the user's finger bends, the receiver's output is lower and lower, and is directly proportional to the degree of finger bending. The result is a low-cost, low-latency, lightweight, and inexpensive way to accurately detect finger bending during teleoperation.

### **1.3.3 Robotic End Effector**

We present a robotic end-effector that uses magnets and hall-effect sensors to sense contact and grasp forces during teleoperation. The end-effector is anthropomorphic, tendon driven, and 3D-printed from soft materials, allowing it to perform a wide range of grasps and potentially allow users to perform more complex teleoperation tasks. The force sensing integrates cleanly into the soft gripper and does not suffer from drift or changes in temperature and humidity.

# Chapter 2

## System Overview

### 2.1 Integrated System

Our proposed teleoperation system contains several distinct hardware components: a robotic arm and gripper, a wearable motion capture system consisting of a data glove and inertial measurement units (IMUs), soft force sensors on the gripper, and haptic feedback devices. The components are integrated as shown in Fig 2.1 and are controlled by a central computer running ROS.

The data flow is as follows, and is outlined in Fig 2.2.

The inertial measurement units sit on the user's upper arm, forearm, and hand, and output the absolute angles of the user's shoulder, elbow, and wrist. This data is transmitted to the central computer for processing. We use these angles to calculate the user's current position in joint space or cartesian space, then map this position to the robot's joint or cartesian space. The mapping outputs a set of desired robot joint angles, and we use a simple PID controller to control the robot joints.

The soft glove outputs a set of signals corresponding to the bend angle of the user's thumb, index, middle, and ring fingers. This data is also transmitted to the central computer for processing, where we map the user's current finger positions to a desired gripper position. We use another PID controller to send the gripper joints to the desired state.

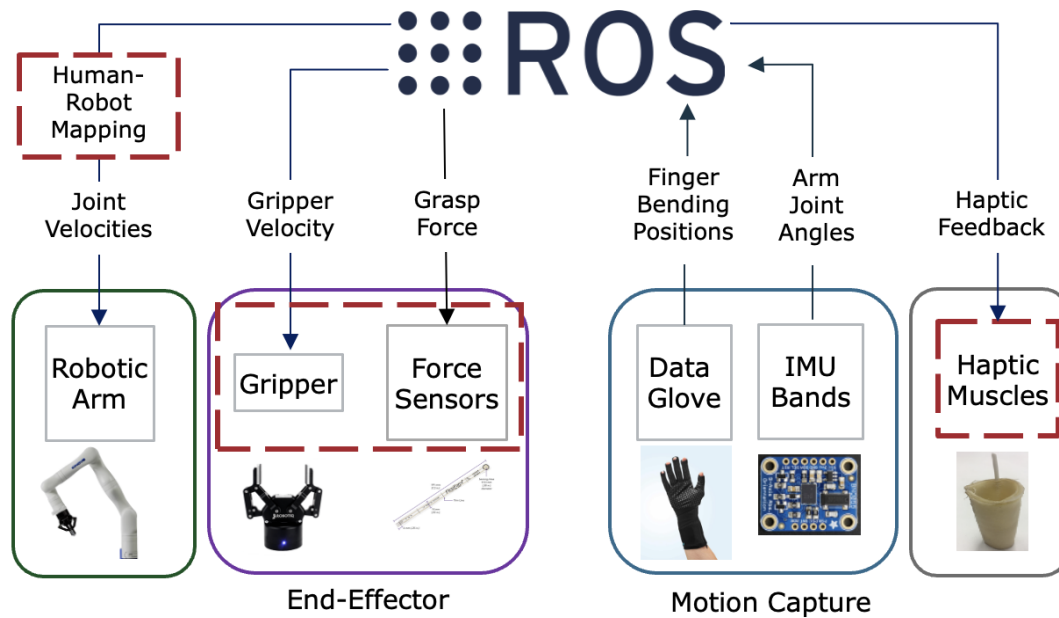


**Figure 2.1:** A system diagram showing how the main subsystems interact. The system uses ROS as its software communication hub, and data is passed as topics from subsystem to subsystem. Our areas of novel contribution are bordered in red.

The two sections above result in a remote robot teleoperation system where the robot shadows the user’s motions in an intuitive way.

During teleoperation, the user will use the robot to manipulate objects in the robot’s surroundings. During manipulation, we read grasp forces, that is, how hard the user is squeezing an object, through force sensors on the robotic gripper. These sensors output a force in pounds which we map to a desired haptic feedback output. Therefore the harder the user squeezes the object, the more haptic feedback they will feel. The user can use this sensation to squeeze the object more or less hard, depending on whether they want to grasp the object firmly or avoid damaging it.

The motion capture and haptic feedback systems offer a closed-loop control system by which a user can teleoperate a robotic arm and adjust their movements to handle fragile objects without deforming or damaging them.

## 2.2 Research Phases Overview

We performed our research and development in four distinct phases, each of which corresponds to a set of user tests, results, and design decisions. The rest of this report is divided by technical subsection, but here we present a timeline of how our final system was developed and the design choices we made following user tests and interviews.

The first phase of research was an initial system that included a simulated robotic arm and the first iteration of our data glove and haptic feedback wearable. The data glove included optical curvature sensors that sat on top of the fingers, and plastic haptic muscles that sat on top of the curvature sensors. We also used inertial measurement units strapped to the user’s arm to capture the user’s arm motions. For our first iteration, we oriented the robot arm on its side and directly mapped human joints to robot joints. Users wore the IMUs and glove and controlled a simulated Kinova Jaco arm and Robotiq 3-fingered gripper. Users were able to pick and place simulated blocks and feel haptic feedback when they grasped a block. This work was published in [67].

The second phase of development used the same motion capture system (data glove and IMUs), but used a physical Kinova Jaco arm and a custom 5-fingered anthropomorphic gripper with a wrist. Because the robot arm was still oriented on its side, we required a separate wrist to accurately orient the gripper for grasping tasks. The anthropomorphic hand also had a first iteration of soft force sensing integrated into its fingertips.

The third phase of research again used the same motion capture system (data glove and IMUs) but we oriented the arm vertically and thus changed the human-to-robot mapping. In the first two phases, we mapped user’s joints directly to the robot joints, but in this phase we used a cartesian mapping scheme for position and orientation control of the end effector. We also refactored the gripper to better embed the force sensors in the fingertips. This work was published in [68] and the work on the gripper was published in [69].

In the fourth phase of research, we redesigned the haptic muscles out of a fabric-silicone hybrid rather than from the heat-sealable plastic we began with. In this phase we also used a different robotic arm (Kinova gen3) and an off-the-shelf gripper (Robotiq 2F-85), and outfitted the gripper



with new force sensors based on force sensitive resistors (FSRs). A part of this work was published in [70]. We also begin to modify how we perform human-to-robot mapping to be more suitable for novice users

The remainder of this dissertation is divided into sections based on the technical subsystems of the full teleoperation section. Each technical section will discuss the different iterations of each subsystem. In Chapter 6, we will revisit these phases and discuss more about how the results from each user test led to the design of the next iteration.

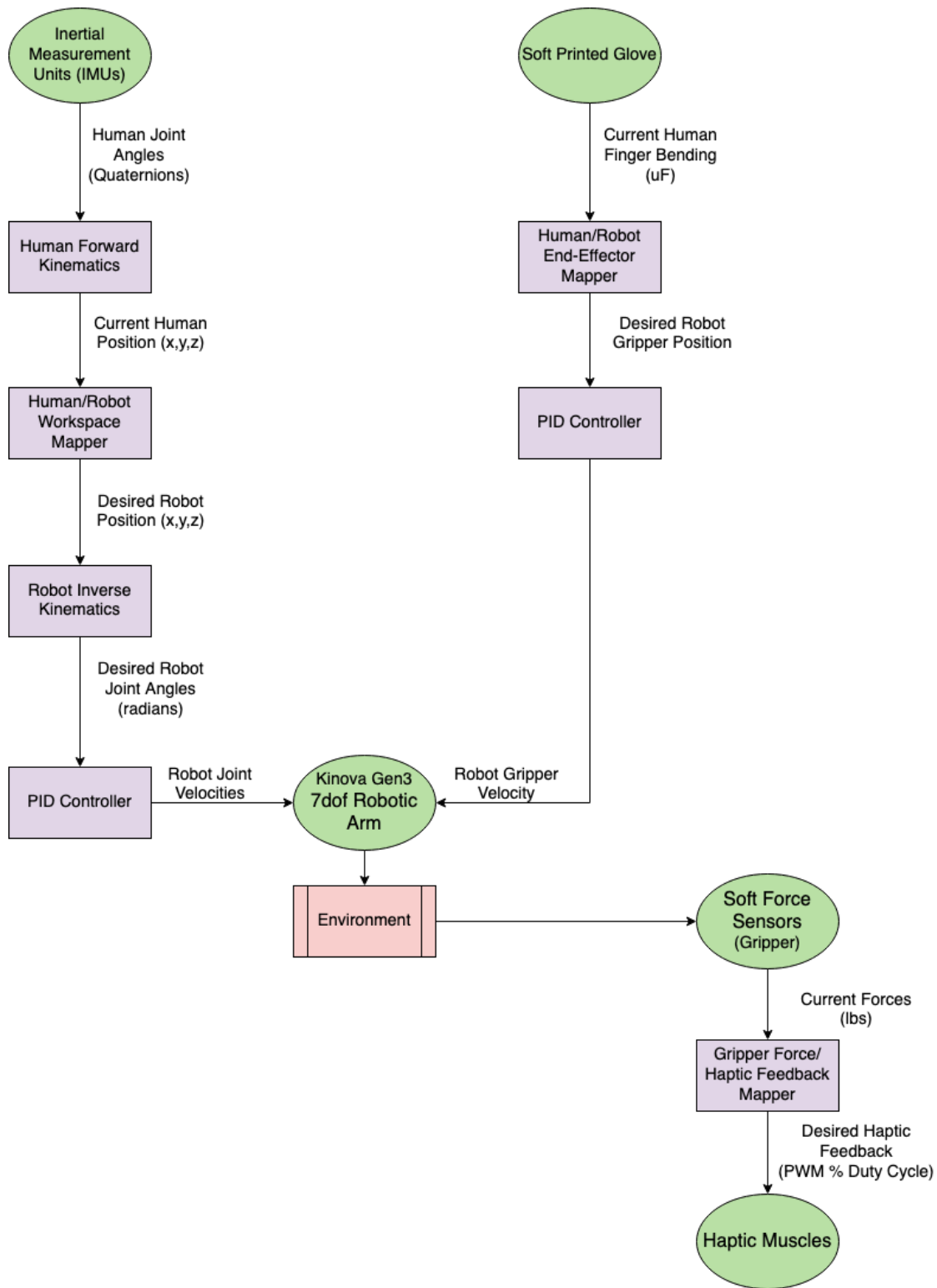


**Figure 2.2:** This software flow shows how data flows from the user to the robotic arm and gripper, and how data from the robotic gripper flows back to the user.

# Chapter 3

## Motion Capture System and User Mapping

### 3.1 Motion Capture Hardware

The wearable motion capture system consists of a data glove and a set of inertial measurement unit (IMU) bands. The glove collects finger bending data while the IMU bands output absolute angles of the shoulder, elbow, and wrist.

#### 3.1.1 Data Glove

The data glove is a soft wearable with embedded sensors that detect finger bending. We used two different gloves in our research, one with custom curvature sensors and one off-the-shelf data glove. The custom curvature sensors are a low-cost option that are nonetheless durable and accurate. The off-the-shelf data glove is lightweight and durable, albeit very costly. We discuss both gloves and the reasoning behind the switch.

#### Optical Curvature Sensors

Our first glove uses optical curvature sensors mounted to the fingers of the haptic glove. Each sensor contains an infrared LED and receiver connected by a flexible black tube to block external light (Fig 3.1). When the user's finger is straightened, the LED and receiver are directly facing each other and the analog signal from the receiver is high. As the user curls their finger, the signal

decreases, as shown in Figure 3.2. Because there is no resistive component to this sensor, the readings do not suffer from drift and other inconsistencies.

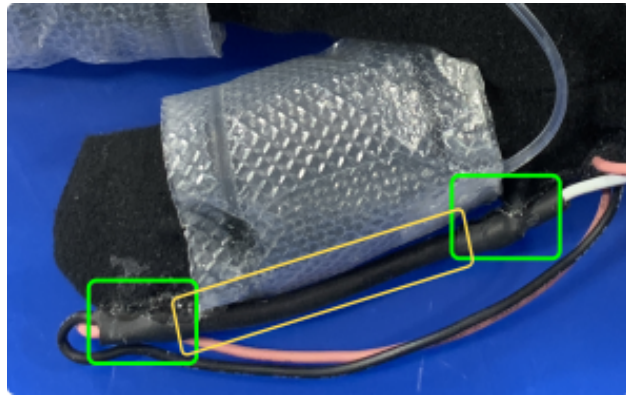


**Figure 3.1:** An optical curvature sensor sitting on the user’s thumb. The infrared emitter and receiver are outlined in green and the flexible black tube in yellow. The curvature sensor sits atop the haptic device (clear plastic).

The curvature sensors sit on top of the haptic muscle, with the infrared LED and receiver sewn directly into the glove. The signals from the receiver are amplified and filtered using a standard operational amplifier circuit, then sent to the analog pin of an Arduino.

We published a version of this glove in [67], where the glove was 3D-printed out of rigid materials and the optical sensors were mounted to the glove between two printed plates that were screwed together. Inspired by off-the-shelf products, we decided to switch to a fabric glove and mount the sensors using fabric glue and stitching. The result was a more lightweight glove (weighing less than 250g), that was also more comfortable to wear.

The optical sensor data glove was a durable and simple option that worked very well for several sets of user tests, as described in Chapter 6. However, we encountered an integration issue when we redesigned the haptic muscle to be manufactured from fabric and silicone rather than plastic, which we discuss further in Chapter 4. When the haptic muscle was plastic, it did not inflate radially enough to bend the optical sensor. However, the fabric-silicone haptic muscles inflate much more and we found that they interfered with the optical sensors by bending the black tube enough to simulate user bending even when the user wasn’t moving. During our pilot teleoperation tests with the fabric haptic muscles and the optical curvature sensors, users found it impossible to grasp an object. When they closed their hand to close the gripper around the object, the object

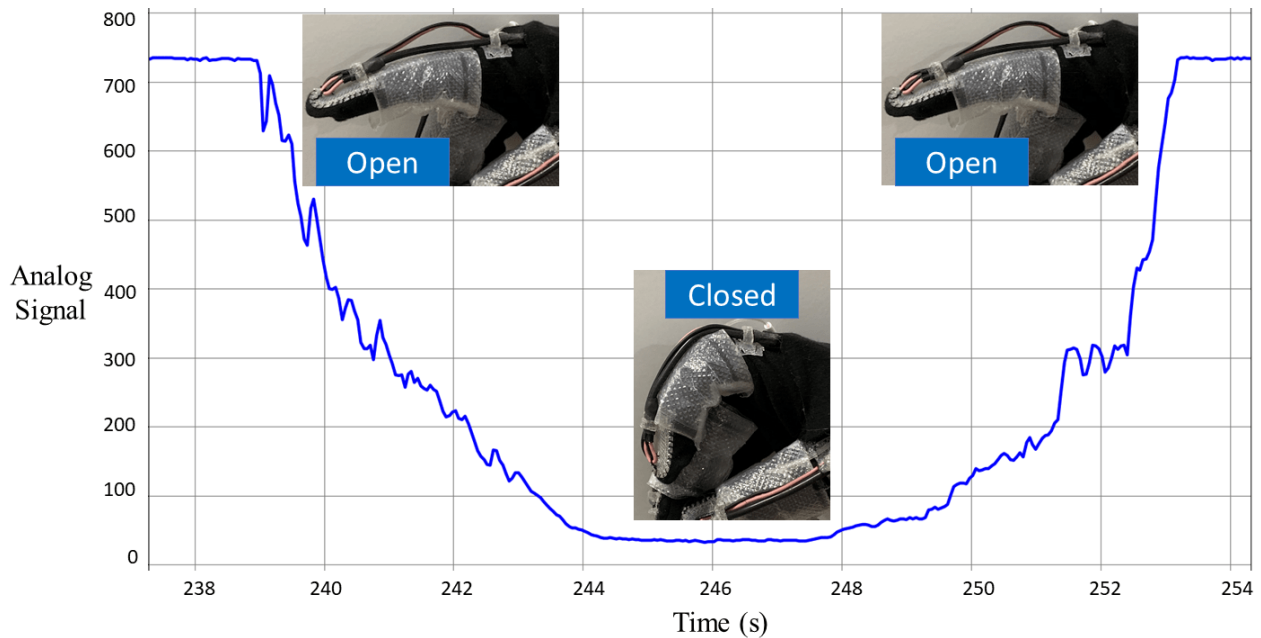


**Figure 3.2:** This plot shows an example of the optical sensor outputting curvature signals when worn by a user. When the user’s finger is straight, light from the LED reaches the receiver, resulting in a high signal. As the user gradually curves their fingers, the light is blocked, resulting in a low signal. This provides an accurate reading of the user’s finger curvature. We find that the signal is consistent when the finger is fully open or closed, and gradually decreases as the user’s finger bends.

triggering the force sensors and haptic feedback. The haptic muscles inflated and bent the sensor as if the user was straightening their hand, and the gripper would open and drop the object.

We therefore required a new data glove design that would not be affected by the haptic devices.

### Capacitive Curvature Sensor

The second glove is an off-the-shelf data glove (StretchSense Supersplay) that uses capacitive curvature sensors attached to the fabric of each finger in the glove.

The capacitive sensors in the StretchSense glove are based on a layered design, where a signal electrode sandwiched between two ground electrodes which are separated by silicone dielectric insulators, forming a flexible parallel plate capacitor as shown in Fig 3.3. When the sensor is stretched, the sensor increases in surface area and decreases in thickness, which increases its capacitance. The sensor is immune to compression, so it sits under the haptic muscle and we observe very little to no crosstalk between the two.



**Figure 3.3:** The StretchSense SuperSplay is an off-the-shelf data glove with capacitive curvature sensing. The curvature sensors are flexible layers that change capacitance when stretched.

The glove contains amplification and filtering circuitry and outputs the capacitance of each of the curvature sensors, two for each finger. For our purposes, we use the sensor on the first knuckle of the thumb, pointer, and middle fingers.

### Gripper Control

We control the gripper using the signals from the data glove by performing a linear mapping between the user and gripper’s open and closed states. We begin each teleoperation session with a calibration routine to record the data glove output when the user’s hand is closed and open. This is because every user outputs a different signal based on their hand size. We can therefore map between the user and the gripper using the following equation, where *map* is a linear mapping function. A diagram showing the mapping concept is shown in Fig 5.1.

$$gripper_{des} = map(user_{current}, [user_{open}, user_{closed}], [gripper_{open}, gripper_{closed}])$$

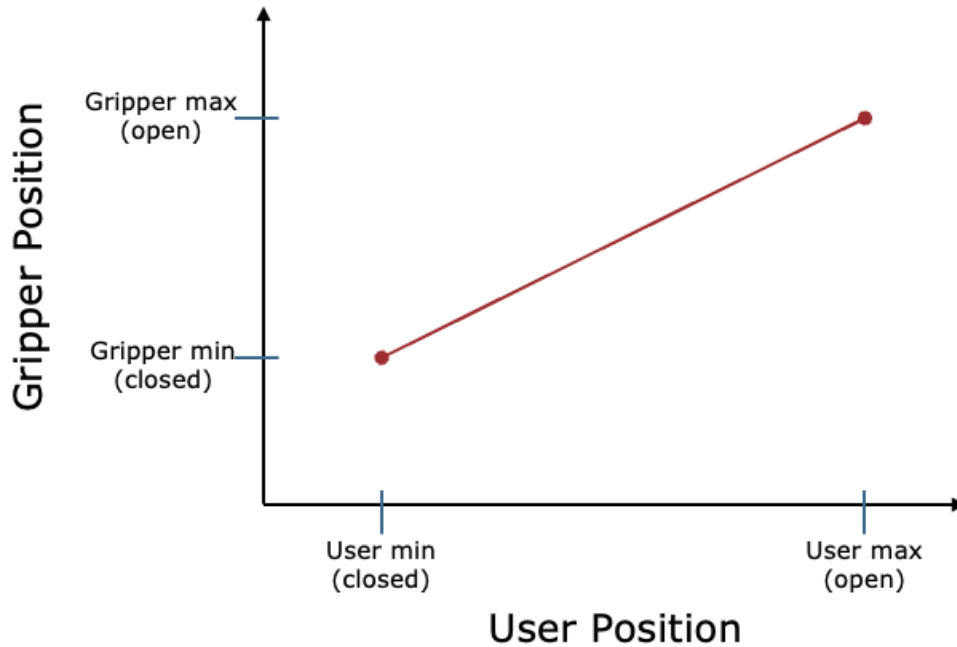


**Figure 3.4:** We use a linear mapping to convert the user’s current position to a desired position for the robotic gripper. We get the user’s minimum and maximum values through a calibration routine at the beginning of each teleoperation test.

### 3.1.2 IMU Bands

We use three inertial measurement units (IMUs) to read the absolute angles of the user’s arm. The IMUs are off-the-shelf boards from Adafruit (BNO055) based on a Bosch chip that contains an accelerometer, magnetometer, and gyroscope. The board outputs absolute angles in quaternions and Euler angles. Each board uses the I2C protocol to connect to a microcontroller. However, the boards only have two hard-coded I2C addresses to choose from, which means only two can be daisy chained and connected to a microcontroller at any one time. Because we need three IMUs, we also add an I2C multiplexer (TCA9548A) that allows us to connect up to 8 IMUs to the microcontroller at once. All three IMUs connect to the multiplexer, which in turn connects to the microcontroller.

We place the IMUs on the user’s upper arm, forearm, and hand as shown in Fig 3.5. This allows us to read rotations from the user’s shoulder, elbow, and wrist. To ensure that the IMUs sit securely on the user, we 3D-printed wearable IMU mounts. We attach the IMUs and relevant connections to a custom PCB, which press-fits into the mount. The mount also include a hole for a 1/2” wide

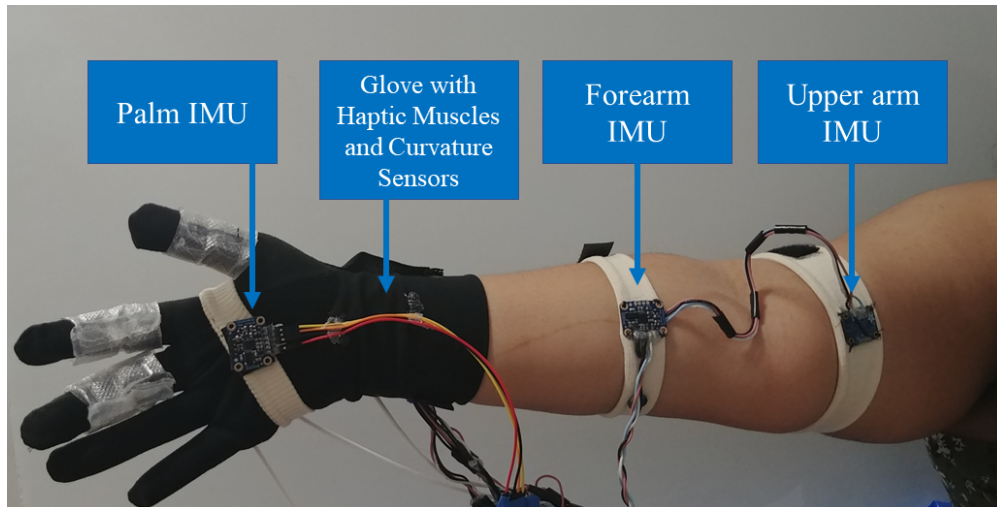


**Figure 3.5:** The user wears 3 IMUs, on the upper arm, forearm, and wrist, to capture their arm motions. The IMUs are connected to each other and the microcontroller using I2C.

elastic band. The elastic band includes a velcro strip that allows it to loop around a user's arm. Each IMU assembly is connected to the next, and to the backpack, by a ribbon cable. This setup is lightweight and comfortable, especially because it is adjustable for each user.

## 3.2 User to Robot Mapping Schemes

### 3.2.1 Joint to Joint Mapping Scheme

One way to achieve intuitive control is to map joints in the Jaco arm directly to corresponding joints that provide similar motions in the human arm. To maximize the intuitiveness of this mapping, the Jaco arm is mounted sideways, so the directions of joint rotations match those of the human body as shown in Fig 3.6. Note that this mapping scheme was implemented on the Kinova Jaco robotic arm.

The first two joints of the Jaco arm map directly to shoulder rotations. The first is based on shoulder flexion and extension, which moves the arm vertically towards and away from a horizontal workspace. The second is based on shoulder abduction and adduction, which pans the entire arm. Both of these positions are directly provided by the IMU mounted on the user's upper arm. The third joint is based on elbow abduction and adduction, which pans the distal half of the arm. This



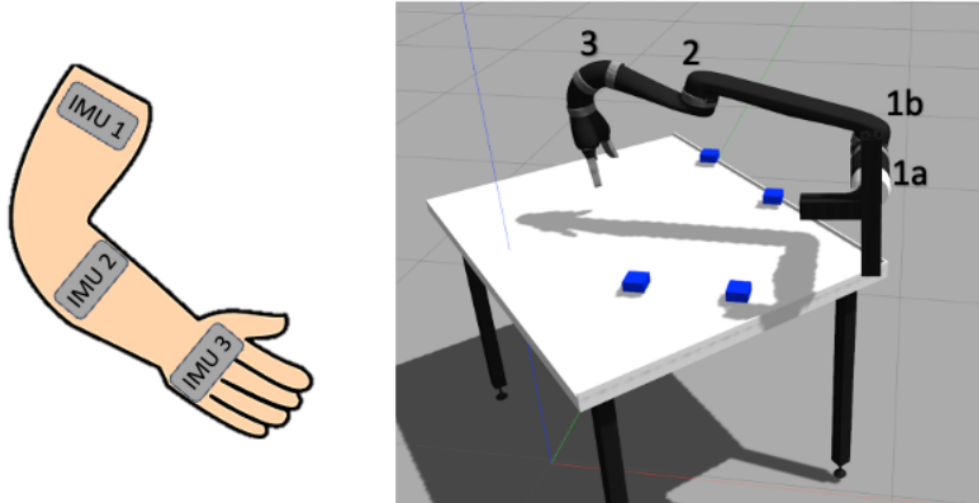


**Figure 3.6:** The human arm and robot are mapped joint-to-joint. The user’s shoulder controls the first two joints, the elbow controls the third, and the wrist controls one of the robot’s wrist joints.

position involves the difference in angle between the upper arm and forearm IMUs, so that panning the entire arm does not result in panning the elbow as well. The fourth and fifth (wrist) joints of the Jaco arm are fixed. The sixth joint is the end effector and is based on wrist rotation.

Using the mapping system above, the IMU data is converted to a set of desired joint angles for the Jaco arm that match the user’s current arm configuration. Under the default position control, Jaco arm tracks position references automatically following a trapezoidal motion profile. To achieve smooth motions, the desired joint positions are sent to a velocity controller that calculates a velocity for each joint based on its current and desired positions via a proportional-derivative (PD) controller. We tuned appropriate PD coefficients that do not overextend the capabilities of the arm through initial experimental studies with the system. A plot of a user’s elbow joint readings from the IMU as well as the movement of the robot arm’s elbow joint during teleoperation is shown in Fig 3.7.

Mapping the user joints directly to the robot joints was very intuitive, and many users told us they were easily able to understand how to move the robot arm around. There were, however, several issues with this setup. Firstly, the robot arm we were using (Kinova Jaco2) could not operate very well turned on its side, because of torque limitations on the lower joints. When

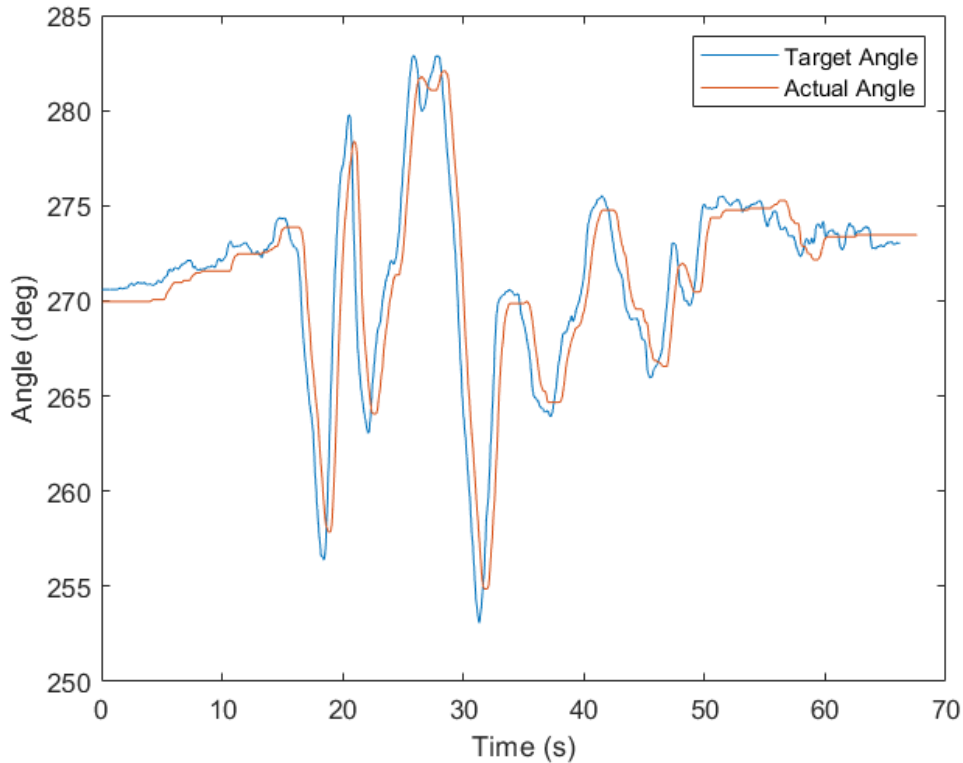


**Figure 3.7:** We asked a user to wear the motion capture system and rotate their elbow parallel to the ground, which teleoperates the elbow joint of the robotic arm. We capture the user data as well as the current joint position output by the robot arm, and plot both here. We find that joint-to-joint mapping is a low-latency form of control because there are no complex kinematics to calculate.

we teleoperated the arm for too long or picked up a heavier object, like a water bottle, the arm overtorqued and jerked around dangerously.

Additionally, while it was very intuitive for users to control the first two joints of the arm, the joint-to-joint scheme limited the robot arm’s range of motion, because all the movements were radial. Users reported during testing that they expected the robot end-effector to move in lines, and the radial motion was difficult to adapt to. The results from these user tests, shown in Phase 2 of Chapter 6, confirm both the mechanical issues with the joint-to-joint scheme, and that users had difficulty aligning the robot arm to pick and place simple objects like a cube or cylinder. For usability purposes, we decided to flip the arm the right way up and work towards a cartesian mapping scheme. We also acquired a Kinova gen3 robotic arm, so the rest of these mapping schemes are implemented on the Gen3.

We therefore consulted the literature on other more common ways to map user motions to robot motions, and we were inspired by systems that use virtual reality headsets for robot arm teleoperation.

### 3.2.2 Cartesian Mapping Scheme

One very common way of translating human arm motions to robot arm motions in the literature is "position-position" control, where we calculate the position of the human arm using forward kinematics calculations, then send the robot arm to the same position using its inverse kinematics. We first cover how we calculate the user's position using the forward kinematics of a human arm.

#### Forward Kinematics of User

The forward kinematics of the user's arm are calculated using the three link lengths (upper arm, forearm, and hand) and the angles given from the IMUs on each joint. For these calculations, we capture the angles from the IMUs in quaternions rather than euler angles. This is because when the IMUs output Euler angles, there are times when two different angles can define the same position and we experience jumping in the angle outputs, especially in pitch and yaw. Reading the angles in quaternions solves this issue, and we immediately convert the angles to euler angles for the calculations.

The forward kinematic calculations are as follows.

The three link lengths are given by  $L_{upper}$ ,  $L_{fore}$ , and  $L_{hand}$ .

The IMUs give us 3 rotation matrices,  $R_{shoulder}$ ,  $R_{elbow}$ , and  $R_{wrist}$ , which are formulated by multiplying the corresponding X, Y, and Z rotation matrices given by the IMU. For example, if the IMU on the upper arm output angles [a, b, c], then

$$\mathbf{R}_{shoulder} = \begin{pmatrix} 1 & 0 & 0 \\ 0 & \cos(a) & \sin(a) \\ 0 & \sin(a) & \cos(a) \end{pmatrix} \times \begin{pmatrix} \cos(b) & 0 & \sin(b) \\ 0 & 1 & 0 \\ -\sin(b) & 0 & \cos(b) \end{pmatrix} \times \begin{pmatrix} \cos(c) & -\sin(c) & 0 \\ \sin(c) & \cos(c) & 0 \\ 0 & 0 & 1 \end{pmatrix} \quad (3.1)$$

The rotation matrices then give us a set of transformation matrices where we multiply the rotation matrix by a matrix representing the corresponding link length. So given  $R_{shoulder}$  above, we get

$$T_{shoulder} = R_{shoulder} \times \begin{pmatrix} 0 \\ 0 \\ -L_{upper} \end{pmatrix} \quad (3.2)$$

$$T_{elbow} = R_{elbow} \times \begin{pmatrix} 0 \\ 0 \\ -L_{fore} \end{pmatrix} \quad (3.3)$$

$$T_{wrist} = R_{wrist} \times \begin{pmatrix} 0 \\ 0 \\ -L_{hand} \end{pmatrix} \quad (3.4)$$

Using the above method to find  $T_{shoulder}$ ,  $T_{elbow}$ , and  $T_{wrist}$ , we can calculate the position of the user's hand. Note that the first point is a simple translation from the user's sternum to their shoulder, so the point is  $[SO_x, SO_y, SO_z]$  where  $SO$  is the offset between the shoulder and the user's sternum. We found this a more convenient and intuitive mapping, where the robot base corresponds to the user's core. Therefore, the following point gives us the position of the user's hand relative to their core.

$$p_0 = [SO_x, SO_y, SO_z] \quad (3.5)$$

$$p_1 = p_0 + R_{shoulder} * T_{shoulder} \quad (3.6)$$

$$p_2 = p_1 + R_{elbow} * T_{elbow} \quad (3.7)$$

$$p_3 = p_2 + R_{wrist} * T_{wrist} \quad (3.8)$$

We calculate the orientation of the user's hand in much the same way, by multiplying the rotation matrices. We thus have the following:

$$r_3 = R_{origin} * R_{shoulder} * R_{elbow} * R_{wrist} \quad (3.9)$$

Where  $R_{origin}$  is the orientation of the user's core and is thus the identity matrix.

While we directly use the calculated orientation as the goal pose for the robotic arm, we cannot directly use the calculated position because the user and robot's workspaces are very different. We therefore have to map the point  $p_3$  with a point in the robot arm's workspace in some intuitive and controllable way.

### **Cartesian Mapping with Workspace Scaling**

In the literature, the most popular way to map the user's workspace into the robot workspace is by simple scaling in Cartesian space. We first calculate the human and robot's reaches respectively. The robot reach is actually further than the edge of the table it is mounted to, so we set its reach value to the distance between the table's edge and the robot base. The user's reach depends on their arm length, and we estimated these values by measuring several peoples' arm lengths and averaging the values. We can thus calculate a scaling factor as the ratio between the two reaches. During teleoperation, we then multiply the user's final position by the scaling factor to calculate the desired position for the robot. We thus have:

$$RobotPosition = p_3 * RobotReach / UserReach \quad (3.10)$$

Fig 3.8 shows a plot showing the user's position, the scaled position, and the robot end-effector's final position over time in the x-axis.

We also add boundaries in cartesian space to ensure that the robot arm does not extend itself or hit the table. This method ensures that the robot arm stays in a reasonable workspace, and theoretically ensures that the user is in a comfortable workspace as well.

When we began performing preliminary user tests with this mapping method, we found several puzzling issues. For some users, especially those with teleoperation or virtual-reality gaming

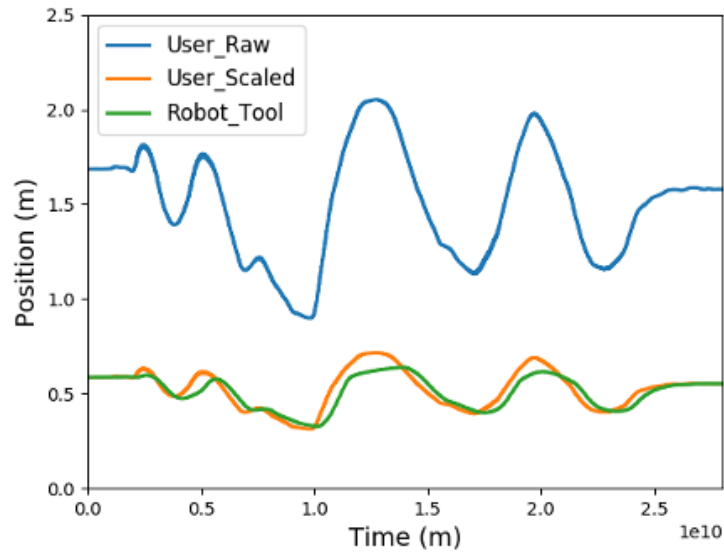


**Figure 3.8:** This is a plot showing the results of workspace mapping with scaling. We capture user data and use a scaling constant to map the user position into the robot workspace. The plot shows an example of the user moving in the x-axis and the resulting motion of the robot arm. We show the user’s raw position, the scaled position, and the robot end-effector’s final position.

experience, the system worked very well, and they were able to perform fairly complex tasks. One user was able to use a plastic knife to cut a banana. Other users who attempted to use the system could barely pick and place one object. We observed that these users could not aim the end-effector effectively, as if they were unsure what movements they had to make to move the arm in the direction they wanted. We also observed that these users seemed to consistently be working in uncomfortable workspaces. It was very difficult to gauge what the problem was, but some users reported they were more comfortable when we manually changed the scaling factor in 3.10 to suit them better.

We realized during these tests that in order to make this teleoperation system work for all users, we had to customize the mapping scheme more. Every user moves differently and has a different working range due to flexibility. We also realized that there was something very intuitive about the joint-to-joint mapping scheme we attempted at first. We therefore tried to combine the two methods into a cartesian-based mapping scheme that would guarantee user comfort while ensuring the robot is using its entire workspace.

## Cartesian Mapping with Workspace Alignment

We present a novel way of mapping user to robot movements using workspace alignment. This method ensures that both the user and the robot are in comfortable workspaces, because we ask the user to define their own workspace before teleoperation. We then use their workspace and align it to the robot workspace in polar coordinates. That is, all our alignment calculations revolve around radii and angles about the user and robot origins.

Before teleoperation, we run a calibration routine where we ask the user to make certain defining poses. The poses are as follows, and give us the following information:

1. Hand by the user's side, indicating how close they want to be to their own body. This gives us  $R_{user-min}$ .
2. Hand stretched out in front, indicating the user's reach. This gives us  $R_{user-max}$ .
3. Hand stretched out to the right side, indicating how far to the right the user can go. This gives us  $\theta_{user-min}$ .
4. Hand stretched out to the left side, indicating how far to the left the user can go. This gives us  $\theta_{user-max}$ .
5. Hand stretched out downwards, indicating the lowest a user wants to reach. This gives us  $height_{user-min}$ .
6. Hand stretched out upwards, indicating the highest a user wants to reach. This gives us  $height_{user-max}$ .

We therefore have two ranges, radius and angle, that define the user's preferred workspace. We can find a similar range that defines the robot workspace by defining similar points of interest. Then, just as we did in the joint-to-joint mapping, we can align these ranges by linearly mapping the user radius to the robot radius, and the user angles to the robot angles. Given the user's position  $p_3 = [x_{user}, y_{user}, z_{user}]$ , the calculations are as follows:

$$R_{user} = \text{sqr}t(x_{user}^2 + y_{user}^2) \quad (3.11)$$

$$\theta_{user} = \arctan(y_{user}/x_{user}) \quad (3.12)$$

$$R_{robot} = \text{map}(R_{user}, [R_{user-min}, R_{user-max}], [R_{robot-min}, R_{robot-max}]) \quad (3.13)$$

$$\theta_{robot} = \text{map}(\theta_{user}, [\theta_{user-min}, \theta_{user-max}], [\theta_{robot-min}, \theta_{robot-max}]) \quad (3.14)$$

The last two equations are a linear mapping of the user's polar position from the user to the robot range. Using these, we can calculate  $x_{robot}$  and  $y_{robot}$  by undoing the polar mapping.

$$x_{robot} = R_{robot} * \cos(\theta_{robot}) \quad y_{robot} = R_{robot} * \sin(\theta_{robot}) \quad (3.15)$$

We calculate the height using a similar linear mapping in the z-axis.

$$z_{robot} = \text{map}(z_{user}, [height_{user-min}, height_{user-max}], [height_{robot-min}, height_{robot-max}]) \quad (3.16)$$

We therefore have a very clear mapping between the user and robot's workspaces, that ensures that the user is comfortable and the robot is using its full range of motion. As above, we validate this scheme by showing the user data and the corresponding robot motion in Fig. 3.9.

### Workspace Alignment Validation

We validate the workspace alignment method by showing how the two methods (scaling and alignment) make use of the robot's workspace. We recorded a simple movement from a user, drawing a circle, then used those movements to teleoperate the robotic arm using both methods. A plot of the user's motion and the robot end-effector's corresponding motions is shown in Fig 3.10.

We can see that the workspace of the robot is much larger using the alignment method, because the user is guaranteed to be able to reach them while in their own workspace. This is not guaranteed using the scaling method, especially because the scaling was based on average arm types and assumptions about user's movement preferences.

We did a latency validation test to ensure that the robot was following the user relatively closely. A plot of user and robot moving in the x-axis is shown in Fig 3.11, and we calculate the latency to



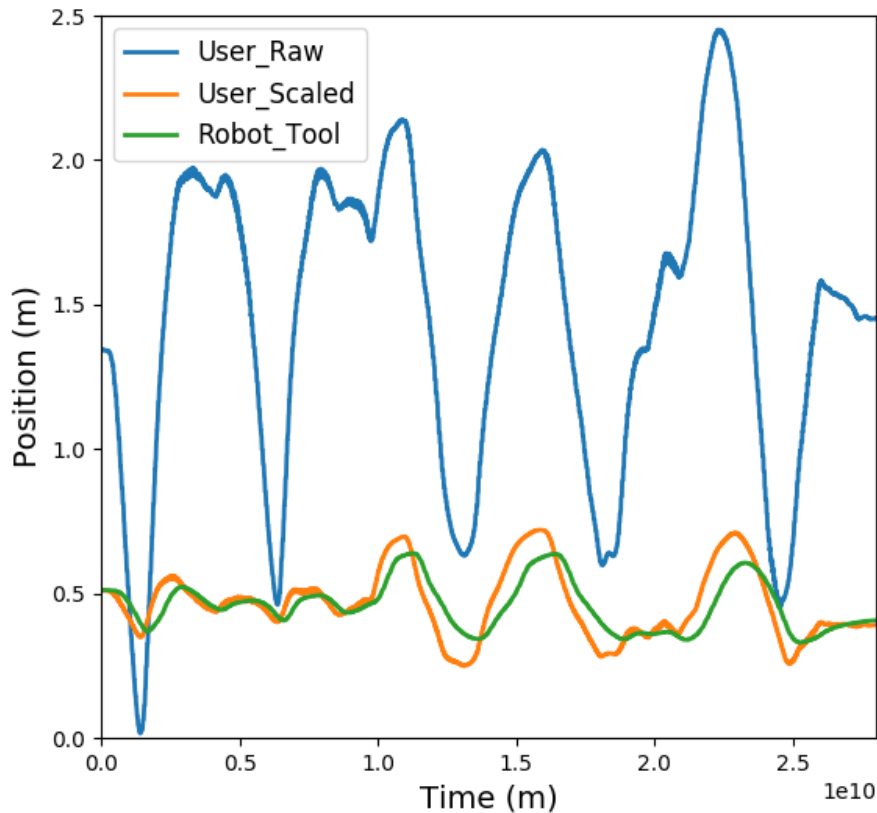


**Figure 3.9:** This plot shows the results of workspace mapping using the proposed alignment technique. We capture user data and use the user’s calibration values to align the user and robot workspaces. The plot shows an example of the user moving in the x-axis and the resulting motion of the robot arm. We show the user’s raw position, the scaled position, and the robot end-effector’s final position.

be an average of 250ms. Occasionally, if the user moves too fast, the robot arm’s kinematics cannot match the user’s speed. However, we find that if the user moves deliberately, the arm follows as expected. This is especially true during pick and place as the user moves deliberately towards the object they are picking.

We also confirm the usability of this method in a number of user tests. In preliminary user tests, we asked 3 users to pick and place one object from one precise target to another, using the scaling method, then the alignment method. The scaling method was successful to only one user, who picked and placed the object in an average of 45 seconds. The other two users could not

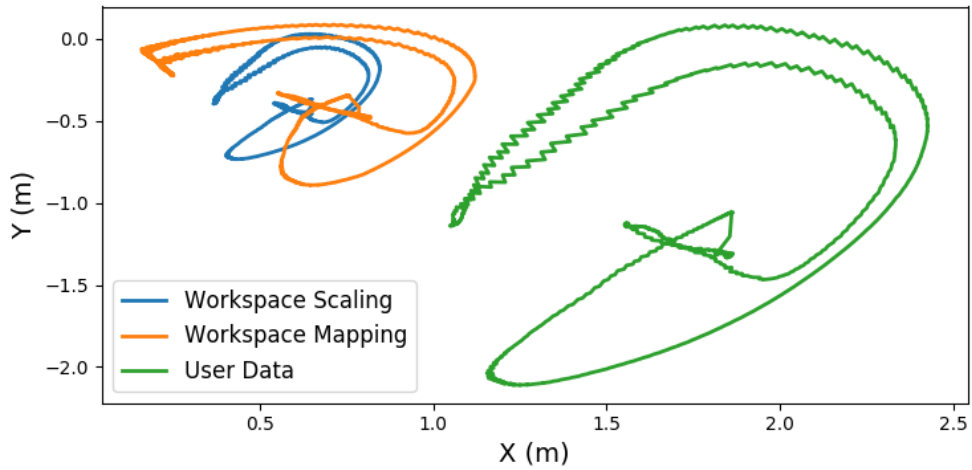


**Figure 3.10:** We asked one user to wear the motion capture system and draw a circle in the air with their hand. We then use both the scaling and alignment mapping methods to calculate the robot's desired position from the same movement. This plot shows the user movement, the desired robot position using the workspace scaling method, and the desired robot position using the workspace alignment method. The alignment method produced a semi-circle that is wider than the scaling method, showing how the user is able to reach a larger workspace using the alignment method.

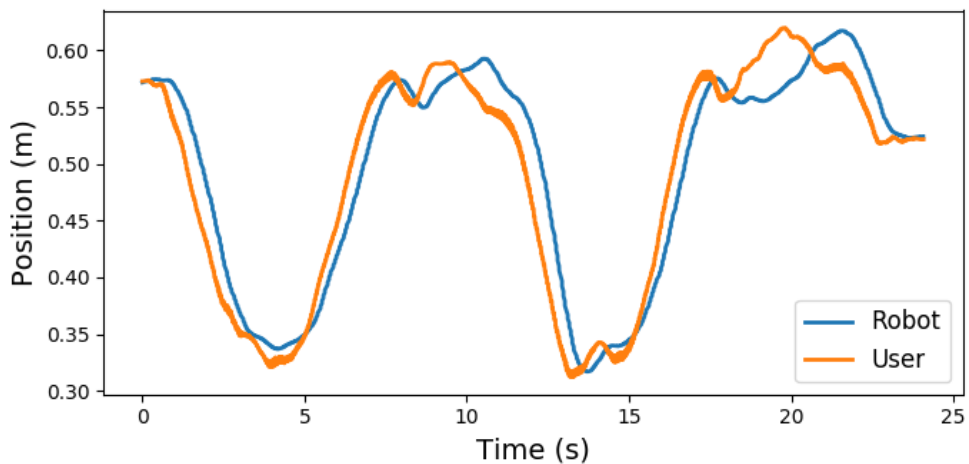


**Figure 3.11:** We asked a user to wear the motion capture system and teleoperate the robot arm in the x-axis, moving left and right several times. We captured their movement and the robot's end-effector position over time to show the latency between the two. We show the robot and user movement in the x-axis and calculate an average latency of 250ms.

accomplish the task without becoming frustrated and tired. The alignment method was successful to all users, who picked and placed the object in an average of 20 seconds. We therefore decided to use this method for our final phase of user testing, as discussed in chapter 6.

# Chapter 4

## Haptic Muscles

### 4.1 Haptic Muscle Design and Control

The haptic muscle is a toroidal structure with two sealed layers and an air pocket for inflation. The structure fits around the user's finger, and when uninflated is easy to bend. When pressurized, as shown in Fig 4.2, the structure inflates around the user's finger and applies a moment force to the knuckle, gently opening the finger. This simulates how a real object in the user's hand would prevent their fingers from closing, thus providing a realistic feeling of grasping something. Because the actuator surrounds the finger, this also provides a contact force on the finger's palmar side.

To control the inflation of the haptic muscles, we use pneumatic solenoid valves (SMC-SAG-070). The valves are 3/2 valves, which means they have three ports and two states. The three ports are Source, Output, and Vent (to atmosphere) as shown in Fig 4.1. The two states are when the Output is connected to the Source and when the Output is connected to the Vent. The Output is by default connected to the Vent, so the valve does not output any pressure. Applying a 5V signal to the valve connects the Output to the Source. Therefore, if we apply a signal that switches between and 5V, such as a PWM signal, we can oscillate the gate between the Output and the Vent. The duty cycle of the PWM signal dictates how long the Output is connected to the Source before switching back to the Vent. The longer the connection between the Output and Source, the more

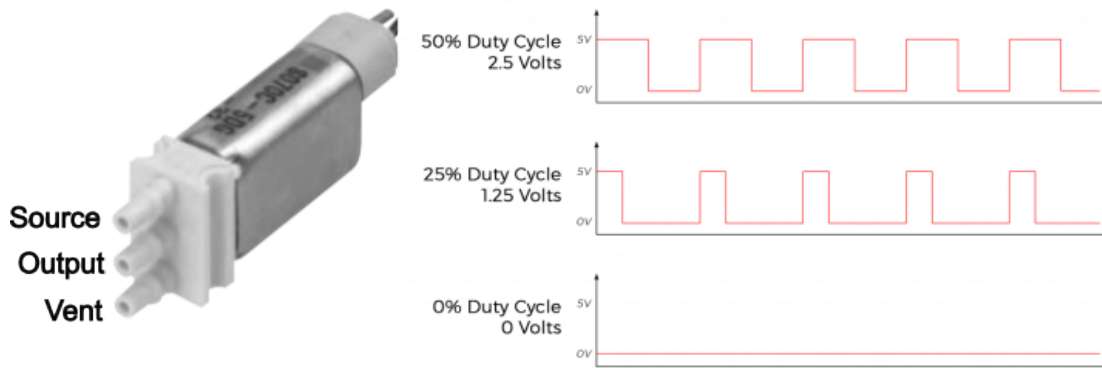


**Figure 4.1:** We control the haptic muscles using solenoid valves that have a constant input air source. By driving the solenoid valve with PWM signals, we can output a certain percentage of the air source to inflate the haptic muscle.

of the source pressure gets pumped to the output. To summarize, the duty cycle of the pulse-width modulation signal determines the percent of the source that flows to the output. In this way, we can controllably inflate and deflate the haptic muscle to any pressure up to the Source pressure. For example, if the source pressure was 40 kPa, and we gave the solenoid valve a PWM signal at 25% duty cycle, the output pressure would be 10 kPa.

## 4.2 Plastic Haptic Muscle Prototype

We manufactured the initial prototypes of the haptic muscles using heat-sealable plastic from Seal-A-Meal food saver bags. The plastic was easy to cut and seal, very lightweight, and air-tight after sealing. The food saver bags were sold with a heat sealer that was the ideal temperature for sealing the plastic without melting it.

Manufacturing these prototypes was a five-step process.

1. We cut one appropriately-sized rectangle with a length and width corresponding to the average circumference and length of a finger. We took circumferences and lengths of several fingers and averaged them to size our haptic muscles. We then cut another rectangle with the same width but slightly longer length. This way, when we lined up the two rectangle's edges, there was a small pocket between them.

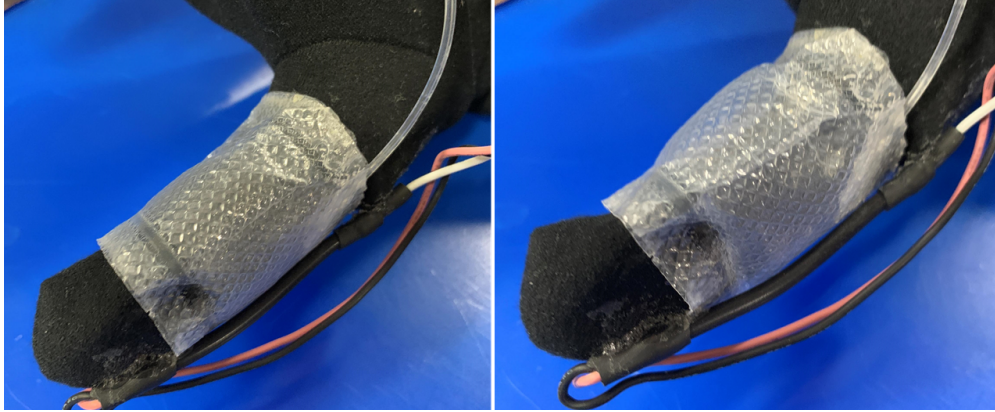


**Figure 4.2:** Initial prototypes of haptic muscles fabricated using heat-sealable plastic deflated (left) and inflated (right).

2. We folded the longer one to size, and sealed three of the four edges using the heat sealer.
3. We sealed the fourth side, leaving a gap large enough for an air tube to fit through.
4. After placing the air tube, we used hot-melt glue to seal the plastic around the air tube. We confirmed that the resulting pouch was air-tight and inflated well before proceeding.
5. Finally, we rolled the pouch into a toroid and sealed it with more hot-melt glue to reinforce the heat-seal.

We integrated initial prototypes of the haptic muscles constructed from a heat-sealable plastic into a data glove. We used the data glove to run tests where several users performed pick-and-place tasks by teleoperating a robotic arm and hand. During teleoperation, we sensed forces at the fingertips of the robotic hand, and directly mapped these forces to the haptic muscle inflation. The users felt a level of feedback proportional to the grasp forces, and were thus able to distinguish good grasps from poor grasps. These tests provided some results towards proving the efficacy of this kind of feedback.

During these teleoperation tests we found several areas of improvement. We received feedback during user interviews that the haptic muscles were uncomfortable to bend and more uncomfortable when inflated because of the "plasticky" feeling. Users also reported that the haptic feedback was rather binary, instead of proportionally following the force sensors' output. In the remainder of this

chapter, we discuss what we learned about the requirements for an ideal haptic muscle, our updated design and manufacturing process, and experiments that helped us choose a suitable material for the process. We wanted to create haptic muscles that could communicate not only grasp quality, but also force applied during a grasp. This would ideally allow a user to handle fragile objects without deforming or dropping them.

## **4.3 Fabric-Silicone Haptic Muscle Prototypes**

### **4.3.1 Design Requirements**

There are several aspects of haptic feedback that are essential to a good teleoperation experience. Haptic feedback should ideally feel natural and intuitive to the user. This means that when there is no feedback, the haptic structure should be unnoticeable. Additionally, the user should easily detect changes in the haptic feedback, and the smaller the detectable change, the more natural the haptics feel. There should be very little delay between force detection on the robot side and haptic feedback detection on the human side. That is, the human and robot should “feel” forces at the same time. Finally, the haptics should be comfortable and any forces applied should not exceed the human pain threshold of 17N [71].

To address these requirements, we chose to construct new haptic muscles using a fabric-silicone composite. The fabric is a ribbed cotton-spandex hybrid that is lightweight, comfortable, and asymmetrically flexible, that is, more elastic perpendicular to the ribs than along them. When inflated, the haptic muscle will inflate around the user’s finger more than along it, allowing us to apply greater kinesthetic forces with lower pressures.

Adding silicone makes the fabric air-tight for pneumatic actuation, and also allows us to add stiffness to the material. The added stiffness allows us to tune the haptic muscle to be elastic enough for comfort, but stiff enough to react to very small changes in input pressure. This ensures the end user will be able to detect minute changes in force during teleoperation.

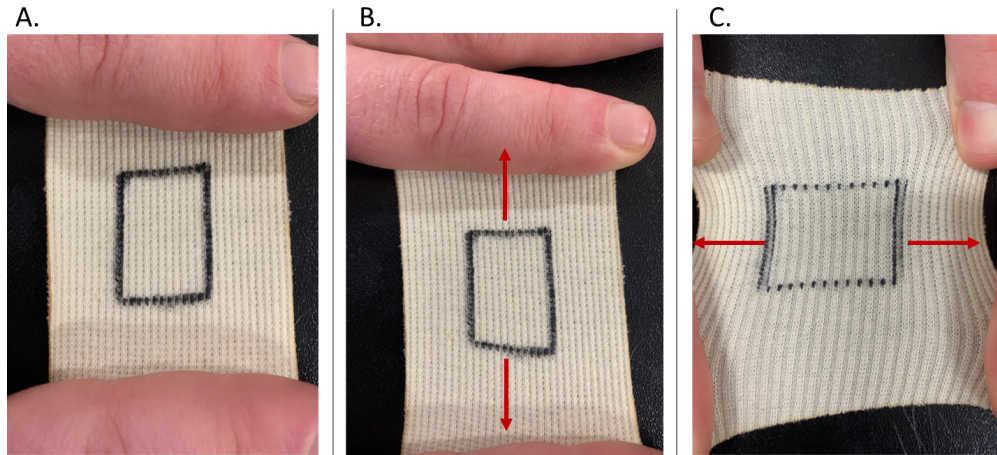


**Figure 4.3:** Cotton-spandex fabric a) in a neutral state b) stretched parallel to the ribs and c) stretched perpendicular to the ribs.

### 4.3.2 Fabrication Process

Constructing haptic muscles from a fabric-silicone composite is a multi-step process that involves applying silicone to the fabric, layering it into a pouch, then rolling the pouch into a toroid that fits around the finger. The specific steps are as follows, and are shown in Fig 4.4.

1. Laser-cut the fabric into two isosceles trapezoids. When rolled into a toroid, the taper allows the haptic muscle to fit snugly around the users' finger rather than fitting loosely at the fingertip. We measured the length and circumference of a diverse range of peoples' fingers and averaged them to get our final measurements. (Fig 4.4A)
2. Coat both sides of each fabric trapezoid with silicone (either Ecoflex 0030 or Dragonskin 10). We placed the fabric in 3D-printed molds before pouring the silicone to minimize leakage. (Fig 4.4B-C) When using Ecoflex 0030, we placed the fabric-silicone pieces in a vacuum chamber to de-gas the silicone.
3. After curing the silicone, place a 3D-printed mask (black) to cover the edges of each trapezoid and apply mold release (Ease Release 200 from Mann). The mask ensures that when the two halves are attached together in the next steps, only the edges are sealed, forming an air-tight pouch. (Fig 4.4D)



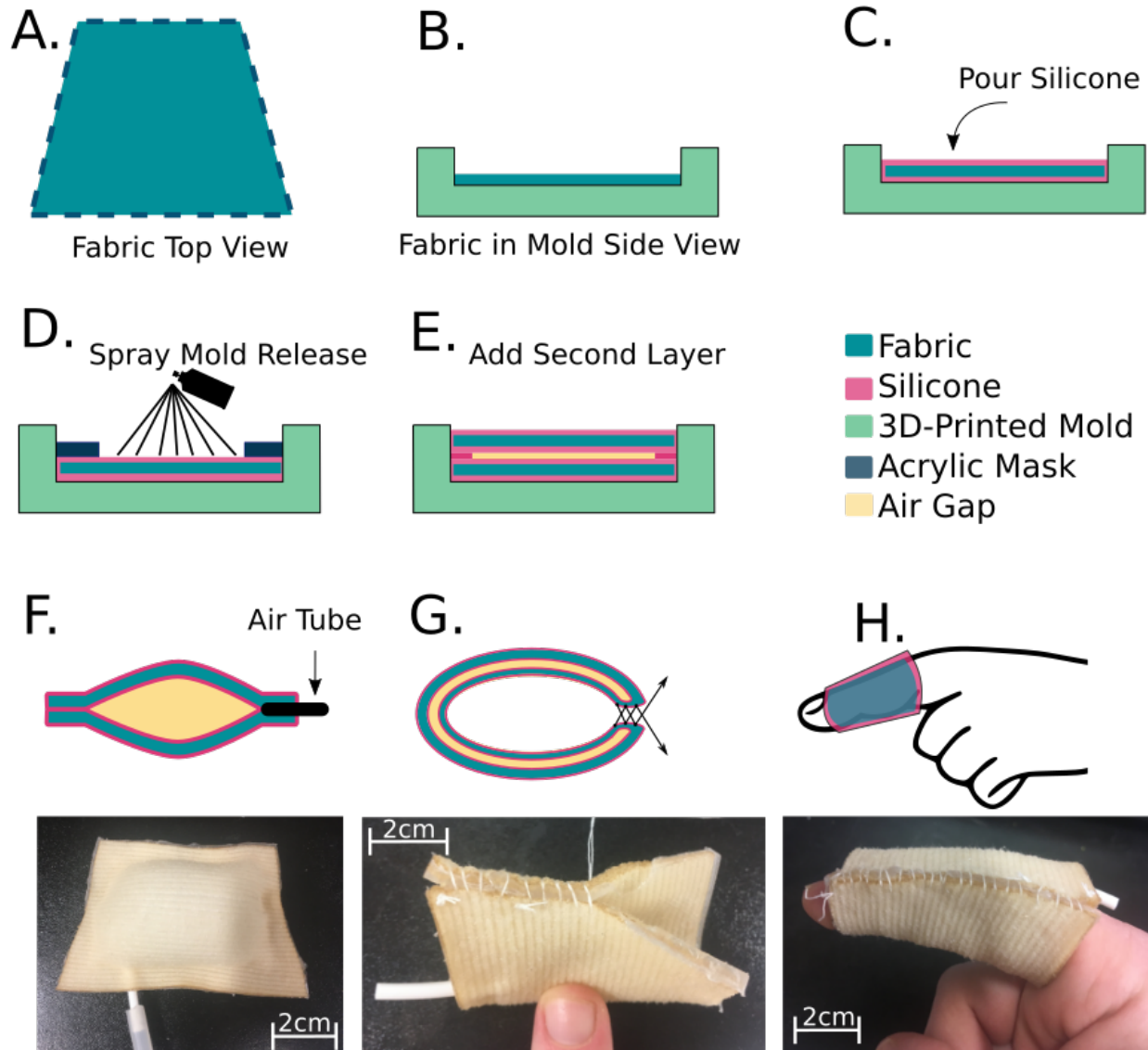


**Figure 4.4:** The manufacturing process to construct one haptic muscle. We coat a trapezoid-shaped piece of fabric with silicone (A-C), spray mold release in the center (D), and add another fabric-silicone piece to create a pouch (E). After inserting an air tube (F), we sew the pouch into a toroid (G).

4. Remove the mask, and pour silicone around the perimeter of one fabric-silicone trapezoid. Lay the second trapezoid on the first. (Fig 4.4E)
5. After curing, remove the pouch from the mold and pierce a tube through the perimeter to allow for air intake. Apply silicone sealer as required to ensure that the pouch remains airtight. (Fig 4.4F)

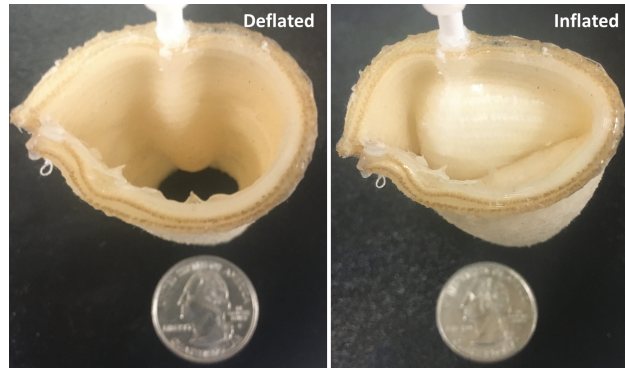


**Figure 4.5:** A complete fabric-silicone haptic muscle deflated (left) and inflated (right).

6. Roll the pouch into a toroid and sew the two edges together. (Fig 4.4G)

The finished haptic muscle is shown in Fig 4.5, both deflated and inflated.

### 4.3.3 Material Selection Experiments

We chose a suitable silicone for the haptic muscles by constructing two versions using two standard silicone types of different stiffnesses (Ecoflex 0030 and DragonSkin 10) and conducting isolated user and pressure response tests. We also included the older haptic muscle design, constructed from heat-sealable plastic, as a control. We performed these tests on all three haptic muscles to gauge their sensitivity, transient pressure response, and controllability.

#### User Sensitivity Tests

We designed user tests to quantify the sensitivity and accuracy of each haptic muscle. The experiments are novel and specific to the haptic muscle design, but are inspired by quantitative haptic tests performed in [10] and [72]. We define “sensitivity” as the smallest change in pressure a user can accurately detect while wearing a haptic muscle. We define “accuracy” as the user’s ability to distinguish between different set pressures. These tests show how well each haptic muscle communicates pressure levels and pressure changes to users, thus proving their ability to communicate grasp quality and force in a teleoperation context.

We performed two user tests on 16 users to determine haptic muscle sensitivity. We chose users who had no prior experience with haptic devices. In each test, we had users wear one haptic

muscle on one finger, close their eyes, and wear headphones to block the sound of the pneumatic valves. In each of the tests, we inflated and deflated the haptic muscle in a particular pattern by varying the PWM duty cycle input of the pneumatic valve controlling the muscle. The tests were respectively dubbed the “Minimal Detectable Change (MDC) Test”, and “Pressure Identification (PI) Test”. Because we were testing haptic muscles of varying materials, and each haptic muscle could withstand a different maximum pressure, we designed the tests around PWM input rather than total pressure input. However, we report the results based on absolute pressure input in kPa.

We created the “Minimal Detectable Change (MDC) Test” to quantify the smallest change in haptic feedback a user could feel when the muscle was already inflated. We began the test at a 40% PWM duty cycle (the haptic muscle partially inflated), then increased the input by 5% for one second before dropping back to 40% for one second. We then increased the pressure by an additional 5%, then repeated the process, dropping back to 40% each time. The input was thus 40%, 45%, 40%, 50%, and so on. We continued this pattern until a user verbally indicated that they noticed the increase in pressure. We repeated this process three times per haptic muscle for a total of 9 tests, and recorded the minimum detected pressure change as a percent duty cycle. Users were allowed to take as many breaks as required for them to stay sensitized to the haptics.

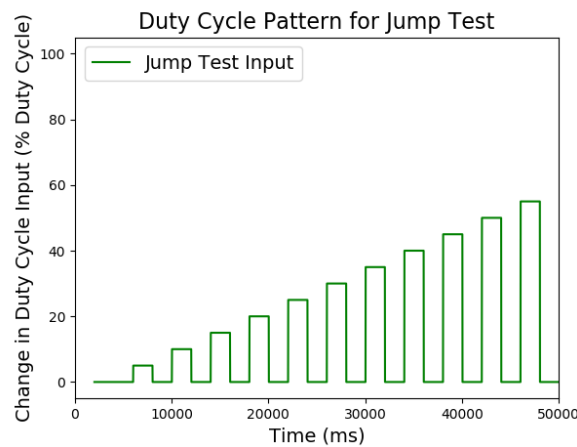


**Figure 4.6:** To perform the Minimum Detectable Change test, we ask a user to wear the haptic muscle, then inflate it partway. We then increase and decrease the PWM duty cycle input in a square wave pattern, gradually increasing the input pressure at each step. The test begins at 40% inflation then slowly increases, with a jump back to 40% inflation between each increase.

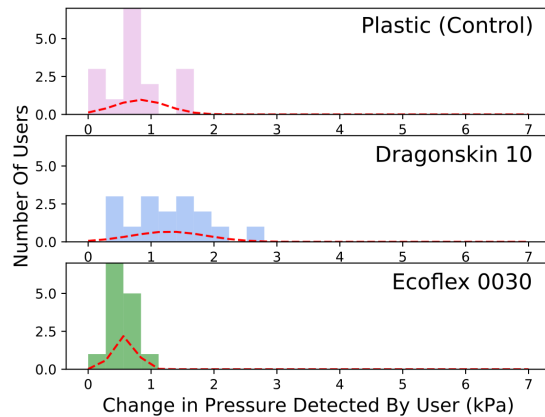


**Figure 4.7:** User results for the “MDC Test”, indicated the change in pressure detected for all three haptic muscles. The haptic muscle made with Ecoflex has the highest sensitivity with the lowest variance. We performed this test on 16 users who had no experience with wearable haptics.

The “Pressure Identification (PI) Test” was a general accuracy test where users had to identify different inflation levels with very little training. We chose 4 evenly spaced inflation levels within the working range of the actuator, between 20% and 100% duty cycle. After allowing the users 2 minutes to get a feel for the different inflation levels, we began the test. We randomly switched between the 4 inflation levels and had the users identify which level they were feeling. We repeated this 12 times for each haptic muscle, for a total of 36 tests, and recorded each user’s accuracy for each haptic muscle. Again, each user was allowed rest time when required.

After performing these tests, we also asked each user to rank the three haptic muscles from most to least comfortable overall.

The results of the tests described above are shown in Table 4.1. The MDC Test results are shown as the minimum change in pressure the users could detect in kPa. The PI Test results are user accuracy, and the User Comfort results are an average ranking across all users. Because the MDC Test results were the most conclusive, we also show a histogram of the user results with fitted normal curves in Fig 4.7. The heat-sealable plastic muscles scored fairly low, quantifying the previous feedback we received that they were uncomfortable and provided very binary haptics, where one pressure was indistinguishable from another. The Dragonskin-based muscles scored similarly, potentially because Dragonskin10 is a very stiff silicone. Though relatively comfortable,

**Table 4.1:** Haptic Muscle Sensitivity Test Results

Test		Heat Sealed Plastic	Ecoflex 0030	Dragonskin 10
MDC Test (kPa)	Mean	0.83	<b>0.56</b>	1.29
	Std Dev	0.41	<b>0.18</b>	0.59
PI Test (accuracy)	Mean	54%	<b>68%</b>	51%
	Std Dev	23%	<b>6%</b>	22%
User Comfort (rank)		3	<b>1</b>	2

Dragonskin10 was too stiff to apply accurate and detectable pressures to users' fingers. In contrast, the Ecoflex0030 haptic muscles scored highly on comfort, accuracy, and sensitivity.

### Transient Pressure Characterization

In order to characterize haptic muscle actuation, and to calculate the time lag in haptic feedback, we characterized each haptic muscles' pressure response. We attached each muscle to a pneumatic valve, then changed the PWM input to the pneumatic valve from 0% to 100% duty cycle. We recorded the internal pressure of the muscle using a pressure sensor inserted into the air pouch (Adafruit MPRLS Ported Pressure Sensor) as shown in Fig 4.8. Note that the initial pressure response is different for all three materials, because of the difference in stiffness and how much input pressure is required to begin inflating each structure.

To calculate the latency, we find the time it takes for each haptic muscle to reach a detectable pressure. That is, we use the results from the previous user tests to find the lowest detectable inflation point, and find the time to reach that point. The Ecoflex and Dragonskin haptic muscles both reach a detectable pressure in 63ms, while the plastic haptic muscle reaches its detectable pressure in 133ms. It has been shown that humans can only sense a haptic feedback delay over 61ms [73]. Therefore, the Ecoflex and Dragonskin actuators will provide haptic feedback with no perceptible delay. The plastic ones, however, have a perceptible delay that our users noticed during testing.

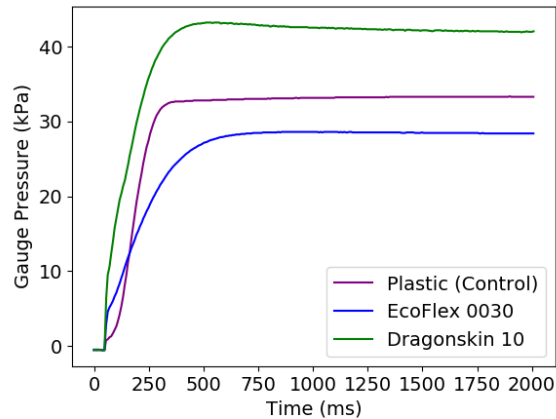


**Figure 4.8:** The transient pressure response of three haptic muscles to immediate (step) full inflation input. This plot shows results from one haptic muscle of each type, and there may be variations across haptic muscles of the same material due to manufacturing differences.

### Duty Cycle and Pressure Relationship

In order to verify that we have direct control over the feedback output by the haptic muscles, we must confirm that the PWM duty cycle input is linearly related to the internal pressure of the haptic muscles. For this test, we incrementally increase the PWM input to the haptic muscles and read the internal pressure as in the previous experiments. We hold each pressure increment for one second. After five cycles of testing, we show the average pressure reading from each increment, as well as standard deviations (Fig 4.9). Note that the x-axis is "% Duty Cycle Input", that is, percent inflated, because each haptic muscle can withstand a different maximum pressure.

Each haptic muscle has a small dead-zone from 0%-20% duty cycle where there is not enough airflow to begin inflation. In teleoperation contexts we would work solely in the 20%-100% duty cycle range.

### Material Selection Results

In the user tests, we found that the fabric-silicone haptic muscle made with Ecoflex0030 was the most effective. Not only did it allow users to detect the smallest changes in pressure (3.3% duty cycle), it also allowed for the most accuracy in the Identification Test and was the most comfortable. We believe that this is because the Ecoflex0030 provides a good balance of extensibility

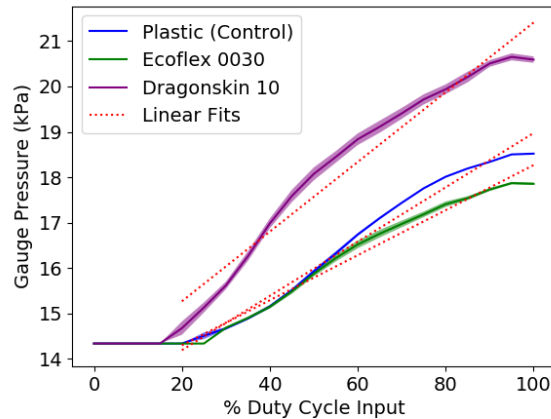


**Figure 4.9:** The duty cycle vs pressure plot for all three haptic muscles, as well as one standard deviation and linear fits. This confirms that the relationship between our input and resulting pressure are approximately linear after an initial duty cycle offset. This plot shows the results after 3 cycles of inflating the haptic muscles, and we show the average, standard deviations, and trendlines across all cycles of each haptic muscle.

and stiffness. The Ecoflex0030 haptic muscle also behaved fairly linearly and had a fast enough pressure response for teleoperation. Therefore, from the perspective of sensitivity, accuracy, and comfort, we can say that the Ecoflex0030 is a clear improvement on the heat-sealable plastic haptic muscles. In the next section, we perform a final validation experiment to show this improvement.

#### 4.3.4 Force Output Validation

The two forces a user experiences with the haptic muscles are a compression force and a restoration force. The compression force squeezes the user’s fingers and conveys a contact force, and the restoration force is what keeps the user’s fingers open, conveying a grasp force. Ideally, the compression force should plateau fairly quickly, ensuring that the force is observable but not uncomfortable. The restoration force should be larger than the compression force because the user’s fingers should be noticeably straightened for the grasp force sensation to feel realistic. Additionally the restoration force should be linear so we can control the amount of grasp force the user feels.

To track both compression and restoration force, we placed a haptic muscle on a 3D-printed 3-jointed tendon-driven finger, as shown in Fig 4.10a. The finger closes when we pull on the palmar

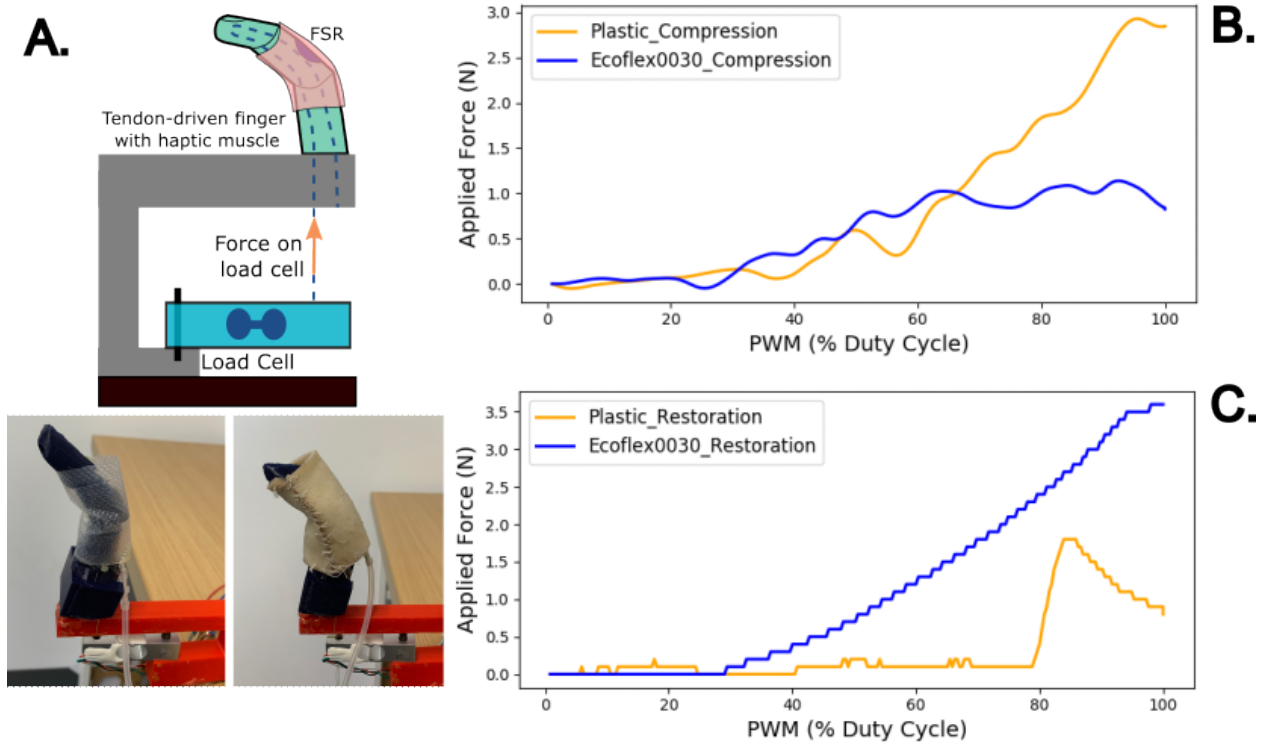


**Figure 4.10:** (a) The setup to track compression forces and restoration forces while inflating the plastic (bottom left) and Ecoflex0030 (bottom right) haptic muscle. It consists of a tendon-driven 3D-printed finger, a force-sensitive resistor (FSR) to track compression, and a load cell to track restoration force. (b) The results of the compression tests for both haptic muscles. (c) The results of the restoration tests for both haptic muscles.

tendon and opens with the dorsal tendon. We mounted a force-sensitive resistor (FSR) on the finger, fixed the dorsal tendon to a mount, then attached the palmar tendon to a load cell. During inflation, the haptic muscle compresses the FSR and attempts to open the finger, pulling on the palmar tendon and, in turn, the load cell. This gives us simultaneous compression and restoration forces as we slowly inflate the haptic muscle.

The results for the compression test are shown in Fig 4.10b. We observe that all forces are well within the pain tolerance threshold of 17N for human fingers [71]. The EcoFlex0030 haptic muscle saturates fairly quickly, providing the ideal binary feedback to communicate contact forces. The plastic muscle has a consistently increasing compression response which is higher than its restoration force.



The results for the restoration test are shown in Fig 4.10c. The Ecoflex0030 haptic muscle provides a restoration force that is linearly related to the PWM input, except for a dead zone which we do not operate in. Additionally, the restoration force is reasonably high, which means the user will actually experience this force during teleoperation. The plastic haptic muscle, however, shows uneven restoration forces during inflation. This uneven force application is because the plastic haptic muscle buckles at the finger joint. The buckle prevents air from reaching beyond the joint for 80% of the inflation, and only the bottom half of the haptic muscle is inflated, which does not apply any restoration force to the finger. At the 80% mark, the air breaks through the buckling and fills the rest of the haptic muscle. We observe a sudden increase in restoration force, and then a decrease as the available air fills a larger pocket. Additionally, the maximum restoration force applied is only 1.5N as compared to the 3.5N applied by the Ecoflex0030 haptic muscle.

These results quantify our previous users' observations that the plastic haptic muscles feel binary and uncomfortable during teleoperation tasks. Because the Ecoflex0030 haptic muscles have a more linear restoration response and a lower compression response, they are more controllable and comfortable. We verify this in Chapter 6 with a comparative teleoperation-related user study.

# Chapter 5

## Robotic End Effector

In this chapter we discuss three versions of robotic end-effectors that we have controlled with various phases of our teleoperation system. The first is a simulated gripper used in phase 1, the second is an anthropomorphic 5-fingered gripper used in phases 2 and 3, and the last is a sensorized off-the-shelf gripper used in phase 4.

The transition from one gripper to the next will be discussed further in Chapter 6, but we summarize here. The initial simulated gripper was sufficient for a proof-of-concept, but was not realistic enough to perform complex tasks or output realistic forces during teleoperation, so we transitioned to a real-world gripper with force sensing in the fingertips. After two iterations of developing novel custom gripper, our user test results in Phase 2 and 3 showed us that an anthropomorphic gripper added too much complexity for us to sufficiently study the motion mapping methods discussed in Chapter 3. We therefore decided to transition to an off-the-shelf gripper for the remainder of this work. In this chapter we present all three versions but focus heavily on the novel custom gripper of Phase 2 and 3 of this work.

The mapping scheme between the user and robot gripper is the same in all cases, and is inspired by the end-to-end mapping presented in [30]. We use a linear mapping to convert the user's current position to a desired gripper position, as shown in Fig 5.1. At the beginning of teleoperation, we ask the user to calibrate the data glove by opening and closing their hand, which gives us their minimum and maximum signals and thus the working range for each individual finger. We then map the user

range linearly to the robot range, either mapping individual fingers to the corresponding robotic finger, or using the average signal from the first three fingers to open and close the gripper.

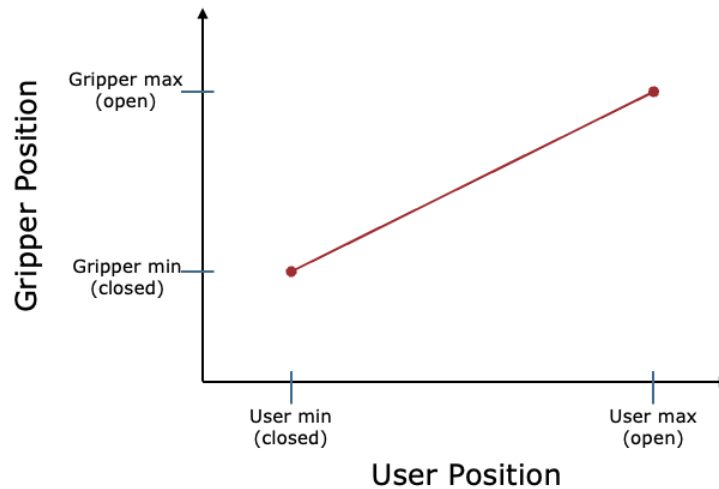


**Figure 5.1:** We use a linear mapping to convert a user’s current finger position to a gripper position. We begin teleoperation by having the user open and close their hand while wearing the data glove. We capture the data glove’s signals in the open and closed position and set this as the user’s working range. We can then linearly map the user’s working range to the robot.

## 5.1 Simulated 3-Fingered Robotiq Gripper

When controlling a simulated robotic arm in the first phase of our research, we used a simulated robotic gripper in Gazebo controlled through ROS. The gripper was modelled after the Robotiq 3-fingered adaptive gripper and we control it using a simulated joint position controller. We used a torque sensing plugin to sense torques at the finger joint, which output a force when we grasped simulated cubes. Additionally, we used Gazebo’s grasp-plugin to ensure that grasped cubes stayed attached to the gripper during teleoperation, simulating a pick, and that the cube fell when the gripper opened, simulating a place.

The rest of this chapter focuses on our real-world gripper solutions.

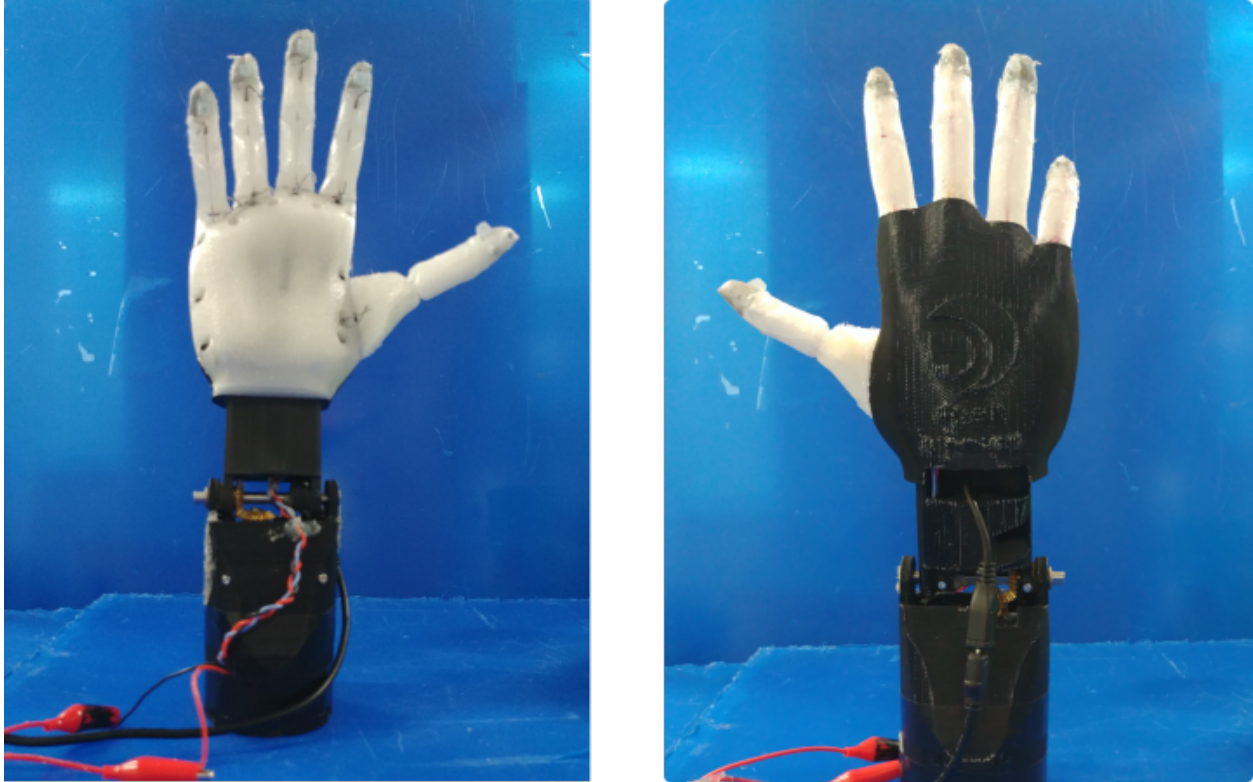


**Figure 5.2:** We 3D print the Ada hand in three distinct pieces. The palm and fingers are one piece, printed from NinjaFlex, a flexible filament. The wrist and back plates are two pieces, printed from rigid ABS.

## 5.2 5-Fingered Anthropomorphic Gripper

### 5.2.1 Ada Hand - Open Source Design

The 5-fingered anthropomorphic robotic hand (Fig. 5.2) is a modified version of the Open Bionics V1.1 Ada Hand [74], which is an open-source 3D-printable hand mainly used for prosthetic robotics research. The fingers are tendon driven and underactuated. The palm and fingers are 3D-printed as a single piece out of Ninjaflex, a flexible thermoplastic polyurethane filament. Thin hinges at the finger knuckles serve as flexure joints, allowing the fingers to bend easily. The hand uses four linear actuators (Actuonix PQ12-R) to flex its fingers: one each for the first, second, and third fingers, and one for both the fourth and fifth fingers.

We thread fishing line from the tip of the linear actuator to the tip of the finger through two holes in the finger. We close each finger by sending the corresponding linear actuator to the beginning



**Figure 5.3:** The fingers of the robotic hand are tendon driven and underactuated. The Ninjaflex fingers allow the fingers to conform to different shapes and perform a variety of grasps such as cylindrical, spherical, tripod, and pinch grasps.

of its stroke, pulling the tendon. Sending the linear actuator to the end of its stroke releases the tendon and opens finger. We can therefore positionally control the robotic hand using pulse-width modulation (PWM) signals from a microcontroller.

We 3D-printed the PCB tray (holding embedded control electronics), back of the hand, and wrist from ABS for more rigid structure. Liquid silicone was painted on the fingers and allowed to cure, which created more friction between the fingers and grasped objects. Because of the compliant nature of the fingers, the underactuated hand can perform a multitude of grasps, such as power, tripod, and pinch grasps (Fig. 5.3) that are commonly used in daily life. This makes it ideal for a teleoperation application because it can perform a broad range of tasks, and its anthropomorphic structure makes for intuitive mapping between the user’s hand and the robotic hand.

## 5.2.2 Soft Force Sensors

The design of the Ada Hand is not sensorized in the open-source version, so we tweaked the design to add force sensing at the fingertips. We were inspired by previous work in our lab to develop soft force sensors based on Hall Effect sensing [1]. In previous work, when exploring how to sense the curvature of soft actuators, our group found that resistive sensors suffer from drift and changes in temperature and humidity. They presented an alternative sensor that senses curvature or force and is more stable.

The soft force sensor proposed in [1] is a silicone pyramid with a 3-axis Hall-Effect sensor at its base and a small magnet suspended near the tip. When the tip of the pyramid is pushed, the magnet moves relative to the sensor and we can read the fluctuations in magnetic field readings in x, y, and z. With some calibration, we can interpret the magnetic field readings as a 3-axis force.

To sensorize the Ada Hand using these soft force sensors, we created a small chamber near the fingertip to house the hall-effect sensor and the magnet, as shown in Fig 5.4. The NinjaFlex walls act as the flexible housing for the magnet, so that when the hand grasps the object, the top of the finger deflects and shifts the magnet with respect to the hall-effect sensor. We can read the magnetic field change due to this deflection and interpret it as a grasp force.

## 5.2.3 5-Fingered Gripper Validation

We integrated the sensorized hand with the data glove presented in chapter 3 and used the glove to grasp several objects with the robot hand. During the grasps we read the force feedback from the hand, as shown in Fig 5.5. We observe that the change in grasping force is very noticeable when the user grasps an object, as expected. We also observe that a rigid object and a soft object result in different grasp forces, likely because the amount of deflection from a rigid object is much higher, while the soft object is more compliant and deflects the fingers less.

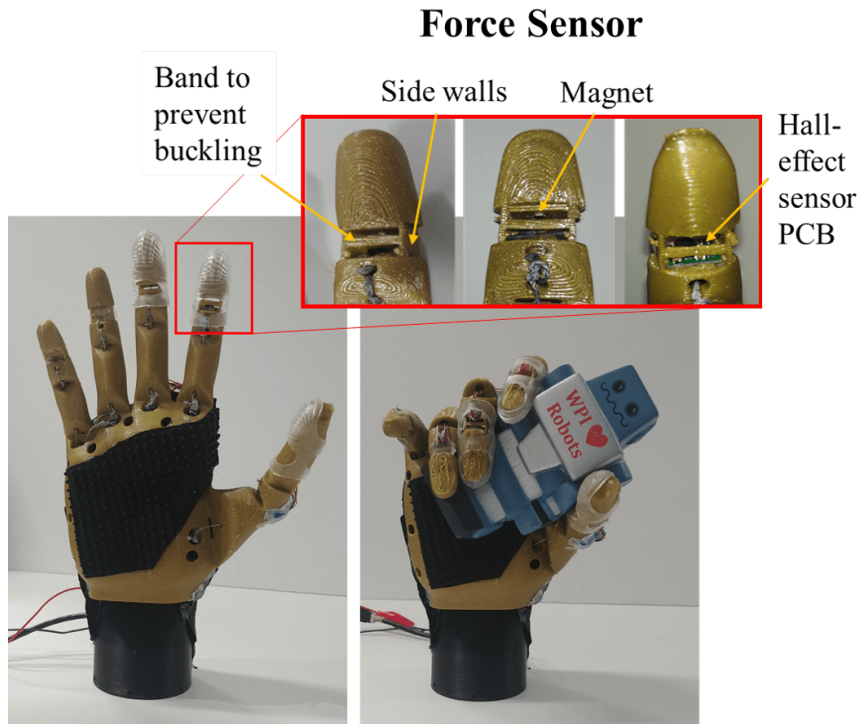


**Figure 5.4:** We sensorize the Ada Hand by adding a chamber in the fingertip to house a hall-effect sensor and a small magnet. This is a novel version of a sensor previously proposed in [1]. The sensor reads finger deflection during grasping which we can interpret as grasp force.

### 5.2.4 5-Fingered Gripper Conclusions

After performing user testing with the 5-fingered anthropomorphic gripper, we found that users struggled to pick and place items as well as we'd hoped. In particular, users struggled to orient the hand precisely to grasp objects where orientation was important, like water bottles and boxes. We discuss this further in chapter 6. Based on our findings, we decided to proceed with a simpler gripper and force sensor setup for the final phase of user testing.

## 5.3 2-Fingered Robotiq Gripper

To simplify the end-effector subsystem, we decided to use a 2-fingered off-the-shelf gripper from Robotiq (2F-85). The gripper connects both physically and electrically to the robotic arm and can be controlled using the same software package the controls the arm. Specifically, we control

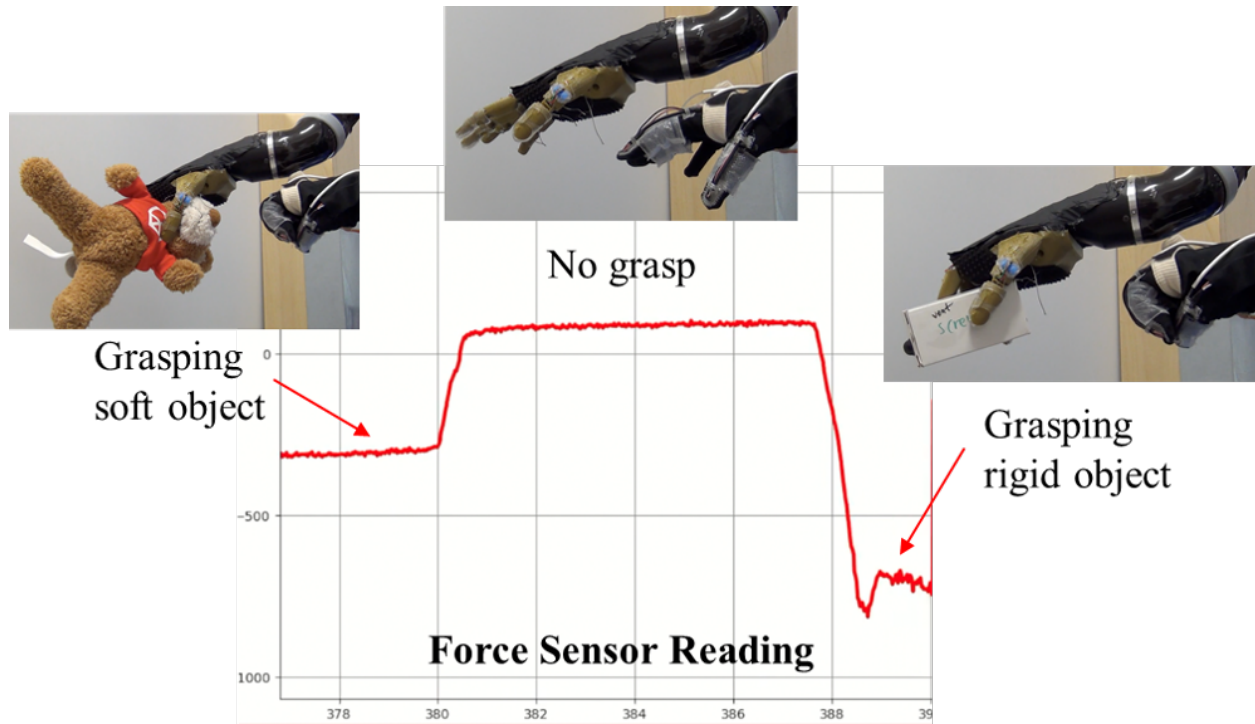


**Figure 5.5:** We sensorize the Ada Hand by adding a chamber in the fingertip to house a hall-effect sensor and a small magnet. This sensor reads finger deflection during grasping which we can interpret as grasp force. In this plot we show a user wearing the data glove presented in Chapter 3 and using it to teleoperate the Ada Hand to grasp a soft toy and a rigid box. The curve shows the sum of the force sensor outputs across all five fingers of the soft gripper. We observe that the force output for a soft object is less than that of a rigid object.

the gripper using velocity-based PD controller using the output from the data glove to calculate a desired gripper position, a position error, and a final velocity.

To sensorize the gripper, we use resistive force sensors from Flexiforce (A401) attached to the gripper’s fingers. We found in early pilot tests that the gripper was very binary, and had no compliance. From working with the anthropomorphic gripper, we knew that adding compliance would improve the force sensor readings and allow us to handle soft objects without deforming them. We therefore added silicone pads (Ecoflex 0030) to the gripper fingers to pad the fingers, as shown in Fig 5.6.

To validate the gripper, one user used the game controller that shipped with the robotic arm to control the gripper and grasp a soft loaf of bread. The signals from the force sensors are shown in Fig 5.7, and show that we can gauge when we are squeezing the bread too hard. While the



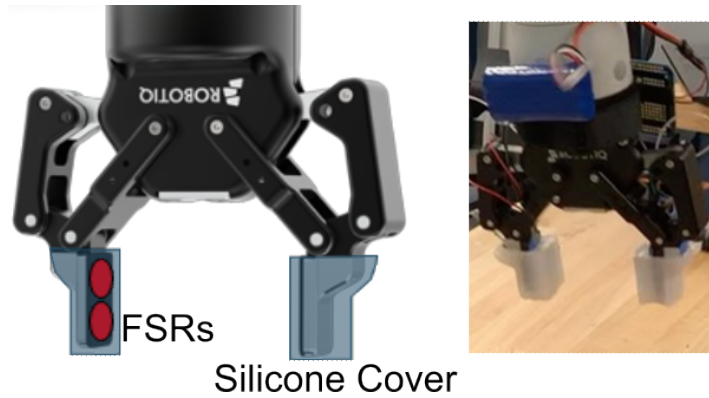


**Figure 5.6:** We add resistive force sensors and silicone pads to the gripper fingers to add sensing and compliance to a rigid off-the-shelf Robotiq gripper.

gripper is not as controllable and dextrous as the 5-fingered anthropomorphic gripper, it may be more intuitive to users to orient, and will thus allow us to have users pick and place a variety of objects.

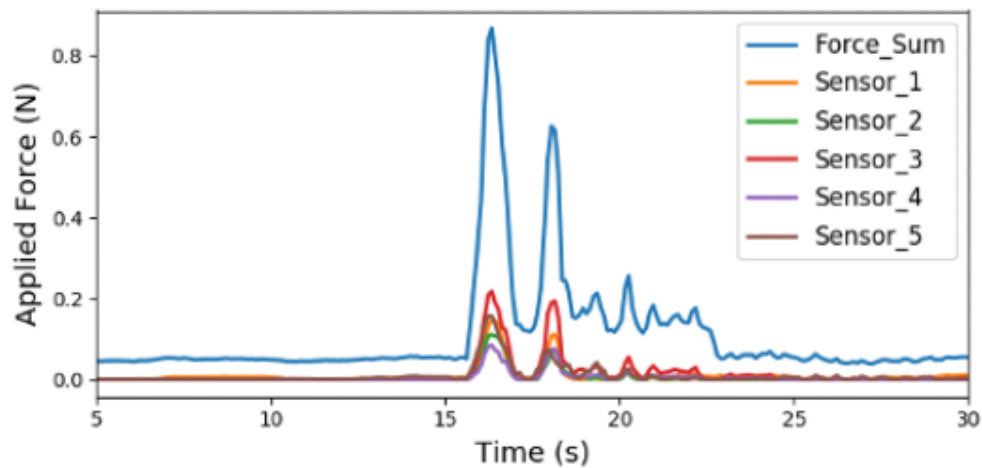


**Figure 5.7:** We asked a user to use a game controller to open and close the gripper around a loaf of bread, and collected the force sensor output. We observe that the user initially squishes the loaf and then opens the gripper somewhat to grasp it more lightly. We see, therefore, that we can use the force sensor data to communicate grasp strength.

# Chapter 6

## User Testing

### 6.1 Phased User Testing

During each phase of development, we designed and ran several user tests to validate the system and certain important subsystems. In this chapter, we present all phases of user testing we performed, as well as the results of the user testing. In each phase, we outline our hypothesis, the system we built to test the hypothesis, the user tests we ran, and the results of the user testing. We also include discussion of how the results of our user tests led us to making certain decisions and improvements to the system. We thus have an iterative process by which we use user-driven design techniques to approach a teleoperation system design that is truly usable by novice users.

Table 6.1 shows each phase of development that corresponds to a set of user tests.

### 6.2 Phase 1

#### 6.2.1 Phase Setup

Phase 1 was the first integration phase in our work, and we were concerned with combining individual technologies into a fully usable system. Give the work done in [67], we had to develop a system that was demoable on the floor of the Wastewater Management Conference in 2018. This required us to create a system that was durable enough to withstand several days of testing, and

**Table 6.1:** This table shows our 4 main phases of development and what version of each subsystem was involved in each phase.

<b>Phase</b>	<b>Curvature Sensors</b>	<b>Robotic Arm</b>	<b>Gripper</b>	<b>Haptics</b>	<b>Mapping</b>
<b>1</b>	Optical	Kinova Jaco2 (sim)	3-Fingered (sim)	Plastic	Joint-to-joint
<b>2</b>	Optical	Kinova Jaco2	5-Fingered with wrist	Plastic	Joint-to-joint
<b>3</b>	Optical	Kinova Jaco2	5-Fingered w/out wrist	Plastic	Cartesian Scaling
<b>4</b>	Capacative	Kinova Gen3	Robotiq 2F-85	Fabric-Silicone	Cartesian Scaling

was easily wearable so many people could quickly try the demo and give us qualitative feedback. It was for this reason that we integrated the motion capture system into a soft data glove. During this phase, which resulted in a proof-of-concept system, we wanted to understand the scope of the problem and learn about how to conduct user studies that were specific to our system.

### 6.2.2 System Description

In phase 1, the system consisted of:

- A motion capture system consisting of IMUs for the arm and optical curvature sensors for the fingers (novel work)
- A simulated Kinova Jaco arm run in Gazebo
- A simulated 3-fingered Robotiq gripper connected to the Kinova Jaco in Gazebo
- Haptic muscles made of heat-sealable plastic (novel work)
- A human-to-robot mapping system based on joint-to-joint mapping

### 6.2.3 User Test Description

We presented this setup at the 2018 Waste Management Conference, where we set up a live demo that visitors could experiment with. They wore the motion capture system and controlled a simulated robotic arm and gripper to pick and place simulated blocks as shown in Fig 6.1. As they

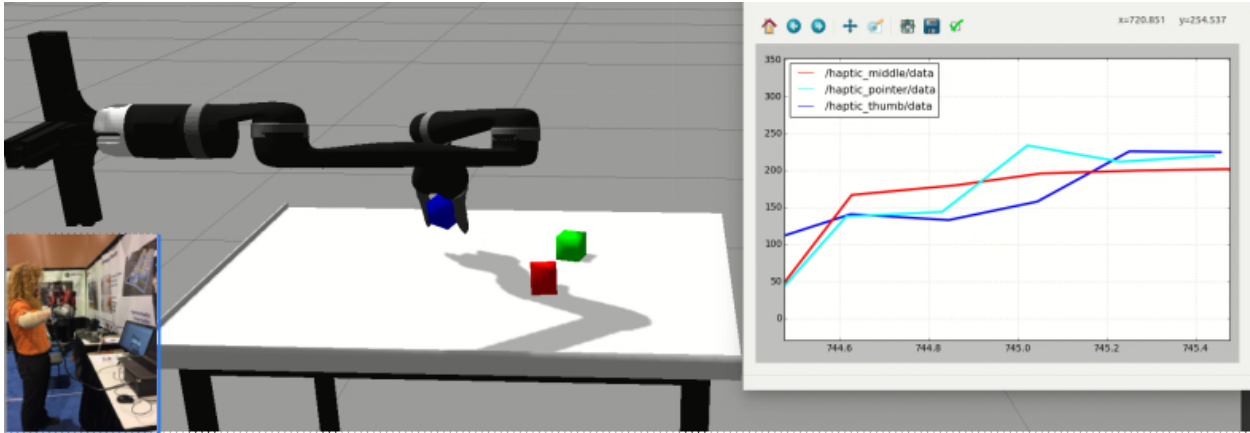


**Figure 6.1:** The simulated setup we presented at the Waste Management Conference in 2018. Users wore the motion capture system and controlled the simulated robotic arm. The plot on the right shows the force output from the gripper as the user grasps a cube. The user felt haptic feedback proportional to the force output through the haptic muscles.

handled the blocks, the haptic muscles gave them a sense of contact and grasp force so they could feel whether they had grasped a block well or not. We observed the users and briefly interviewed them to gauge how intuitive the robot arm control was and how well the haptic feedback was working. We observed how long it took them to pick up a cube, asked them questions about the comfort of the motion capture system, and when they did pick up a cube asked them questions about the comfort and realism of the haptic feedback. Over the course of three conference days, we worked with approximately 20 users who had never seen or used a teleoperation system before, and most were not engineers.

## 6.2.4 User Test Results

We synthesized our findings into several qualitative statements:

1. The joint-to-joint control was very easy to understand, but somewhat limited the robot arm's workspace because the user could not move in a straight line in any direction, and instead had to move in arcs because all movement was based on direct joint rotation.

2. The haptic feedback was very easy to understand and allowed users to gauge whether they had grasped the block or not. In many cases, users noted that their grasp was poor or they missed the block before it became visually obvious in the simulation.
3. The force sensors on the simulated gripper were the limiting factor in this system because the forces included both contact and grasp forcing, which sometimes confused the user because the visual feedback and haptic feedback were different.

### **6.2.5 User Test Conclusions and Future Work**

After synthesizing our findings, we concluded that the motion capture system and haptic feedback mechanisms were satisfactory and worth continuing with. However, to gauge the real use of haptic feedback during teleoperation, we would need higher resolution and realism in the force sensing on the robotic gripper. We also decided to experiment with a more realistic gripper. In our next phase, we decided to replace the simulation with a physical robotic arm (Kinova Jaco) and a custom anthropomorphic gripper with force sensing in the fingertips (as discussed in section 4).

## **6.3 Phase 2**

### **6.3.1 Phase Setup and Hypotheses**

After proving out the system in Phase 1, in Phase 2 we wanted to bring those results into the real-world by implementing our system on a real robotic arm. We hypothesized that, given a more realistic gripper, we might increase the complexity of tasks which would later allow us to show the efficacy of the haptic feedback in the teleoperation system. We also hypothesized that, because users were able to control the simulated robot arm using joint-to-joint mapping, they would be able to do the same with the real robotic arm. We therefore designed our system with the 5-fingered anthropomorphic gripper discussed in Chapter 5, and rotated and mounted the arm sideways to match the simulation from Phase 1. We wanted to run user experiments to gauge task performance quantitatively, and also ask a specified set of questions to gather qualitative data.

During very initial pilot tests with the author and two colleagues, we noted that the presence of haptic feedback did not affect either performance time nor user comfort. We observed that this was due to the teleoperation system being difficult to use. We therefore designed our user test in Phase 2 to understand the difficulty and quantify it across more users.

### **6.3.2 System Description**

In phase 2, the system consisted of:

- A motion capture system consisting of IMUs for the arm and optical curvature sensors for the fingers
- A physical Kinova Jaco
- An anthropomorphic gripper with 5 fingers and a movable wrist (novel work)
- Haptic muscles made of heat-sealable plastic
- A human-to-robot mapping system based on joint-to-joint mapping

### **6.3.3 User Test Description**

To test the teleoperation system for usability and intuitive control, we performed a pick-and-place user tests with 9 individuals, 7 males and 2 females. All individuals were right-handed engineering students between the ages of 19 and 33.

The task completed by users was to place a water bottle and a small box into a larger box as shown in Figure 6.2. This required the users to precisely position the arm and grasp each object. After each user was fitted with the device and given an explanation of the teleoperation scheme and task, we gave them 5 minutes to practice with a sample bottle and box. After 5 minutes, we replaced the items with another bottle and box and, when the user was ready, began a timer. During the timed portion of the test, we recorded how long it took each user to pick and place each item successfully, as well as the number of times the item fell (was knocked over) or was dropped.

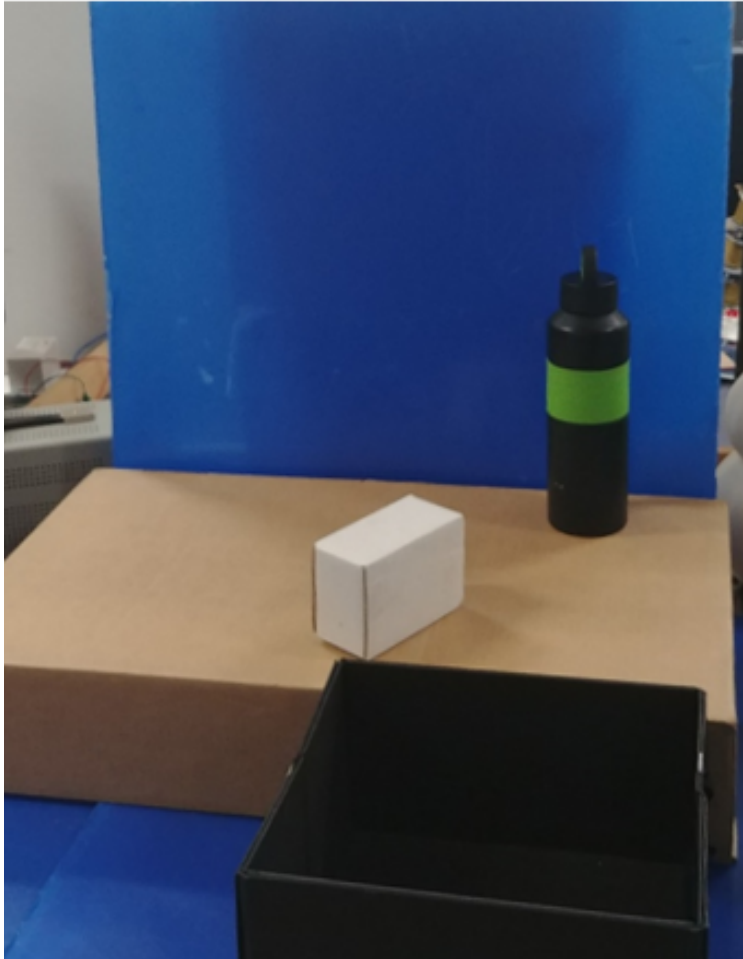


**Figure 6.2:** To test the usability of the system, users were asked to grasp a small box and a water bottle and place them into the larger black box.

### **6.3.4 User Test Results**

Of the 9 users we worked with, 8 were able to place the small box in the box, and all 9 users could place the water bottle in the box. Tables 6.2 and 6.3 summarize the performance results in manipulating a cylindrical bottle and a rectangular box respectively for all users and also breaks down results by experienced and inexperienced users. This was because we noted a significant difference in physical and mental comfort between users who had never used the system and users who had practiced with the system before, even for only 30 minutes. We wanted to quantify this difference in task performance. For both objects, users with more experience performed much better than those with no experience, both in time to complete the task and number of drops and

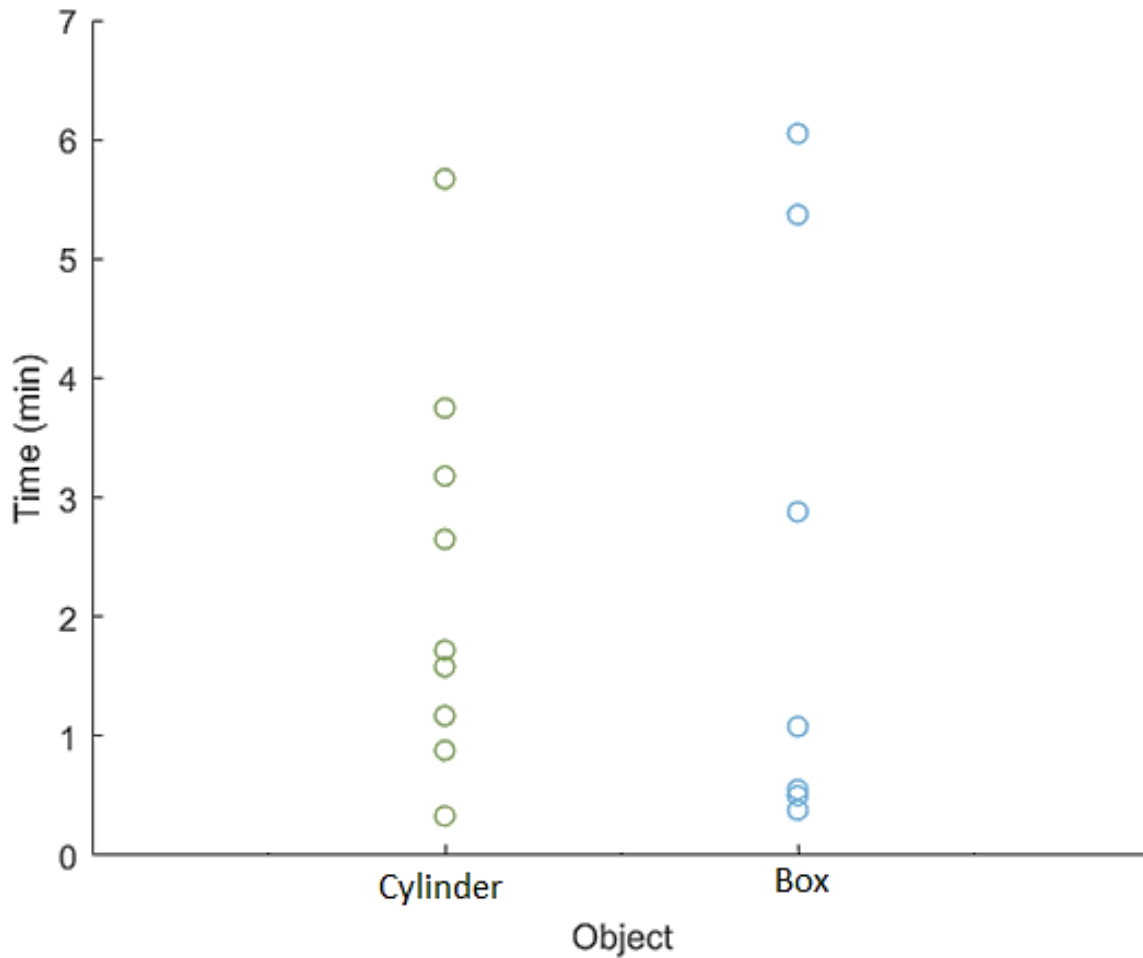


**Figure 6.3:** During the timed portion of the user test, 5 out of 9 users were able to complete the entire task in under 5 minutes, and 2 out of 3 experienced users completed the task in under 2 minutes. On average users took less time to pick and place the box than the bottle, but experienced users dealt with both objects fairly quickly.

**Table 6.2:** User performance in picking and placing a cylindrical bottle (9 users, 6 inexperienced and 3 experienced)

<b>Bottle</b>	Time (min)	Number of Drops	Number of Falls
All Users	$2.33 \pm 1.67$	$0.67 \pm 0.87$	$2.33 \pm 2.26$
Inexperienced	$3.02 \pm 1.60$	$0.83 \pm 0.98$	$3.00 \pm 2.28$
Experienced	$0.93 \pm 0.63$	$0.33 \pm 0.58$	$1.00 \pm 1.73$

falls. This demonstrates that the system works best with some amount of training or practice, but that even with only 5 minutes of training the system is intuitive enough to perform simple tasks.



**Table 6.3:** User performance in picking and placing a rectangular box (9 users, 6 inexperienced and 3 experienced)

<b>Box</b>	<b>Time (min)</b>	<b>Number of Drops</b>	<b>Number of Falls</b>
All Users	$1.98 \pm 2.26$	$0.00 \pm 0.00$	$1.11 \pm 1.62$
Inexperienced	$2.73 \pm 2.48$	$0.00 \pm 0.00$	$1.50 \pm 1.87$
Experienced	$0.48 \pm 0.09$	$0.00 \pm 0.00$	$0.33 \pm 0.58$

We found that the largest challenge for our users was positioning the anthropomorphic hand. The lack of a fully opposable thumb and sideways wrist motion made precise grasping difficult without practice because there was very little room for error in grasp position and orientation. During user tests, the number of falls was much greater than drops on average because while a successful grasp was very stable once achieved, users tended to knock over objects while trying to position the hand for grasping. We also found that users had to place the hand very precisely to engage the force sensors, because the contact point of the sensors was too small.

With experience, however, users were able to perform much more complex tasks than the pick-and-place test. In other trials with the system, experienced users could stack objects, pour beads from one cup to another, and perform a more elaborate pick-and-place task very quickly. Our hypotheses were therefore disproven; users had a rather difficult time with the joint-to-joint mapping on the real-world robot.

### **6.3.5 User Test Conclusions and Future Work**

After synthesizing our results from this user test, we concluded that the major limitations of this system lay in the anthropomorphic gripper's wrist and the orientation of the robotic arm. We also realized that our attempts to test whether the haptics were useful in a teleoperation context were limited by the quality of the teleoperation scheme. We therefore decided to redesign the gripper without a wrist and with better integrated force sensors. We also decided to begin running separate user tests for teleoperation system and haptic feedback efficacy.

## **6.4 Phase 3**

### **6.4.1 Phase Setup and Hypotheses**

After Phase 2, we realized that the human-robot motion mapping scheme was more important to the system than we previously realized, and required separate testing from the haptic feedback testing. We therefore made separate hypotheses about the teleoperation scheme, the haptic feedback, and the full teleoperation system and tested them all. Firstly, we hypothesized that using a teleoperation scheme from literature, that is, end-to-end mapping between the user and robot, would result in a more usable system than the joint-to-joint mapping. We also hypothesized that the haptic muscles would be useful in communicating grasp quality to a user, and that this would be more evident when their vision was occluded. Finally, we hypothesized that the full teleoperation system would be usable by novice users, that users would take less time to pick and place objects than in Phase 2, and that the presence of haptic feedback would increase task performance.

### **6.4.2 System Description**

In phase 3, the system consisted of:

- A motion capture system consisting of IMUs for the arm and optical curvature sensors for the fingers
- A physical Kinova Jaco
- An anthropomorphic gripper with 5 fingers
- Haptic muscles made of heat-sealable plastic
- A human-to-robot mapping system based on cartesian mapping with scaling

### **6.4.3 User Test Description: Grasp Quality**

To test the first hypothesis about the haptic muscles, we devised an experiment using only the data glove and the robotic hand to test the system's ability to convey grasp quality with the soft

force sensors and haptic muscles. We performed this test with 10 users, all engineers but a mix of roboticists and non-roboticists, none of whom had experience with haptic feedback systems.

A user wore the haptic glove and looked at a computer screen, which showed live footage of a table surface. One of the authors held the wrist of the robotic hand, and the user could see the hand and some objects on the screen. The author placed the robotic hand over an object so the object was partially or fully occluded, and the user closed their fingers to grasp the object. Using their view from the screen and the haptic feedback through the glove, the user reported whether the robotic hand was grasping the object securely or insecurely. After their guess, the author lifted the robotic hand and object to find the true grasp quality; if the object stayed grasped, it was secure, and if the object fell immediately or after a slight disturbance, it was insecure. After 1 to 3 minutes of practice, we recorded the true grasp quality and whether the user's guess was correct or incorrect. We repeated this test for four objects both with and without haptic feedback, performing a total of 12 grasps per object (6 with and 6 without feedback).

We then turned off the camera to test a user's ability to determine grasp quality using only the haptic feedback they felt through the glove. Rather than identifying between a successful and unsuccessful grasp, we wanted to test levels of grasp security and asked users to rate the grasp from 1 to 3, 1 being least secure and 3 being most secure. After lifting the robotic hand, if the object fell immediately, the grasp would be rated a 1. If it was grasped securely, it was rated a 3. If the object slipped after a slight disturbance, it was a 2. Each object was grasped 6 times for this test, and we again recorded the user's guess and the true grasp quality. During both tests, we tried to give users an equal number of secure and insecure grasps to identify.

#### **6.4.4 User Test Results: Grasp Quality**

The results of the two experiments are presented in the Tables 6.4 and 6.5. For the first test using the camera, we found that without feedback, users were able to identify good grasps 73% of the time and poor grasps 51% of the time. With feedback, they correctly identified good grasps with 95% accuracy and poor grasps with 74% accuracy. Users also reported that they felt more confident of their answers with the haptic feedback.

**Table 6.4:** Grasp Quality Test with Visual Feedback

	No Haptic Feedback	Haptic Feedback
<b>Secure Grasp, Correct</b>	66	97
<b>Secure Grasp, Incorrect</b>	25	5
<b>Insecure Grasp, Correct</b>	54	71
<b>Insecure Grasp, Incorrect</b>	52	25

**Table 6.5:** Grasp Quality Test with no Visual Feedback

	Reported Grasp Quality		
	1	2	3
<b>Actual Grasp Quality</b>			
1	49	23	10
2	2	11	14
3	2	8	61

For the blind test, users were 60% accurate at identifying poor grasps and 86% accurate at identifying good grasps. They were also fairly accurate at reporting a middle-level quality of grasp; when users said the grasp was a two, the grasp turned out to be either a one or a two 81% of the time. For both a one or a two grasp, the object slipped at some point during the grasp, either upon initial lifting or after the object was lifted and experienced a small disturbance. Users were more likely to label a middle-level grasp as a 1 than a 3, which is ideal for teleoperation purposes.

During these tests, some users reported feeling an object slipping from their grasp, which highlights the capabilities of the soft force sensors to detect slip as well as the haptic muscles to convey nuanced forces.

### 6.4.5 User Test Description: System Teleoperation

To test the intuitive nature of the teleoperation system and effect of feedback on the entire system, we performed user testing with a series of pick-and-place tasks. We performed this test on 12 users, 8 of whom had no experience with a teleoperation system, and 4 of whom had used our system for 30 minutes to 2 hours prior to testing. We again made this distinction to gauge how quickly users became familiar with the system and to test whether experience affected how the users reacted to the haptic feedback.



**Figure 6.4:** To test our system, users picked up 5 randomly ordered objects, each with and without feedback, and placed them in a box. Objects are placed on the table one at a time.

Users were told to pick up a given object and place it in a nearby box as quickly as possible. After giving each user five minutes of practice time to become accustomed to the system, we tested them with five objects, each with and without haptic feedback, for a total of ten tasks. The five objects were a soft teddy bear, a robot-shaped stress toy, a paper cup, a cardboard box, and an empty plastic water bottle. These ten tasks were randomized to account for user learning during the test, and the position and orientation of each object were kept constant for all trials. We recorded the time required to complete each task, starting from when we told the user to begin and ending when the object landed in the box. A sample of the pick-and-place task, with multiple items on the table, is included in the supplementary video.

#### **6.4.6 User Test Results: System Teleoperation**

During the user study, all subjects completed every task. In the presented data, we define an inexperienced user as someone who was introduced to the system for the first time during user testing. An experienced user had worked with the system during development or for previous publications, and had about 30 minutes to 2 hours of practice before user testing. Analysis of the experienced and inexperienced users' data showed that subjects' teleoperation skills improve with practice.

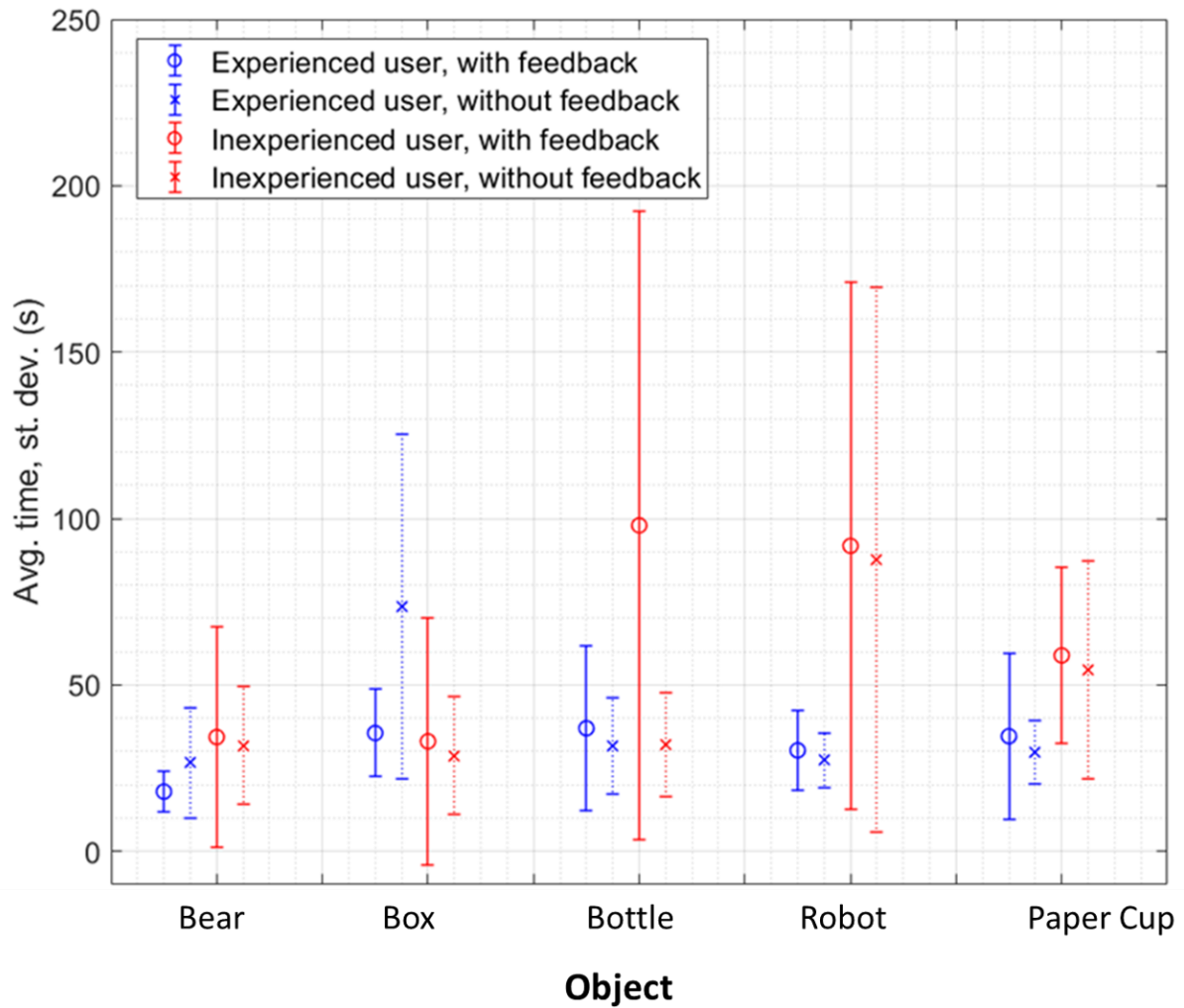


**Figure 6.5:** Pick and place user study results with/without feedback for experienced users and inexperienced users. We tested 12 users, 8 inexperienced and 4 experienced. The center point is the average time to complete the pick-and-place task for each object, and the error bars represent the standard deviation among users.

When analyzing the time taken for tasks with and without haptic feedback, we found significant differences between the inexperienced and experienced users. The average task completion times were greatly reduced for some objects, as were the standard deviations. We also observe that in the experienced users, 2 objects benefited from the haptic feedback and the other objects had similar average times. The average time to complete a pick-and-place task for inexperienced users was 55.1 seconds, and for experienced users was 34.6 seconds.

The inexperienced users struggled more with controlling the robotic arm, so the benefits of the haptic feedback are less visible. Teleoperating the robotic arm proved slightly difficult during user testing. Though we tested the teleoperation scheme in simulation, the real robotic arm seemed to have additional safety measures to prevent self-collisions and over-torqueing the motors. Because of these rather unpredictable measures, the arm was sometimes unable to follow a user's pose, and thus stop moving. Additionally, the hand was somewhat difficult to align because its thumb is not opposable. These issues added to the time and effort required to perform a pick-and-place task, and many users relied mostly on visual feedback to align the arm and hand. Though the first set of experiments prove the intuitiveness and usefulness of the pneumatic feedback, the teleoperation system requires some improvements before users can fully make use of the haptics. However, the average task completion time of 55.1 seconds for inexperienced users, and clear improvement of experienced users with more practice time, shows the promise of this teleoperation system. Additionally, experienced users were able to complete more challenging tasks, like placing a small box in a cup.

#### **6.4.7 User Test Conclusions and Future Work**

After synthesizing the results from both user tests, we concluded that the system required a rather drastic change to move the research forward. Firstly, the haptic feedback, though proven useful in communicating grasp quality, also proved to be rather binary. That is, it only told users whether the grasp existed or not, and not enough of the nuance that we hoped for given the resolution of the haptic muscle control. We therefore concluded that this was a materials issue, and decided to

experiment with using different materials to construct the haptic muscles. After the redesign, we also realized we needed a different data glove and decided on an off-the-shelf solution.

Secondly, the robotic arm and gripper were becoming a limitation due to the kinematics of the Kinova Jaco and the anthropomorphic gripper. The Kinova Jaco has a non-spherical wrist, which made orientation control in the cartesian space rather difficult. Additionally, the anthropomorphic hand did not have an opposable thumb, which made grasping certain objects challenging. In order to focus on the teleoperation scheme and the haptic feedback mechanism, we decided to use a more convenient robotic arm (Kinova gen3), and an off-the-shelf gripper (Robotiq 2F-85).

## **6.5 Phase 4**

### **6.5.1 Phase Setup and Hypotheses**

We made several improvements to the system based on the user test results from Phase 3, both quantitative and qualitative. As before, because the motion mapping and haptic feedback subsystems are themselves complicated, we make separate hypotheses about each and test them before conducting full system user studies. We hypothesize that the fabric-silicone haptic muscles will allow users to better handle delicate and fragile materials, because we have seen in Chapter 4 that they apply more linear forces and are more sensitive. We also hypothesize that a workspace alignment scheme that we developed and discussed in Chapter 3 will be more usable than the workspace scaling scheme and allow users to complete tasks faster and more comfortably. Finally we hypothesize that adding haptic feedback to the teleoperation system will improve task performance and lower task load.

### **6.5.2 System Description**

In phase 4, the system consisted of:

- A motion capture system consisting of IMUs for the arm and an off-the-shelf data glove with capacitive curvature sensors



- A physical Kinova Gen3
- A Robotiq 2F-85 gripper with force sensing on the fingers
- Haptic muscles made of a fabric-silicone composite (novel work)
- A human-to-robot mapping system based on cartesian mapping with workspace alignment (novel work)

### **6.5.3 User Test Description: Novice Haptic Study**

To focus on the interaction between the force sensors and haptic feedback mechanism, we designed a simpler pick and place test for novice users. This is a parallel to the grasp quality tests we ran in Phase 3, but are a clearer indicator of how users make use of grasp quality feedback. We performed this test with 12 users, a mix of roboticists and non-roboticists, none of whom had experience with the teleoperation system.

Users wore the data glove and were able to open and close their hand to control the robotic gripper. Rather than controlling the robotic arm with IMUs, they were also given a computer keyboard which sent the robotic arm to pre-programmed positions for a pick-and-place task. To remove variables related to visual feedback, we blocked the users' view of the physical robot and instead showed them a monitor with a live feed from a camera facing the robot. The user test setup and the users' view are shown in Fig 6.6. Their task was to pick and place a small soft toy, and we instructed users to be as gentle as possible with the toy.

The sequence was as follows: 1) the user pressed a button to move the arm from its "home" position to hover over the soft toy, 2) the user closed their hand (thus closing the gripper) until they were confident that they had grasped the toy 3) the user pressed the button to send the arm to a position over a bin and 4) the user opened their hand, causing the gripper to drop the toy into the bin. They completed this task with no haptic feedback, while wearing the plastic haptic muscles presented in the previous paper, and while wearing the Ecoflex0030 haptic muscles presented in this paper.

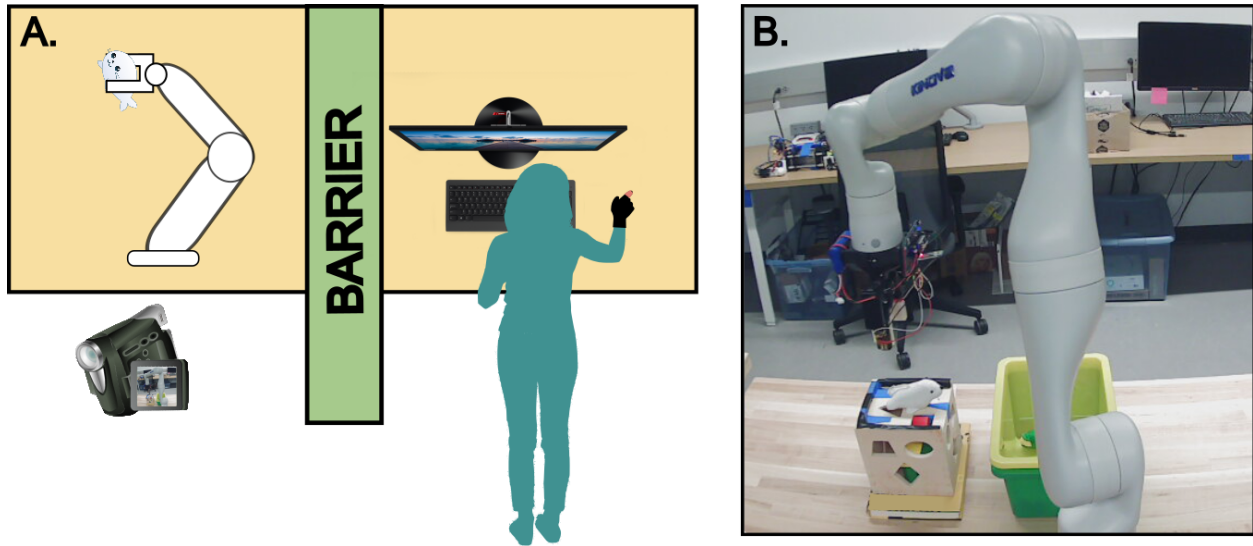


**Figure 6.6:** User test setup simulating remote teleoperation with a robotic arm and gripper. (a) The setup includes a camera pointing at the robot with the video fed to the monitor, and a barrier to prevent the user from seeing the physical robot. The user wears a data glove with haptic muscles and controls the arm with the glove and a keyboard. (b) The user watches a monitor which streams live video of the robot arm.

**Table 6.6:** Novice Haptic Test Results (12 users)

	Avg Max Force	Number of Drops (Total)	Avg Challenge Rating
Without Haptics	0.947 N	6	6.2
Plastic Haptic Muscles	0.698 N	3	5.1
Ecoflex0030 Haptic Muscles	<b>0.457 N</b>	<b>0</b>	<b>4.7</b>

After practicing twice in each scenario, users performed the pick and place task 5 times with each type of feedback, for a total of 15 tests. During the tests we kept track of how many times they dropped the soft toy. After each set of 5 tests, we asked users to rate how challenging it was to handle the soft toy delicately, from 0 (not at all challenging) to 10 (extremely challenging).

#### 6.5.4 User Test Results: Novice Haptic Study

We synthesized the pick and place results by calculating the maximum force applied during each attempt by averaging the highest 10 force readings. We then took an average of maximum force readings across all users for each scenario. We also averaged their ratings from the user experience questions. The results of these user tests are shown in Table 6.6.

Without haptic feedback, a user only has visual cues about whether the object they are handling is deforming or not, which are not sufficient. With haptic feedback, users are able to first detect contact, then gauge whether the grasp strength is sufficient to transport the object without dropping or damaging it. One novice user stated that the silicone-based haptic muscles allowed them to more accurately gauge how hard they were grasping the soft toy because “the sensation was more linearly related to the amount I was squishing it”. These user tests demonstrate that the new sensitivity gained from the re-design of the haptic muscles greatly improves the teleoperation experience as well as the capabilities of the teleoperation system. They also emphasize the results of the previous force output experiments that showed the plastic haptics to be too binary to allow for fragile object handling during teleoperation.

### **6.5.5 User Test Description: Novice Teleoperation Study**

We wanted to test the effects of all the changes to the teleoperation system by redoing the user test from Phase 3, where users picked and placed 4 differently shaped objects. We tested 10 users with the teleoperation system using similar or the same objects: a soft bear, a box of appropriate size, a robot-shaped stress toy, and a paper cup. We did not test with the water bottle because the off-the-shelf gripper made the pick too difficult in pilot testing. For this round of testing, all our users were inexperienced with the system.

We began each test by having the users wear the motion capture system and perform a calibration routine, as discussed in section 3, to align the user and robot workspaces. We then allowed the user 10 minutes of training in which they picked and placed various shaped objects. During this time, users could choose to recalibrate the arm and change their preferred workspaces to ensure maximum comfort. The first 5 minutes of training were without haptic feedback, and the second 5 minutes were with haptic feedback.

After training, we laid all 4 objects on the table, in rather random locations that we were sure were within the robot workspace. We wanted to add this slight difficulty to show the capabilities of the new mapping system. We then told the user which object to pick and place. We then counted down to ensure that our timer began when the user intended to complete the task. We stopped

the timer when the user placed or dropped the object into the box, and recorded the time. After the users finished picking and placing all 5 objects, we paused teleoperation and asked them to fill the NASA TLX (Task Load Index) survey which reported how challenging the task was from various angles, such as mental load, physical load, and frustration. We repeated this 6 times, 3 times with haptic feedback and 3 without. We alternated whether the haptic feedback was on or off to compensate for user learning through the task.

### **6.5.6 User Test Results: Novice Teleoperation Study**

The first major result of this test is that across all users, who were all inexperienced, the average time to pick and place an object with our system was 18.63 seconds, as compared to 44.85 seconds as shown in Phase 3 user testing. This shows that the teleoperation system as a whole has improved tremendously in intuitiveness and usability for performing tasks that use the entire table as a workspace. in Fig 6.7 of the user test results for each object, along with the averages and standard deviations across users. We see that the average has reduced greatly, as has the standard deviation because more users are more comfortable using the system.

We also find that the time to pick an object decreases with more experience, as shown in Fig 6.8 where we show each user's average task time across all objects per run. We see that there are a few outliers, but in general users take less time to complete later runs because they quickly overcome any initial discomforts or nervousness from the initial trials.

When comparing trials with haptics versus without haptics, we find that task completion time is not affected by haptics. This is probably because once a user is comfortable using a teleoperation system for a pick and place task, they can generally visually ascertain whether they have grabbed the object or not, and haptics does not significantly speed up their task time. We did find, however, that having haptics present led to greater satisfaction and less negative feeling during the task, as shown by the responses to the NASA TLX survey. Across all users, the "negative feeling", that is, the average of all the questions related to demand or frustration, decreased when the haptics were present, as shown in Fig 6.9. Because the haptic feedback decreased the demand on the user, this

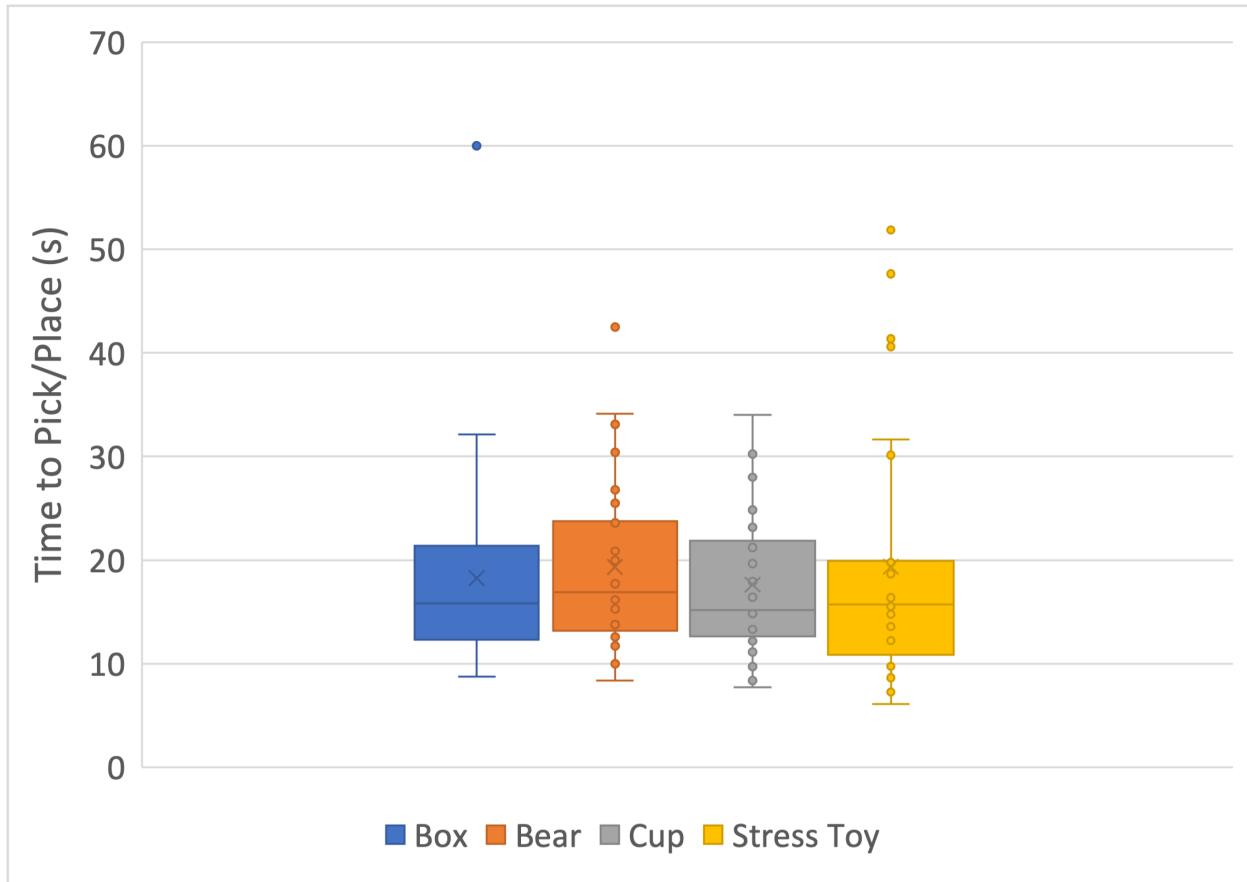


**Figure 6.7:** We performed a pick-and-place test with 10 users and 4 objects of varying size and stiffness to gauge how well they can use the system. The results that users perform an average pick and place in 18.63 seconds. We find that the new human-robot mapping scheme improves both average performance and standard deviation of task completion time. This shows that more users are more comfortable with the system with very few outliers who struggled more.

indicates that haptics will be helpful in more complex tasks, particularly with more experienced users.

### 6.5.7 User Test Description: Expert Teleoperation Study

As a final study to show the potential of the new haptic muscles in a full teleoperation setting, we ran a pilot test with an expert user who has trained on the teleoperation system for several hours. They used the system, including full control of the robotic arm and gripper, to pick and place soft baked fruit bars (Kellogg’s Nutrigrain). The fruit bars were particularly fragile and brittle, prone to cracking and deforming during even normal handling. The expert performed this task with no

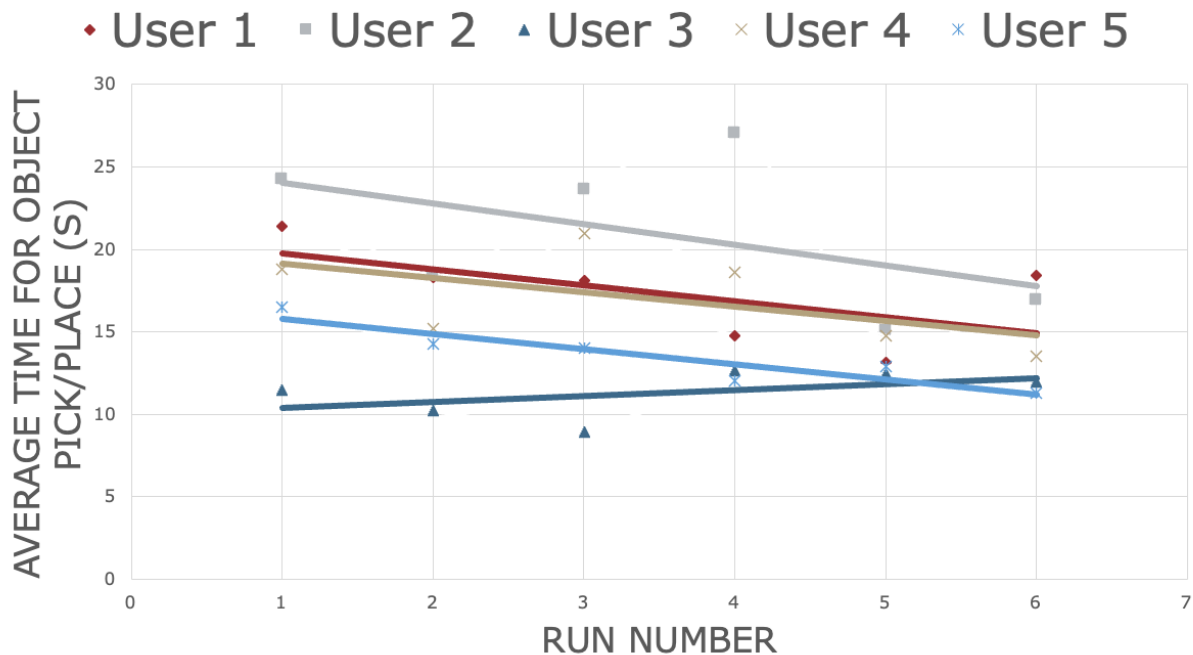


**Figure 6.8:** We performed a pick-and-place test with 10 users and 4 objects of varying size and stiffness to gauge how well they can use the system. We find that, in general, users complete the pick and place more quickly as they gain experience with the system. In this plot we show a sample of 5 users and their average pick and place times over the course of testing. The trendline shown shows a slight downward trend when comparing completion times over all 6 runs of the experiment.

haptic feedback and while wearing the Ecoflex0030 haptic muscles. They completed 3 tests in each scenario, for a total of 6 tests.

### 6.5.8 User Test Results: Expert Teleoperation Study

Two representative plots of the expert test are shown in Fig 6.10. The expert user applied on average 58% less force given haptic feedback, and this was reflected in the state of the fruit bars after testing. The attempts with haptic feedback resulted in intact fruit bars with little to no damage, while all attempts without feedback and with plastic haptic muscles resulted in deformed or entirely broken bars. The more sensitive haptic muscles allowed the user to adjust their grasp to keep hold of the fruit bar (Fig 6.10b). These preliminary results are very promising, and we will continue to explore the capabilities of the Ecoflex0030 haptic muscles with more expert users in future work.

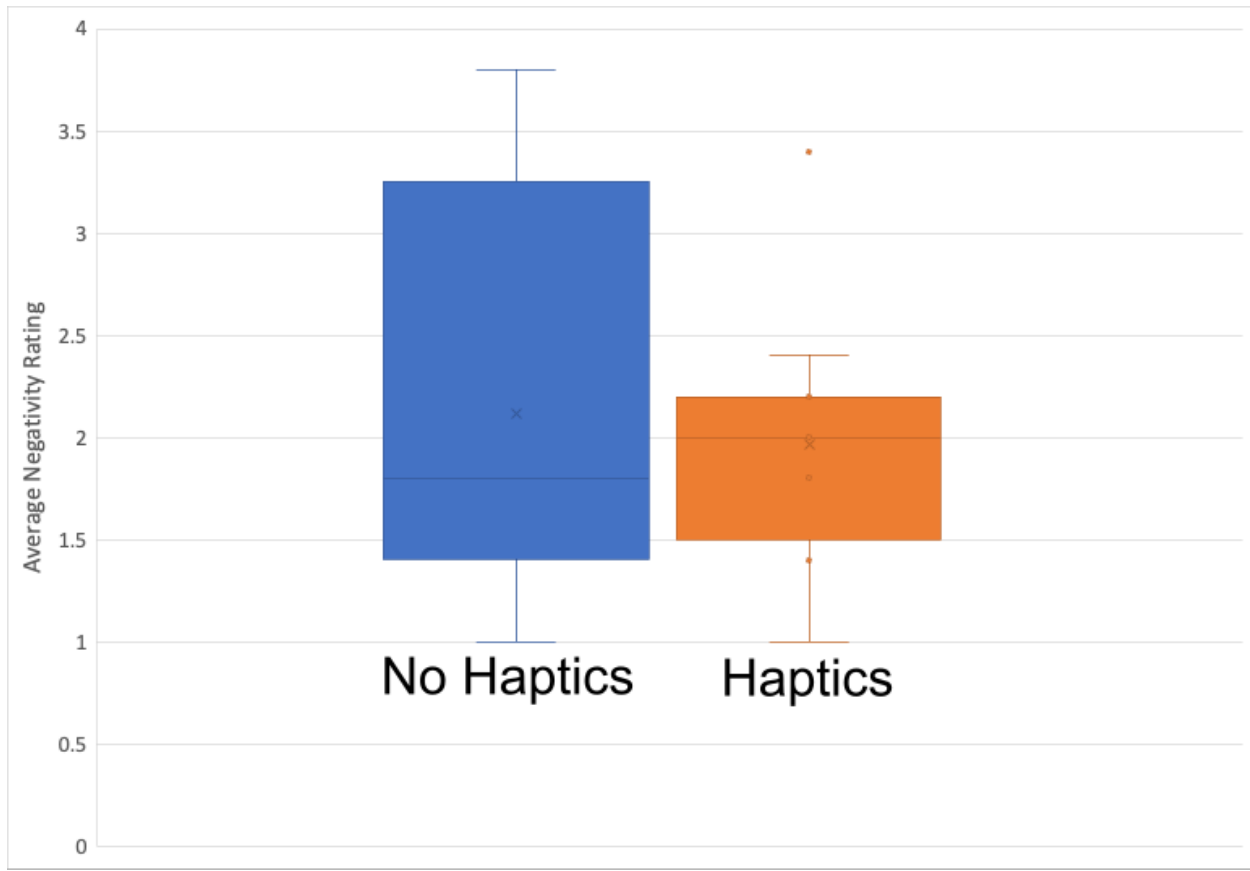


**Figure 6.9:** We performed a pick-and-place test with 10 users and 4 objects of varying size and stiffness to gauge how well they can use the system. After each run of picking and placing 4 objects, we asked them to fill out a NASA Task Load Index survey. We calculate "average negativity" as the average of the user's responses to the task load questions. We find that the presence of haptic feedback decreases users' average negativity and therefore mental load during the task.

### 6.5.9 User Test Conclusions and Future Work

After synthesizing our results from the novice and expert user tests, we found that the teleoperation system was much improved and allowed novice users to perform pick and place tasks with as little as 10 minutes of training. We also found that these novice users gain confidence with the system very quickly, showing how the intuitiveness of our system has improved. We showed that the haptic feedback decreased mental load during pick and place tasks, and allowed expert users to successfully pick and place delicate fruit bars several times.

During these tests, we found that the limiting factor was the off-the-shelf gripper, which proved slower to control than the robotic arm itself. Additionally, the two fingers were not enough to grasp

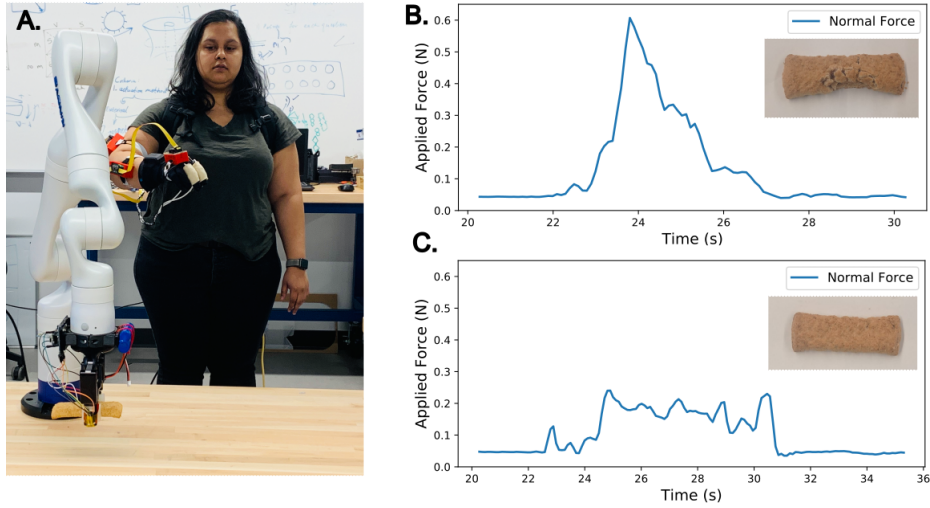


**Figure 6.10:** Teleoperation experiment to pick and place a soft fruit bar by an experienced user: (a) without haptic feedback and (b) with haptic feedback. The plots show normal force applied during the task, as well as the state of the fruit bar at the end of the attempt.

more complex shapes, and the silicone pads covering the force sensors were slightly thick and bulky. We therefore suggest that the next step to improving this system is to use a better-equipped gripper with force sensing, such as an improved version of the anthropomorphic gripper presented in section 5.



# Chapter 7

## Broader Impacts

### 7.1 Broader Impact

Our goal over the course of this project has been to develop and test a solid and usable teleoperation system that provides haptic feedback in a useful and intuitive way. We have achieved this goal, and to prove the usability of the system we have developed many user tests that show how the haptic feedback improves user performance in specific tasks. The result is a generic system that has been proved out with “toy” problems, which is sufficient for technical research purposes.

This teleoperation system can potentially be integrated into larger systems in spaces such as space exploration, medical care, and warehouse logistics. However, each application has a different set of benefits, requirements, and concerns that would change how we implement the teleoperation system. This is partially because each field has a different set of technical requirements and tasks to be done, but also because each setting has a different user who wants to interact with the system in a different way. In this broader impacts section, I will discuss the technical and human factors requirements of each field, and explore how we can innovate responsibly in these different sectors. I will begin to address what factors to consider when considering applying teleoperation technology in industry and research space, and how such considerations can define future teleoperation research. I will also discuss integrating the teleoperation with artificial intelligence systems and the

potential for human-drive AI models. Finally I will conclude with a discussion on the importance of STEM education and outreach, and my experiences with outreach and mentorship.

## **7.2 Responsible Innovation In Different Sectors**

### **7.2.1 Space Exploration**

One major benefit of remote teleoperation is the ability for a user to perform tasks in remote or dangerous locations while staying safe. One example of this is space exploration. It is prohibitively expensive to send astronauts into space, and even after extensive training astronauts find life on the ISS fairly difficult. Additionally, planets like Mars and Venus are extremely dangerous environments, so they can only be explored by autonomous rovers. Robot teleoperation has the potential to accelerate space research by allowing people to perform more complicated tasks without relying on an astronaut or autonomous system [5].

To integrate our teleoperation system into a space exploration system would require us to dive deeper into user experiences that are specific to deep-space tasks. Firstly we consider what tasks might be done in space, and we find in the literature that target grasping, particularly in cluttered environments, is an important aspect of extraterrestrial exploration [75]. We also find that users expect to be in controlled and isolated environments, and do not mind being tethered to large teleoperation systems. By exploring what objects a teleoperated robot is expected to work with, we can make design decisions about the end-effector of the robot, and potentially reduce the complexity of the teleoperation system.

One large consideration is the time delay between the user and robot movement due to the distance between them [76]. This delay is at minimum 0.4 seconds but is usually between 3 and 6 seconds, which greatly interferes with the telepresence experience. This delay affects both robot movement and haptic feedback, and it is very difficult for a user to utilize the haptic feedback well at such latencies. Much research that addresses teleoperation for space exploration revolves around this latency problem, and there are several proposed solutions, including predictive models for control and force feedback. Many of these solutions involve some basic autonomy to help

the teleoperator with simple motions [77]. The idea of assistive teleoperation is not new, but it remains a deeply technical problem, and there is more research to perform to gauge how factors like user trust and comfort are affected by teleoperation. During our studies, we find that users enjoy having full control of the robotic arm, and if the robot behaved unexpectedly they would be uncomfortable.

## **7.2.2 Warehouse Logistics**

A second benefit of robot teleoperation systems is the transfer of effort between the user and the robot [78]. A user can teleoperate a robot to lift a heavy object or apply large forces without overextending or injuring themselves. This can be especially helpful to warehouse workers, who tend to suffer from stress injuries in their arms, legs, and backs due to repeatedly lifting heavy items. According to a Bureau of Labor Statistics report, “transportation and warehousing increased from 206,900 cases in 2020 to 253,100 cases in 2021” [79]. Remote teleoperation can allow workers to stay more stationary, help them lift heavy objects without strain, and sometimes complete tasks in inherently dangerous spaces, such as around forklifts. This can allow workers to be safer, more efficient, and more satisfied with their jobs.

When considering robots that work in warehouses, much of the current research focuses on mobile robots that can travel around the warehouse [80], similar to space exploration robots. The difference is that a mobile robot on a warehouse floor may have to interact with other workers. This leads to questions of trust and safety, and if the user were remote, we may consider whether other workers would be wary of a robot that seems autonomously intelligent even though it is under someone’s direct control [81]. Perhaps this situation would require the robot to have a screen in which the user is visible, or perhaps the user should be able to speak through the robot. Unlike the space exploration scenario, warehouse workers may not appreciate semi-autonomous assistance during teleoperation and may want as much control as possible.

Another consideration is the location of the teleoperator in a warehouse scenario. Because a warehouse is, for the most part, not an inherently dangerous place, they may prefer to be very close to the robot, or they may prefer to be in another building. Some studies explore the use

of virtual reality or augmented reality systems that perform mobile robot teleoperation, but these studies focus on keeping the worker far from the robot [82][83]. If the worker would prefer to be in the warehouse, we would have to consider the comfort and portability of the system over long periods of use. The current version is portable and comfortable for a relatively short user study, but may become uncomfortable over a full workday. Another consideration if the user is very active is user intentionality, that is, whether a user movement is meant to control the robot or not. If, for example, another warehouse worker accidentally jostled the user, we would not want the robot to respond. Current studies in autonomous obstacle avoidance and the use of virtual reality spaces that keep the user remote show that there is some work to do to enhance the realism and sense of control in such experiences.

In the warehouse scenario, we can look at the teleoperator, robot, and human warehouse workers as a whole system that needs to interact seamlessly, safely, and with trust. In comparing the space exploration and warehouse logistics sectors, it is clear that the more people are involved, the more questions there are about human factors, trust, and human-robot interaction.

### **7.2.3 Medical Care**

The COVID-19 pandemic clearly showed the challenges of performing normal nursing tasks when dealing with a severely contagious disease [84]. While some of these tasks can be autonomous, people in hospitals look to nurses for personalized care and comfort. A teleoperated nursing system would allow nurses to provide this care while themselves staying distanced and comfortable [85][86]. This has the potential to address issues like burnout, physical stress, and contagion in medical care spaces. It has also been shown that higher levels of telepresence in the system could “provide a stronger feeling of a person to person interaction for both users, in comparison to video and phone calls” [87].

As with the warehouse logistics example, we must consider both the teleoperation user and the human (likely a patient) interacting with the teleoperated robot. In the case of medical care, the patient would likely be from a vulnerable population; they may be elderly, disabled, or a child. This vulnerability adds to the questions of safety and trust, because patients must be treated with

immense care. If the nursing tasks involve physically interacting with a patient, we must perform intense reliability testing to ensure the teleoperated robot cannot harm anyone, even if the nurse controlling it makes a mistake, is jostled, or loses control. There is also the question of whether a patient would feel cared for and comfortable if they are staying at a hospital full of robots, even if the robots are teleoperated. In medical spaces, it has been shown that seeing and hearing the operator increases trust and comfort in patients [88].

In the medical scenario, using robots to help with tasks, however menial, raises many concerns about safety and trust, as well as the comfort and satisfaction of the people being cared for. The fact that these people may be from vulnerable populations increases the importance and complexity of these concerns.

### **7.3 Teleoperation-Driven AI**

Artificial intelligence (AI) has become one of the next big things in technology. Every day there seems to be a new article about the cutting-edge discoveries researchers are making in AI, and how the new AI is growing more powerful and "intelligent". Currently, AI is causing major concerns in the media and in industry because some people worry it is growing too powerful and we cannot understand it. There are also concerns that, given new advances in robotic manufacturing and control, this super-intelligent AI will be able to act on the physical world in unpredictable and scary ways.

Because my work is in the realms of robotics, and because teleoperation can be used as a tool for artificial intelligence, I will briefly touch on some of these concerns and how teleoperation has the potential to help.

Artificial Intelligence is a term many people use to describe the development of computer systems that can perform tasks normally associated with human intelligence, such as visual perception, speech recognition, and decision-making. There is, however, a concern that such automated and "intelligent" systems are devoid of transparency. Machine learning algorithms are black boxes, which are trained on many inputs until it gives a reasonably correct output. Even the programmers

of such algorithms are not certain why they output what they do, which becomes an issue when the outputs are questionable or based on biased data.

Our research falls under an interesting category of autonomy that depends on human demonstrations. This gives us the opportunity to be more transparent than most autonomous system developers about how the autonomy was built in the first place. In many AI cases, the input data comes from a large database that is too large for anyone to properly vet, which increases the lack of transparency and trust in such systems. In our case, however, the input data is provided by real people, and part of our goal is to ensure that the expert demonstrators need not be roboticists.

It is clear that we are already being exposed to AI models that can be very helpful in our daily lives (like ChatGPT) but that are also causing concerns about AI development in general. Learning from demonstration through teleoperation has the potential to democratize robot training and thus expose more non-technical people to the idea of robot autonomy. This has the potential to help increase trust in other autonomous systems, especially if aided by increased education and awareness of AI.

## **7.4 STEM Education and Outreach**

As automation and robotics change the definition of work and the kinds of tasks people do in the workplace, it is vital that our education systems keep up with these new developments. During my time at WPI, I have had many opportunities to be part of education and outreach programs, especially those that encourage people from minority populations to pursue a STEM education. During these processes I learned about leadership, communication, and the power of diversity on STEM teams.

WPI has many outreach programs, and many of them are tailored to grade-school children. One of these was TouchTomorrow, a day-long event in Worcester where many groups from WPI showcased their work to children and parents in the Worcester area. The event was free to attend, which made it an amazing opportunity to interact with young children who may not have been exposed to STEM yet. It was a chance to show them how interesting and impactful a STEM

career could be. In turn, we learned how to explain our research, which is generally published in academic journals, to young children so they would understand what we were working on. In particular, I learned to add much more background and impact factor to my explanations, while keeping the technicals light and understandable. I believe every engineering student should have this opportunity to practice engineering communication in such an intense and exciting way.

Another of WPI's outreach programs, titled WRAMP (Womens' Research and Mentorship Program), gave me the opportunity to work with a diverse group of high school women from the Worcester area and introduce them to robotics research. As the team leader, I was responsible for designing the project we would work on together, as well as helping them think through solutions to the technical problems they faced in the lab. This was a delicate balance of engineering and teaching, and not only did it change the students' lives, it changed me as well.

The students I worked with included a young woman on the autism spectrum, a Hispanic woman who had never coded before, an adopted Guatemalan woman with an identity crisis, and a Chinese American woman with deep-set imposter syndrome. Across the board, this program helped these women feel more comfortable with who they were, and convinced them that engineering could be an exciting and impactful career to pursue. The program also gave me a deeper understanding of the importance of diversity in teams. My group was always giving me new ideas, like using soft robots as fidget toys or pouring silicone over crafting beads to make a coaster. This experience convinced me that diversity is not just a vague moral idea, but a concrete advantage for an engineering team. Finally, I learned the importance of breaking the student-teacher model and creating a comfortable environment for my mentees to share ideas. Their ideas and the conversations we had gave our team new insights and pivoted our research in amazing and unexpected ways.

Introducing young people to STEM, especially those from underserved populations, is the only way to keep up with current changes in technology and the workforce. I look forward to continuing this work and seeking opportunities to mentor and excite students in STEM fields.

# Chapter 8

## Conclusions and Future Work

This report has covered our six years of research regarding intuitive teleoperation of a robotic arm and hand, and the use of soft materials as haptic feedback devices. We have discussed the system we built, delved into the details of each subsystem, reported on the various phases of the system, and presented the results of various phases of user testing. Finally, we explored the broader impacts of this research from various industrial and research angles. From this research we have several conclusions and insights about the fields of robot teleoperation and haptics.

Robot arm teleoperation is a unique field where we develop a complex and moving system with many parts, then invite novice users to take full control of the system. Teleoperation is equally a technical and user-oriented problem, and in this report we have explored and addressed both kinds of issues. Our goal, to create a system usable by any novice user, is a goal we have addressed by using better grippers and building better haptic devices, but also by considering what a user considers intuitive in a human-to-robot mapping scheme. Our ideas about what make a good teleoperation system have come from technical papers but also from interviews with users and much synthesis of the qualitative feedback they have given us. We therefore have a unique experience of developing a teleoperation system in multiple phases using user-oriented design principles and user testing to help define the phases of work.

Given the improvement of the teleoperation system over time, we can say that we have achieved our goals. In a user test with only novice users, we showed a reduced task time by about 60% as



compared to an older user test with novice and expert users. We have enabled users to pick and place fragile and brittle objects, and we have done so using a system that is lightweight, low-cost, and portable. We have also found that haptic feedback decreases users' mental and physical load even during simple pick-and-place tasks. As ongoing research, we have explored teleoperation of anthropomorphic hands, and various end-effector force sensing modalities, and we have developed a 3D-printable anthropomorphic hand with accurate force sensing that does not experience drift.

There are several paths forward for our research regarding improving the teleoperation system. Firstly, we have proven the efficacy of the haptic feedback, but can do more to increase the comfort and usability of the haptics, such as choosing thinner fabrics, making them adjustable, and using thinner layers of silicone. Secondly, we have proved that an anthropomorphic hand is useful for teleoperation but also that it can complicate the user experience, so we might research more intuitive hands and hand-mapping schemes. Finally, we can begin exploring a particular sector where teleoperation can be useful, such as warehouse logistics or at-home care, and tailor the system to do complex tasks within those spaces.

# Bibliography

- [1] A. Dwivedi, A. Ramakrishnan, A. Reddy, K. Patel, S. Ozel, and C. D. Onal, “Design, modeling, and validation of a soft magnetic 3-d force sensor,” *IEEE Sensors Journal*, vol. 18, no. 9, p. 3852–3863, May 2018.
- [2] S. Swart, H. J. Zietsman, N. D. Goslett, and P. M. S. Monteiro, “Ocean robotics for sustainable, long-range marine resource and ecosystem management in the 21st century: natural environment,” *CSIR Science Scope*, vol. 8, no. 2, p. 102–103, Jan 2015.
- [3] A. Schweikard and F. Ernst, *Medical Robotics: Introduction*. Cham: Springer International Publishing, 2015, p. 1–27. [Online]. Available: [https://doi.org/10.1007/978-3-319-22891-4\\_1](https://doi.org/10.1007/978-3-319-22891-4_1)
- [4] L. Schmidt, J. Hegenberg, and L. Cramar, “User studies on teleoperation of robots for plant inspection,” *Industrial Robot: An International Journal*, vol. 41, Jan 2014.
- [5] T. Sheridan, “Space teleoperation through time delay: review and prognosis,” *IEEE Transactions on Robotics and Automation*, vol. 9, no. 5, p. 592–606, Oct 1993.
- [6] C. Preusche, T. Ortmaier, and G. Hirzinger, “Teleoperation concepts in minimal invasive surgery,” *Control Engineering Practice*, vol. 10, no. 11, p. 1245–1250, Nov 2002.
- [7] J. Petereit, J. Beyerer, T. Asfour, S. Gentes, B. Hein, U. D. Hanebeck, F. Kirchner, R. Dillmann, H. H. Götting, M. Weiser, M. Gustmann, and T. Egloffstein, “Robdekon: Robotic systems for decontamination in hazardous environments,” Sep 2019, p. 249–255.

- [8] R. G. Boboc, H. Moga, and D. Talaba, "A review of current applications in teleoperation of mobile robots," *Bulletin of the Transilvania University of Brasov. Engineering Sciences. Series I*, vol. 5, no. 2, p. 9–16, 2012.
- [9] W. s. Liu and Y. Li, "The research for control strategies and methods of teleoperation system," in *World Automation Congress 2012*, Jun 2012, p. 1–4.
- [10] A. Bolopion and S. Régnier, "A review of haptic feedback teleoperation systems for micromanipulation and microassembly," *IEEE Transactions on Automation Science and Engineering*, vol. 10, no. 3, p. 496–502, Jul 2013.
- [11] R. Rahman, M. S. Rahman, and J. R. Bhuiyan, "Joystick controlled industrial robotic system with robotic arm," in *2019 IEEE International Conference on Robotics, Automation, Artificial-intelligence and Internet-of-Things (RAAICON)*, Nov 2019, p. 31–34.
- [12] K. Yamashita, Y. Kato, K. Kurabe, M. Koike, K. Jinno, K. Kito, K. Tatsuno, and M. T. Sqalli, "Remote operation of a robot for maintaining electric power distribution system using a joystick and a master arm as a human robot interface medium," in *2016 International Symposium on Micro-NanoMechatronics and Human Science (MHS)*, Nov 2016, p. 1–7.
- [13] M.-F. Crainic and S. Preitl, "Ergonomic operating mode for a robot arm using a game-pad with two joysticks," in *2015 IEEE 10th Jubilee International Symposium on Applied Computational Intelligence and Informatics*, May 2015, p. 167–170.
- [14] A. Dünser, M. Lochner, U. Engelke, and D. R. Fernández, "Visual and manual control for human-robot teleoperation," *IEEE Computer Graphics and Applications*, vol. 35, no. 3, p. 22–32, May 2015.
- [15] R. Alves, R. Vassallo, E. Freire, and T. Bastos-Filho, "Teleoperation of a mobile robot through the internet," in *Proceedings of the 43rd IEEE Midwest Symposium on Circuits and Systems (Cat.No.CH37144)*, vol. 2. Lansing, MI, USA: IEEE, 2000, p. 930–933. [Online]. Available: <http://ieeexplore.ieee.org/document/952906/>

- [16] L. V. Herlant, R. M. Holladay, and S. S. Srinivasa, “Assistive teleoperation of robot arms via automatic time-optimal mode switching,” *Proceedings of the ... ACM SIGCHI. ACM Conference on Human-Robot Interaction*, vol. 2016, p. 35–42, Mar 2016.
- [17] M. Micire, M. Desai, J. L. Drury, E. McCann, A. Norton, K. M. Tsui, and H. A. Yanco, “Design and validation of two-handed multi-touch tabletop controllers for robot teleoperation,” in *Proceedings of the 16th international conference on Intelligent user interfaces*, ser. IUI ’11. New York, NY, USA: Association for Computing Machinery, Feb 2011, p. 145–154. [Online]. Available: <https://dl.acm.org/doi/10.1145/1943403.1943427>
- [18] D. Rakita, “Methods for effective mimicry-based teleoperation of robot arms,” in *Proceedings of the Companion of the 2017 ACM/IEEE International Conference on Human-Robot Interaction*. Vienna Austria: ACM, Mar 2017, p. 371–372. [Online]. Available: <https://dl.acm.org/doi/10.1145/3029798.3034812>
- [19] M. Takagi, Y. Takahashi, S. Yamamoto, H. Koyama, and T. Komeda, “Vision based interface and control of assistive mobile robot system,” in *2007 IEEE 10th International Conference on Rehabilitation Robotics*, Jun 2007, p. 341–346.
- [20] F. Marić, I. Jurin, I. Marković, Z. Kalafatić, and I. Petrović, “Robot arm teleoperation via rgbd sensor palm tracking,” in *2016 39th International Convention on Information and Communication Technology, Electronics and Microelectronics (MIPRO)*, May 2016, p. 1093–1098.
- [21] F. Kobayashi, K. Kitabayashi, H. Nakamoto, and F. Kojima, “Hand/arm robot teleoperation by inertial motion capture,” in *2013 Second International Conference on Robot, Vision and Signal Processing*, Dec 2013, p. 234–237.
- [22] Q. He, Z. Zheng, X. Zhu, H. Zhang, Y. Su, and X. Xu, “Design and implementation of low-cost inertial sensor-based human motion capture system,” in *2022 International Conference on Cyber-Physical Social Intelligence (ICCSI)*, Nov 2022, p. 664–669.

- [23] J.-H. Kim, N. D. Thang, and T.-S. Kim, “3-d hand motion tracking and gesture recognition using a data glove,” in *2009 IEEE International Symposium on Industrial Electronics*, Jul 2009, p. 1013–1018.
- [24] B. Fang, F. Sun, H. Liu, and D. Guo, “A novel data glove using inertial and magnetic sensors for motion capture and robotic arm-hand teleoperation,” *Industrial Robot: An International Journal*, vol. 44, no. 2, p. 155–165, Jan 2017.
- [25] K. Kukliński, K. Fischer, I. Marhenke, F. Kirstein, M. V. aus der Wieschen, D. Sølvason, N. Krüger, and T. R. Savarimuthu, “Teleoperation for learning by demonstration: Data glove versus object manipulation for intuitive robot control,” in *2014 6th International Congress on Ultra Modern Telecommunications and Control Systems and Workshops (ICUMT)*, Oct 2014, p. 346–351.
- [26] M. Pan, Y. Tang, and H. Li, “Review of the state-of-the-art of data gloves,” Dec 2022, p. 402–405.
- [27] X. Zhu, X. Wang, and Y. Ma, “Design and development of teleoperation interactive system for 7-dof space redundant manipulator,” in *2021 5th International Conference on Automation, Control and Robots (ICACR)*, Sep 2021, p. 179–183.
- [28] B. Omarali, K. Althoefer, F. Mastrogiovanni, M. Valle, and I. Farkhatdinov, “Workspace scaling and rate mode control for virtual reality based robot teleoperation,” in *2021 IEEE International Conference on Systems, Man, and Cybernetics (SMC)*, Oct 2021, p. 607–612.
- [29] K. Kamali, I. A. Bonev, and C. Desrosiers, “Real-time motion planning for robotic teleoperation using dynamic-goal deep reinforcement learning,” in *2020 17th Conference on Computer and Robot Vision (CRV)*, May 2020, p. 182–189.
- [30] R. Li, H. Wang, and Z. Liu, “Survey on mapping human hand motion to robotic hands for teleoperation,” *IEEE Transactions on Circuits and Systems for Video Technology*, vol. 32, no. 5, p. 2647–2665, May 2022.

- [31] E. Sartori, P. Fiorini, and R. Muradore, “Cutaneous feedback in teleoperated robotic hands,” Oct 2016, p. 686–691.
- [32] A. Frisoli, M. Solazzi, F. Salsedo, and M. Bergamasco, “A fingertip haptic display for improving curvature discrimination,” *Presence*, vol. 17, no. 6, p. 550–561, Dec 2008.
- [33] J. H. Low, W. W. Lee, P. M. Khin, N. V. Thakor, S. L. Kukreja, H. L. Ren, and C. H. Yeow, “Hybrid tele-manipulation system using a sensorized 3-d-printed soft robotic gripper and a soft fabric-based haptic glove,” *IEEE Robotics and Automation Letters*, vol. 2, no. 2, p. 880–887, Apr 2017.
- [34] S. D. Laycock and A. M. Day, “Recent developments and applications of haptic devices,” *Computer Graphics Forum*, vol. 22, no. 2, p. 117–132, 2003.
- [35] R. P. Khurshid, N. T. Fitter, E. A. Fedalei, and K. J. Kuchenbecker, “Effects of grip-force, contact, and acceleration feedback on a teleoperated pick-and-place task,” *IEEE Transactions on Haptics*, vol. 10, no. 1, p. 40–53, Jan 2017.
- [36] K. Fujimoto, F. Kobayashi, H. Nakamoto, and F. Kojima, “Development of haptic device for five-fingered robot hand teleoperation,” in *Proceedings of the 2013 IEEE/SICE International Symposium on System Integration*, Dec 2013, p. 820–825.
- [37] Z. MA and P. Ben-Tzvi, “Rml glove—an exoskeleton glove mechanism with haptics feedback,” vol. 20, p. 641–652, Apr 2015.
- [38] S. Nisar, M. O. Martinez, T. Endo, F. Matsuno, and A. M. Okamura, “Effects of different hand-grounding locations on haptic performance with a wearable kinesthetic haptic device,” *IEEE Robotics and Automation Letters*, vol. 4, no. 2, p. 351–358, Apr 2019.
- [39] S. Baik, S. Park, and J. Park, “Haptic glove using tendon-driven soft robotic mechanism,” *Frontiers in Bioengineering and Biotechnology*, vol. 8, p. 541105, Oct 2020.

- [40] M. Bouzit, G. Burdea, G. Popescu, and R. Boian, “The rutgers master ii-new design force-feedback glove,” *IEEE/ASME Transactions on Mechatronics*, vol. 7, no. 2, p. 256–263, Jun 2002.
- [41] B. Jumet, Z. A. Zook, D. Xu, N. Fino, A. Rajappan, M. W. Schara, J. Berning, N. Escobar, M. K. O’Malley, and D. J. Preston, “A textile-based approach to wearable haptic devices,” in *2022 IEEE 5th International Conference on Soft Robotics (RoboSoft)*, Apr 2022, p. 741–746.
- [42] S.-Y. Teng, P. Li, R. Nith, J. Fonseca, and P. Lopes, “Touchfold: A foldable haptic actuator for rendering touch in mixed reality,” in *Proceedings of the 2021 CHI Conference on Human Factors in Computing Systems*, ser. CHI ’21. New York, NY, USA: Association for Computing Machinery, May 2021, p. 1–14. [Online]. Available: <https://dl.acm.org/doi/10.1145/3411764.3445099>
- [43] Y. Sun, Y. S. Song, and J. Paik, “Characterization of silicone rubber based soft pneumatic actuators,” Nov 2013, p. 4446–4453.
- [44] N. Elango and A. A. M. Faudzi, “A review article: investigations on soft materials for soft robot manipulations,” *The International Journal of Advanced Manufacturing Technology*, vol. 80, no. 5, p. 1027–1037, Sep 2015.
- [45] “Design and characterization of a novel fabric-based robotic arm for future wearable robot application,” Dec 2017, p. 367–372.
- [46] [Online]. Available: <https://robotiq.com/products>
- [47] G. E. Loeb and R. Johansson, “Biomimetic tactile sensor,” Feb 2010. [Online]. Available: <https://patents.google.com/patent/US7658119/en>
- [48] J. Nichols Cook, A. Sabarwal, H. Clewer, and W. Navaraj, “Tactile sensor array laden 3d-printed soft robotic gripper,” in *2020 IEEE SENSORS*, Oct 2020, p. 1–4.

- [49] T. Q. Dinh, J. I. Yoon, J. Marco, P. Jennings, K. K. Ahn, and C. Ha, “Sensorless force feedback joystick control for teleoperation of construction equipment,” *International Journal of Precision Engineering and Manufacturing*, vol. 18, no. 7, p. 955–969, Jul 2017.
- [50] J. R. McKinsey and G. T.-C. Chiu, “Interfacing a force-feedback joystick with a hydraulic robot arm,” in *2007 International Symposium on Computational Intelligence in Robotics and Automation*, Jun 2007, p. 497–503.
- [51] T. Klamt, M. Schwarz, C. Lenz, L. Baccelliere, D. Buongiorno, T. Cichon, A. DiGuardo, D. Droschel, M. Gabardi, M. Kamedula, N. Kashiri, A. Laurenzi, D. Leonardis, L. Muratore, D. Pavlichenko, A. S. Periyasamy, D. Rodriguez, M. Solazzi, A. Frisoli, M. Gustmann, J. Roßmann, U. Süß, N. G. Tsagarakis, and S. Behnke, “Remote mobile manipulation with the centauro robot: Full-body telepresence and autonomous operator assistance,” *Journal of Field Robotics*, vol. 37, no. 5, p. 889–919, 2020.
- [52] L. Meli, G. Salvietti, G. Gioioso, M. Malvezzi, and D. Prattichizzo, “Multi-contact bilateral telemanipulation using wearable haptics,” in *2016 IEEE/RSJ International Conference on Intelligent Robots and Systems (IROS)*, Oct 2016, p. 1431–1436.
- [53] M. Dascalu, M. S. Teodorescu, A. Plavitu, L. Milea, E. Franti, D. Coroama, and D. Moraru, “Tele-operated robotic arm and hand with intuitive control and haptic feedback,” *American Journal of Aerospace Engineering*, vol. 1, no. 44, p. 21, Dec 2014.
- [54] D. S. Pamungkas and K. Ward, “Tele-operation of a robot arm with electro tactile feedback,” in *2013 IEEE/ASME International Conference on Advanced Intelligent Mechatronics*, Jul 2013, p. 704–709.
- [55] L. Takayama, “Putting human-robot interaction research into design practice,” in *2022 17th ACM/IEEE International Conference on Human-Robot Interaction (HRI)*, Mar 2022, p. 1–1.
- [56] J. Pérez, J. Aguilar, and E. Dapena, “Mihr: A human-robot interaction model,” *IEEE Latin America Transactions*, vol. 18, no. 09, p. 1521–1529, Sep 2020.



- [57] X. Mu, L. Tan, Y. Tian, and C. Wang, “Recent development of human-robot natural interaction in spatial cognition tasks,” vol. 01, Aug 2016, p. 446–450.
- [58] “Human robot interaction in collaborative manufacturing scenarios: Prospective cases,” Nov 2022, p. 1–6.
- [59] Z. Chu, J. Wang, X. Jiang, C. Liu, and L. Li, “Mind-vr: A utility approach of human-computer interaction in virtual space based on autonomous consciousness,” in *2022 International Conference on Virtual Reality, Human-Computer Interaction and Artificial Intelligence (VRHCIAI)*, 2022, p. 134–138.
- [60] R. Jayaswal and M. Dixit, “A study on human-computer interaction based on surveillance tasks,” in *2022 IEEE World Conference on Applied Intelligence and Computing (AIC)*, 2022, p. 384–390.
- [61] T. Li, H. Wang, D. Fan, D. Wang, L. Yin, and Q. Lan, “Research on virtual skiing system based on harmonious human-computer interaction,” in *2022 International Conference on Virtual Reality, Human-Computer Interaction and Artificial Intelligence (VRHCIAI)*, 2022, p. 106–110.
- [62] S. Saxena, P. Saxena, and S. K. Dubey, “Various levels of human stress their impact on human computer interaction,” in *2013 International Conference on Human Computer Interactions (ICHCI)*, 2013, p. 1–6.
- [63] Z. Yan, R. Kantola, and P. Zhang, “Theoretical issues in the study of trust in human-computer interaction,” in *2011 IEEE 10th International Conference on Trust, Security and Privacy in Computing and Communications*, 2011, p. 853–856.
- [64] Y. J. Vite and Y. Hu, “The role of attention and cognitive workload in measuring levels of task complexity within virtual environments,” Mar 2023, p. 651–652.
- [65] W. Moroney, D. Biers, F. Eggemeier, and J. Mitchell, “A comparison of two scoring procedures with the nasa task load index in a simulated flight

- task,” in *Proceedings of the IEEE 1992 National Aerospace and Electronics Conference@<sub>N</sub>AECON1992, May1992, p.734–740vol.2.*
- [66] S. Pirasmepulkul, A. Caracappa, P. Luxsuwong, C. D. Onal, W. Michalson, T. Khuu, and M. Luo, “Haptic glove as a wearable force feedback user interface,” 2017-11-09.
- [67] E. Skorina, R. Rameshwar, S. Pirasmepulkul, T. K. Khuu, A. Caracappa, P. Luxsuwong, M. Luo, W. R. Michalson, and C. Onal, *Soft Robotic Glove System for Wearable Haptic Teleoperation - 18373*, Jul 2018, no. INIS-US-20-WM-18373. [Online]. Available: <https://www.osti.gov/biblio/22977681>
- [68] S. Li, R. Rameshwar, A. M. Votta, and C. D. Onal, “Intuitive control of a robotic arm and hand system with pneumatic haptic feedback,” *IEEE Robotics and Automation Letters*, vol. 4, no. 4, p. 4424–4430, Oct 2019.
- [69] A. M. Votta, S. Y. Günay, D. Erdoğan, and Önal, “Force-sensitive prosthetic hand with 3-axis magnetic force sensors,” Sep 2019, p. 104–109.
- [70] R. Rameshwar, E. H. Skorina, and C. D. Onal, “Fabric-silicone composite haptic muscles for sensitive wearable force feedback,” in *Proceedings of the 16th International Conference on PErvasive Technologies Related to Assistive Environments*, ser. PETRA ’23. New York, NY, USA: Association for Computing Machinery, 2023, p. 33–41. [Online]. Available: <https://doi.org/10.1145/3594806.3594853>
- [71] A. Ozcan, Z. Tulum, L. Pinar, and F. Başkurt, “Comparison of pressure pain threshold, grip strength, dexterity and touch pressure of dominant and non-dominant hands within and between right-and left-handed subjects,” *Journal of Korean Medical Science*, vol. 19, no. 6, p. 874–878, Dec 2004.
- [72] C. Pacchierotti, S. Sinclair, M. Solazzi, A. Frisoli, V. Hayward, and D. Prattichizzo, “Wearable haptic systems for the fingertip and the hand: Taxonomy, review, and perspectives,” *IEEE Transactions on Haptics*, vol. 10, no. 4, p. 580–600, Oct 2017.

- [73] A. J. Doxon, D. E. Johnson, H. Z. Tan, and W. R. Provancher, “Human detection and discrimination of tactile repeatability, mechanical backlash, and temporal delay in a combined tactile-kinesthetic haptic display system,” *IEEE transactions on haptics*, vol. 6, no. 4, p. 453–463, 2013.
- [74] Jan 2016. [Online]. Available: <https://openbionicslabs.com/obtutorials/ada-v1-assembly>
- [75] X. Wang, W. Xu, B. Liang, and C. Li, “General scheme of teleoperation for space robot,” Jul 2008, p. 341–346.
- [76] H. Chen, P. Huang, and Z. Liu, “Modeling and forecasting of time delay about the space robot teleoperation system,” Jul 2019, p. 529–534.
- [77] T. Sheridan, “Space teleoperation through time delay: review and prognosis,” *IEEE Transactions on Robotics and Automation*, vol. 9, no. 5, p. 592–606, Oct 1993.
- [78] M. Hajduk, P. Jencik, J. Jezny, and L. Vargovcik, “Trends in industrial robotics development,” vol. 282, p. 1–6, 2013.
- [79] [Online]. Available: <https://www.bls.gov/respondents/iif/>
- [80] “Towards remote teleoperation of a semi-autonomous mobile manipulator system in machine tending tasks,” Nov 2019. [Online]. Available: <https://dx.doi.org/10.1115/MSEC2019-3027>
- [81] R. Inam, K. Raizer, A. Hata, R. Souza, E. Forsman, E. Cao, and S. Wang, “Risk assessment for human-robot collaboration in an automated warehouse scenario,” vol. 1, Sep 2018, p. 743–751.
- [82] M. E. Walker, H. Hedayati, and D. Szafir, “Robot teleoperation with augmented reality virtual surrogates,” in *2019 14th ACM/IEEE International Conference on Human-Robot Interaction (HRI)*, Mar 2019, p. 202–210.
- [83] —, “Robot teleoperation with augmented reality virtual surrogates,” in *2019 14th ACM/IEEE International Conference on Human-Robot Interaction (HRI)*, Mar 2019, p. 202–210.

- [84] T. Lancet, “Covid-19: protecting health-care workers,” *The Lancet*, vol. 395, no. 10228, p. 922, Mar 2020.
- [85] H. Lv, D. Kong, G. Pang, B. Wang, Z. Yu, Z. Pang, and G. Yang, “Gulim: A hybrid motion mapping technique for teleoperation of medical assistive robot in combating the covid-19 pandemic,” *IEEE Transactions on Medical Robotics and Bionics*, vol. 4, no. 1, p. 106–117, Feb 2022.
- [86] A. Naceri, J. Elsner, M. Tröbinger, H. Sadeghian, L. Johannsmeier, F. Voigt, X. Chen, D. Macari, C. Jähne, M. Berlet, J. Fuchtmann, L. Figueredo, H. Feußner, D. Wilhelm, and S. Haddadin, “Tactile robotic telemedicine for safe remote diagnostics in times of corona: System design, feasibility and usability study,” *IEEE Robotics and Automation Letters*, vol. 7, no. 4, p. 10296–10303, Oct 2022.
- [87] N. Feizi, M. Tavakoli, R. V. Patel, and S. F. Atashzar, “Robotics and ai for teleoperation, tele-assessment, and tele-training for surgery in the era of covid-19: Existing challenges, and future vision,” *Frontiers in Robotics and AI*, vol. 8, 2021. [Online]. Available: <https://www.frontiersin.org/articles/10.3389/frobt.2021.610677>
- [88] K. Kraft and W. D. Smart, “Seeing is comforting: Effects of teleoperator visibility in robot-mediated health care,” in *2016 11th ACM/IEEE International Conference on Human-Robot Interaction (HRI)*, Mar 2016, p. 11–18.